國立交通大學

光電工程研究所

博 士 論 文

應用版畫色序法實現高畫質低功率之
節能液晶顯示器

A High Image Quality and Low Power Consumption
Eco-LCD Using Stencil Field-Sequential-Color Method

研 究 生：林芳正

指導教授：謝漢萍 博士

黃乙白 博士

中 華 民 國 九 十 八 年 八 月

應用版畫色序法實現高畫質低功率之
節能液晶顯示器

A High Image Quality and Low Power Consumption Eco-LCD

Using Stencil Field-Sequential-Color Method

研 究 生：林芳正　　　　　　Student：Fang-Cheng Lin

指導教授：謝漢萍 博士　　　　Advisors：Dr. Han-Ping D. Shieh
　　　　　黃乙白 博士　　　　　　　　　Dr. Yi-Pai Huang

國 立 交 通 大 學

光 電 工 程 研 究 所

博 士 論 文

A Dissertation
Submitted to Institute of Electro-Optical Engineering
College of Electrical and Computer Engineering
National Chiao Tung University
in partial Fulfillment of the Requirements
for the Degree of
Doctor of Philosophy
in
Department of Photonics
August 2009
Hsinchu, Taiwan, Republic of China

中華民國 九十八 年 八 月

應用版畫色序法實現高畫質低功率之
節能液晶顯示器

博士研究生：林芳正　　　　指導教授：謝漢萍 教授

黃乙白 助理教授

國立交通大學　　光電工程學系/光電所

摘　　要

全球化的氣候異常變遷已被公認為近年來最重要的環保問題，面對這樣的窘境，開發且廣泛使用節能家電用品成為讓地球永續發展的重要一環。有鑑於電視相關顯示產品的用電量約佔家用電的百分之十，因此，本論文除了提升顯示器的影像品質外，更朝向低耗能的環保液晶顯示技術發展。

本論文將液晶顯示器視為一組雙面板的顯示架構，包含一個高解析度的液晶面板與一個可獨立調變光強度且由發光二極體 (LED) 組成的低解析度背光面板。在此雙面板的架構下，分為兩個階段針對背光及液晶兩面板提出不同於先前的方法，進一步提升高動態範圍 (high dynamic range, HDR) 及色序型 (field-sequential color) 兩大顯示技術的顯像品質。

首先，在第一階段針對背光部分，提出 IMF (Inverse of a Mapping Function) 背光決定法。IMF 可依據不同輸入影像，演算出符合該畫面特性的動態背光映對函數 (mapping function)。從實驗結果發現，利用 IMF 背光決定法，除了提升液晶顯示器的對比度外，在維持與傳統液晶顯示器相同的最高亮度下，更大幅降低30%的電能消耗。

在第二階段部分，由於色序型液晶顯示器在不需要彩色濾光片的情形下，可提升三倍的光使用率以進一步降低電能消耗，但色序型顯示器確有著致命的潛在缺陷：色分離現象。此缺陷將大幅降低影像品質，甚至造成人眼觀看時的不舒適感，因此提出優化無彩色濾光片液晶面板的方法。不同於先前需要超過 300Hz 的子畫面更新頻率，我們提出低於 240Hz 的版畫概念色序型液晶顯示技術 (Stencil-FSC) 來抑制色分離現象並巧妙的將高動態範圍技術應用於傳統的色序型顯示技術。如同版畫技巧，Stencil-FSC 先將三原色的影像內容初步集中於第一個子畫面，如此一來，可大幅降低剩下各子畫面的亮度，僅用來補足第一個子畫面顯示不足的顏色。經由 80 張不同影像內容的模擬結果，色分離平均抑制量為傳統色序型顯示器的 50%，從實際的拍攝結果也幾乎察覺不出色分離現象。

最後，我們將 Stencil-FSC 的概念硬體實現於 32 吋的色序型液晶顯示器。實驗量測結果顯示其不僅提升影像對比至 26,000:1、114% NTSC 的色域表現，同時，更大幅降低平均電能消耗至 35 瓦特以下，相當於傳統同尺寸 LED 背光液晶顯示器耗電量的 20%。在如此低耗能高品質的顯示技術下，期許未來人類在與親朋好友享受高品質多媒體影像的同時，也能為地球的永續發展盡一分心力。

A High Image Quality and Low Power Consumption Eco-LCD Using Stencil Field-Sequential-Color Methods

Doctoral Student: Fang-Cheng Lin   **Advisors: Dr. Han-Ping D. Shieh**

Dr. Yi-Pai Huang

Department of Photonics & Institute of Electro-Optical Engineering
National Chiao Tung University

ABSTRACT

Climate change is now widely recognized as a major environmental problem. In creating a sustainable world, energy-efficient household electronics should be developed and popularized. Since TV-related activity occupies 10% of overall household power usage, developing high image performance and low power consumption "Eco-LCDs" becomes the main subject in this dissertation.
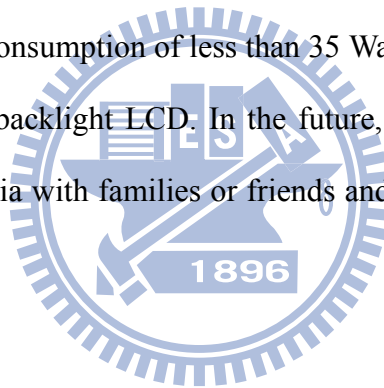
An LCD was studied as a dual-panel structure: a low resolution controllable LED backlight and a high resolution LC panel. Based on this dual-panel concept, we divided this dissertation into two stages and proposed novel methods to improve both high dynamic range (HDR) and field-sequential color (FSC) technologies.

In the first stage, we proposed the IMF method to optimize HDR-LCD backlight signals. IMF provided a dynamic backlight gamma to achieve high contrast ratio and high brightness images while reducing average power consumption by 30% when compared to the same size LED backlight LCD.

Furthermore, an FSC-LCD enhanced the optical throughput by a factor of 3 because of getting rid of color filters. However, the FSC-LCD is still facing a lethal issue, color breakup

(CBU). In the second stage, we proposed the Stencil-FSC method at less than 240Hz field rate to suppress CBU. This method was much different from the prior CBU suppression methods which usually used field rate more than 300Hz. Stencil-FSC ingeniously applied local HDR technology to an FSC-LCD. The originality of Stencil-FSC was to use a multi-color image concentrating image luminance in a single field. The intensities of the residual primary-color sub-frames were therefore greatly reduced. Through simulations, CBU was suppressed by 50% for eighty test images when compared to conventional RGB-driving and made CBU almost imperceptible in experimental photos.

In addition, this dissertation successfully demonstrated the Stencil-FSC method on a 32-inch FSC-LCD to yield a high dynamic contrast of 26,000:1, a wide color gamut of 114% NTSC, and average power consumption of less than 35 Watts which was equivalent to 20% of the same size full-on LED backlight LCD. In the future, we expect that human beings will enjoy high quality multimedia with families or friends and simultaneously maintain a healthy Earth.

ACKNOWLEDGEMENTS

TABLE OF CONTENTS

FIGURE CAPTIONS

xiii

TABLE LIST

Chapter 1

INTRODUCTION

Concerns about saving energy and protecting the environment are gradually increasing. After the documentary, "An Inconvenient Truth," featuring Al Gore in 2006, the global warming issue receives wide attention [1]. The greenhouse effect makes the Earth warmer. Polar bears almost have no place to live on the Earth (Fig. 1-1). Climate change is now widely recognized as a major environmental problem. When facing the climate change, energy-efficient household electronics should be developed and popularized. A recent study by PG&E in California estimated that 10% of overall household power usage was devoted to TV-related activity. Consequently, reducing power consumption becomes one of the main subjects in current liquid crystal display (LCD) manufacturing.

(a) Rising CO_2 concentration   (b) A helpless polar bear
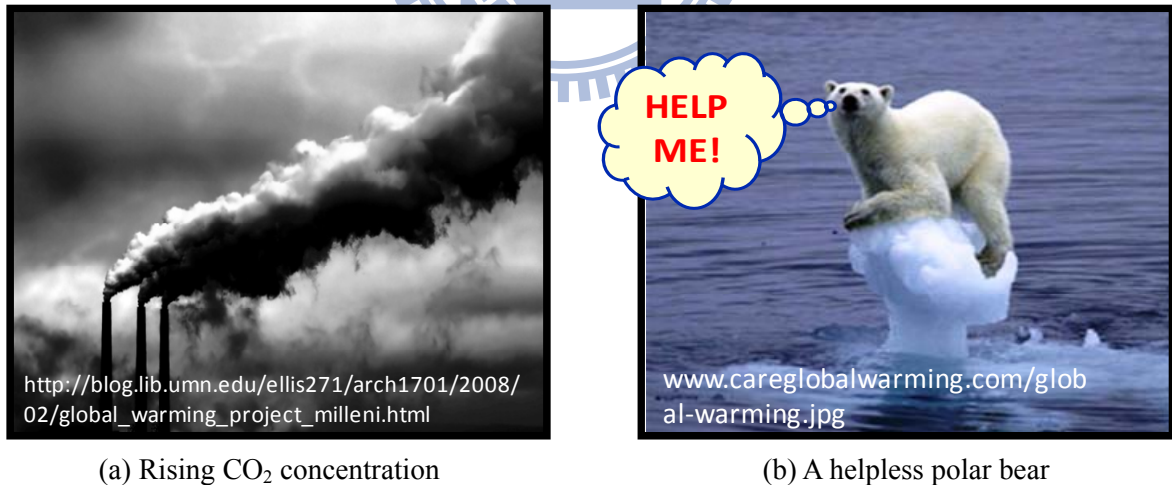
Fig. 1-1   Cause and effect of global warming. (a) Cause: rising carbon dioxide concentration and (b) a consequence: a helpless polar bear.

The history of LCDs can be traced to the year 1964. G. Heilmeier was the first person to turn a clear liquid milky by applying electricity at Radio Corporation of America (RCA).

Heilmeier also had the foresight to imagine that a wall-sized full-color LC display was achievable. T. Peter Brody fabricated the first active matrix LCD in 1972, which was initially limited to small display applications, like calculators, watches, etc. In 1988, Sharp demonstrated the first active matrix full-color and full-motion LCD panel. Until 1991, M. Aramoto of Sharp's Audio-Video Group introduced the first wall-hanging- television product, the "Liquid Crystal Museum." Heilmeier's dream had become a reality [2][3].

Fig. 1-2   The first wall-hanging televisions fabricated by Sharp Cooperation [2].

In the past decades, thin film transistor liquid crystal displays (TFT-LCDs) have become the most wide-spread display technology for applications ranging from small mobile devices, car navigation systems, laptops, and monitors to large-sized TV applications and projectors, etc. The high number of LCD applications can be attributed to several features, such as high resolution, high brightness, light weight, and a thin profile.

1.1 Thin Film Transistor Liquid Crystal Displays (TFT-LCDs)

A traditional TFT-LCD is composed of two main structures: a backlight module and an LC panel, as shown in Fig. 1-3. As liquid crystals (LCs) are not emissive, TFT-LCDs must rely on additional light sources (e.g. CCFLs or LEDs) which are generally behind the LC cell and are called "backlight." The LC panel is basically a sandwich structure with LC molecules

filled between two glass substrates: a TFT-array glass and a color-filter glass. The TFT-array glass consists of a polarizer and TFTs. The number of TFTs is three times more than the number of pixels. The LC controls the light transmission using different molecular orientations that vary in accordance with the applied voltage. The color-filter glass is composed of a polarizer (analyzer) and a color-filter layer. In the color filter, each pixel segment is made up of three primary-color (red, green, and blue) sub-pixels approximate 150 micro-meters in size for a 37-inch LCD.
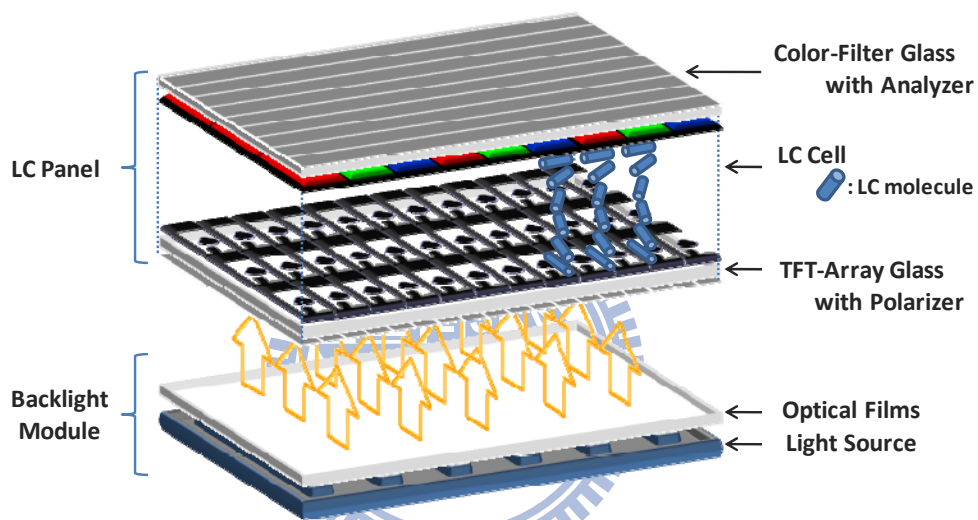
Fig. 1-3   Traditional LCD structure: a backlight module and an LC panel.

The TFT-LCD is generally illuminated using a constant full-on backlight which consists of conventional cold cathode fluorescence lamps (CCFLs). The backlight polarization state changes to the linear state after propagating through a polarizer on the TFT-array glass. Different voltages between these two glasses control LC orientations and create different phase retardations due to the LC birefringence property. When the linear polarized lights propagate through the LC cell, the polarization states are modulated by differing LC orientations. Consequently, lights from different sub-pixels continue to propagate into red, green, and blue color filters in different intensities and become colorized. After passing through the analyzer, a color image is finally created through human eye spatial synthesis.

1.2 Issues of Current TFT-LCDs

Although LCDs have many advantages, some issues still must be improved. The notorious issues are low optical throughput, imperfect "dark" state, low color saturation, and others. A traditional LCD backlight system is generally illuminated by a full-on CCFL backlight. The generated light propagates through an optical stack comprised of a set of polarizers, color filters, and diffusers. Substantial proportions of light are scattered and absorbed by these components. Overall, approximately only 5~8% of backlight reaches the front-of-screen image, more than 90% of backlight is consumed (Fig. 1-4). Second, an imperfect dark state is due to light leakage from LCs and a pair of non-ideal crossed polarizers; the poor image contrast ratio of conventional LCDs results in fuzzy images. An additional issue is that CCFL spectrum widely covers all visible wavelengths (e.g. 400~700nm) and the transmittance spectra of color filters are not pure peaks at red, green, and blue (Fig. 1-5(a)). Therefore, the primary colors perceived by human eyes in a conventional LCD are often made up of several different frequencies resulting in color gamut shrinkage. Fig. 1-5(b) illustrates that the color gamut of RGB-LED backlight is much larger than that of CCFL backlight [4]. Images produced on LCDs with backlights employing CCFLs and RGB-LEDs are compared in Fig. 1-6 in which the RGB-LED backlight LCD shows a more vivid color image.

These issues are attributed to the full-on CCFL backlight and color filters which absorb more than 70% backlight intensity. Consequently, LCD manufacturing utilizes the light emitting diode (LED) which is high power efficiency and near point light source to replace conventional CCFL backlight. In addition, the inefficient color filters are removed to enhance the poor optical throughput and save 19% of the material cost in a typical 32-inch LCD panel, as illustrated in Fig. 1-7 [5].
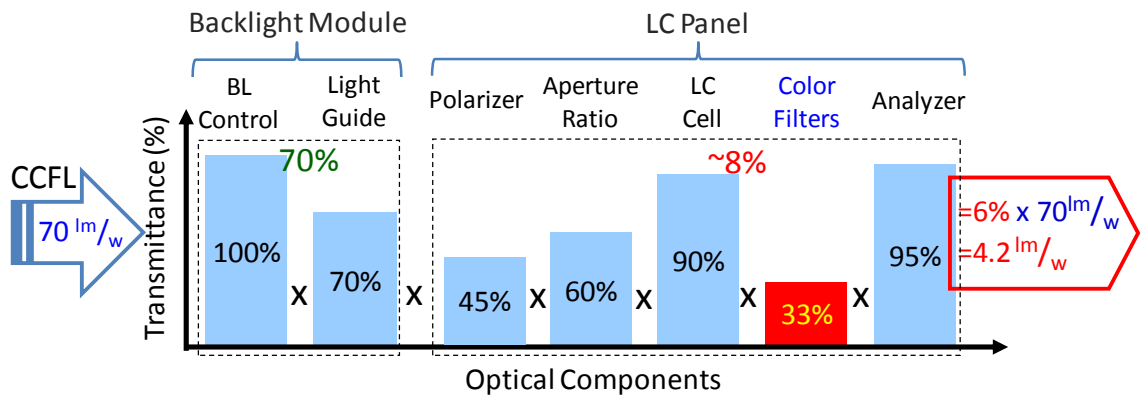
Fig. 1-4 Low optical throughput in a CCFL-backlight LCD attributed to the low optical transmittance efficiency of optical components.

(a) Spectra of light sources and color filters   (b) Color gamut with different BLs
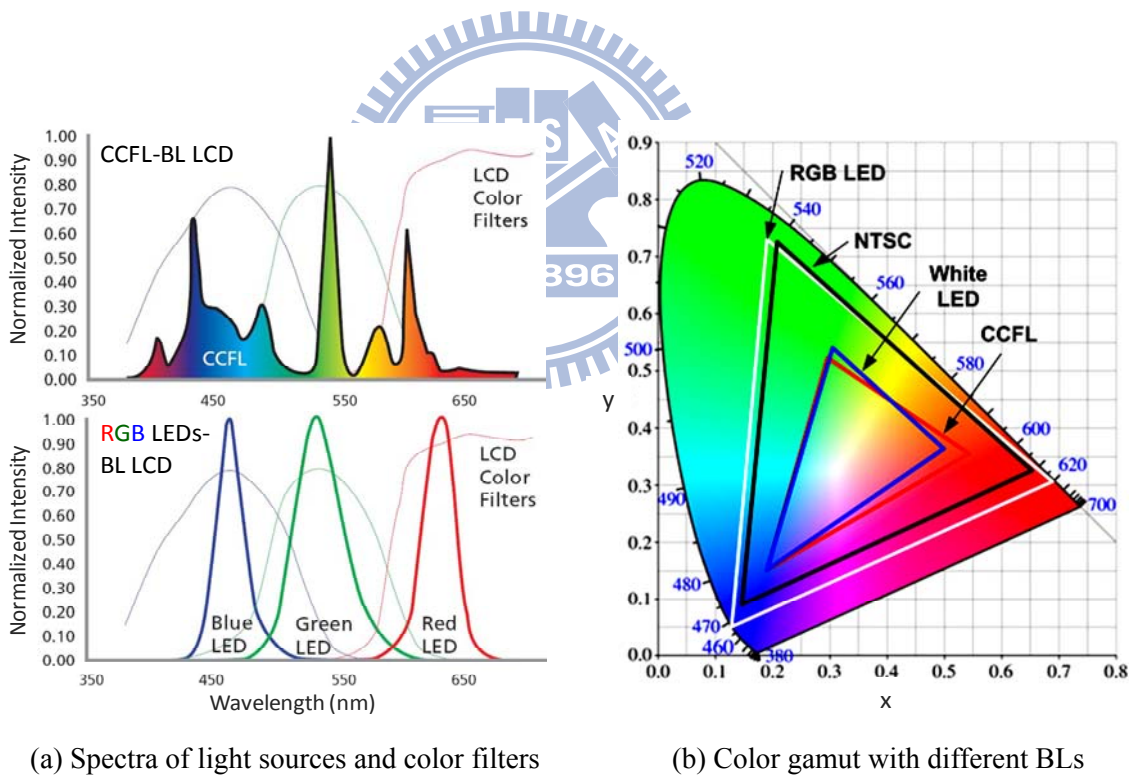
Fig. 1-5 (a) Typical color filter transmittance spectra with illuminant spectra of a CCFL backlight (top) and a RGB-LED backlight (bottom). (b) LCD color gamut with backlights employing the RGB LEDs, CCFLs and white LEDs [4].

(a) CCFL BL LCD   (b) RGB-LED BL LCD
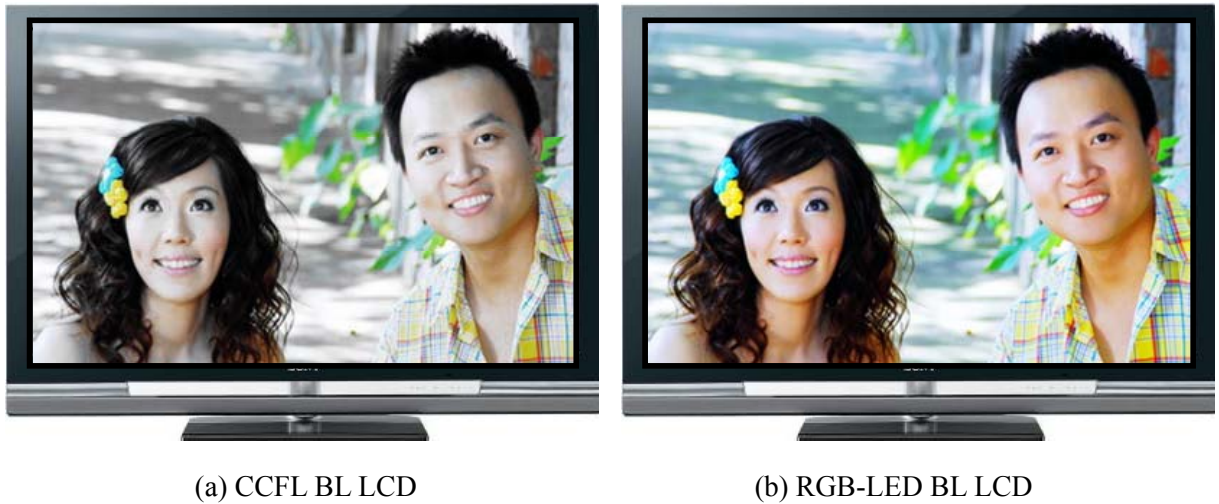
Fig. 1-6　Differing image color saturation and contrast ratio abilities in (a) CCFL backlight and (b) RGB-LED backlight LCDs.
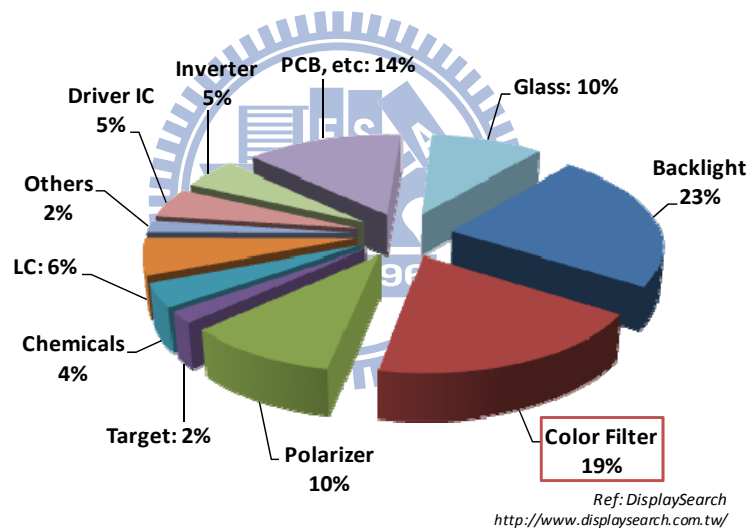
Fig. 1-7　A typical materials cost structure of a 32-inch LCD panel (Q4' 2008)[5].

1.3　LED-based LCD Technologies

Light emitting diodes (LEDs) are praised for several advantages, such as being mercury-free, having small form factor, a long lifetime, high power efficiency, wide color gamut, and fast switching operation [6]. Therefore, LEDs are being applied to the LCD backlight system and not only save power but also enable the panel lighter and thinner [7]. The advanced technologies of scanning backlight driving [8], high dynamic range [9]-[15],

and field-sequential color [16]-[21] are swiftly developed resulting from this new option for backlight systems.

1.3.1 High Dynamic Range Display Systems

Scenes in the real-world contain a dynamic range over 10 orders of luminance magnitude from starlight to sunlight (Fig. 1-8). The human visual system perceives over 5 orders in real time and evolves to all ranges through long-time adaptation [22]. However, in spite of recent advances in cell technology, the dynamic range of current state-of-the-art LCDs is typically limited to only three orders of magnitude; especially the dark region of the picture is not truly dark because of light leakage. Therefore, using LED light sources as a backlight instead of CCFLs, the backlight panel is locally dimmed and greatly increases the dynamic range of such a display while simultaneously substantially reducing power consumption. This type of display is also called the "high dynamic range (HDR) display."

10^{-3}	10^{-2}	10^{-1}	1	10	10^2	10^3	10^4	10^5	10^6	**Luminance**
Star	Quarter moon	Full moon	Twilight	Family living room	LCD	overcast day	Sunny day	Full daylight	Direct sunlight	**(lux)**
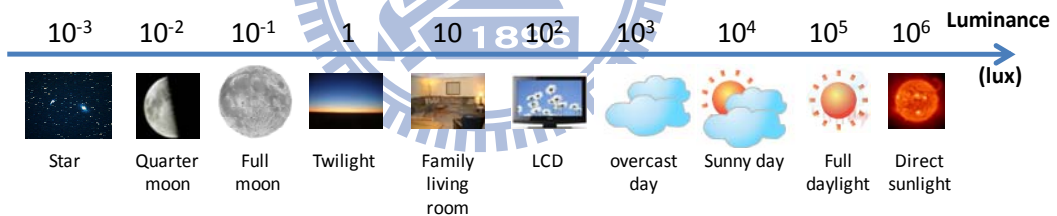
Fig. 1-8   Real world dynamic range with 10 orders of luminance magnitude.

Local dimming backlights effectively combined a low-resolution display (the backlight) with a high-resolution one (the LC panel), as shown in Fig. 1-9. These backlights generated only the amount of light required to correctly represent the video content while dimming under dark areas. Therefore, a high dynamic range/high contrast image was achieved using an HDR display. However, many image details were lost while applying an excessively dark backlight determination method even though LC signals were compensated [23], as illustrated in Fig. 1-10.
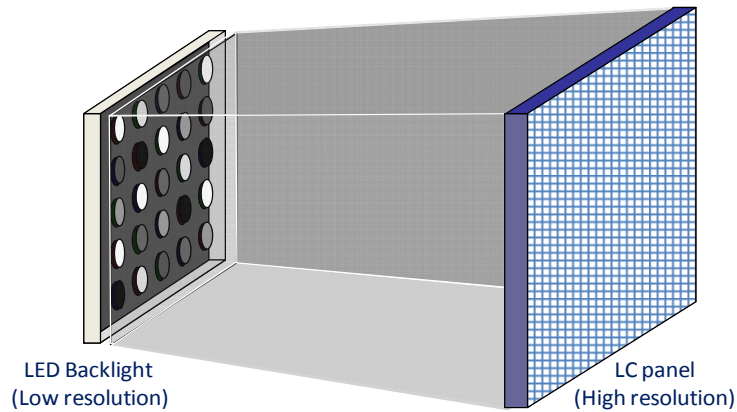
Fig. 1-9   An LC-TV with a local dimming backlight can be regarded as the superposition of two displays with different spatial resolutions: a low resolution backlight (left) and a high resolution LC panel (right).

(a) Full-on BL LCD   (b) HDR-LCD
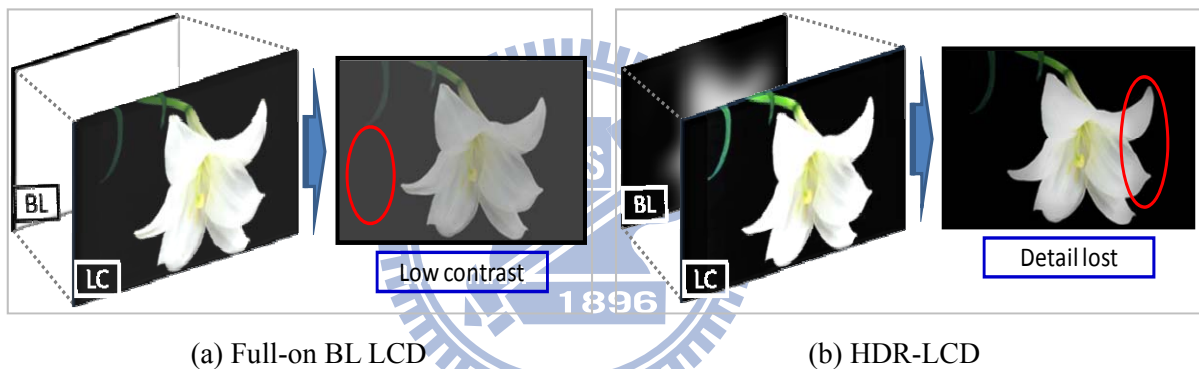
Fig. 1-10   (a) Light leakage results in a low contrast image on a full-on backlight LCD, and (b) an excessively dark backlight signal results in image detail lost on an HDR-LCD.

1.3.2 Field-Sequential Color LCDs

A high optical throughput field-sequential color (FSC) LCD without color filters was proposed to further reduce power consumption [16]-[21]. By rapidly displaying red (R), green (G), and blue (B) field-images sequentially, a full-color image was created by temporal color synthesis, as illustrated in Fig. 1-11(a). To prevent luminance flicker, the three-primary colors system required a minimum refresh rate of 180Hz. Consequently, fast-response LEDs were applied to LCD backlight systems to replace conventional CCFLs. After removing color filters, FSC-LCDs possessed many benefits, such as high optical

throughput, wide color gamut, low material cost, three times the possible screen resolution, and other features compared to LCDs with color filters.

However, FSC-LCDs still face an inherent visual artifact, color breakup (CBU), which occurs when relative velocities exist between the screen object and the human eye. This may occur during both smooth motion pursuit (eye velocity is slower than 90 degree/sec) and particularly saccadic movement (eye velocity is faster than 90 degree/sec) [24]-[30]. During eye movements, the separated R, G, and B sub-pixels of an image degrade image quality and cause viewer discomfort, as shown in Fig. 1-11(b). Once the CBU issue is overcome, a low power consumption and high image quality LCD becomes feasible.

	Time Sequentially	Relative velocity

Data Load	LC Set	LED Flash	Data Load	LC Set	LED Flash	Data Load	LC Set	LED Flash

Red   Green   Blue

5.56 ms

1 frame (60 Hz): 16.7 ms

CBU Image

(a) FSC-LCD mechanism   (b) Color breakup
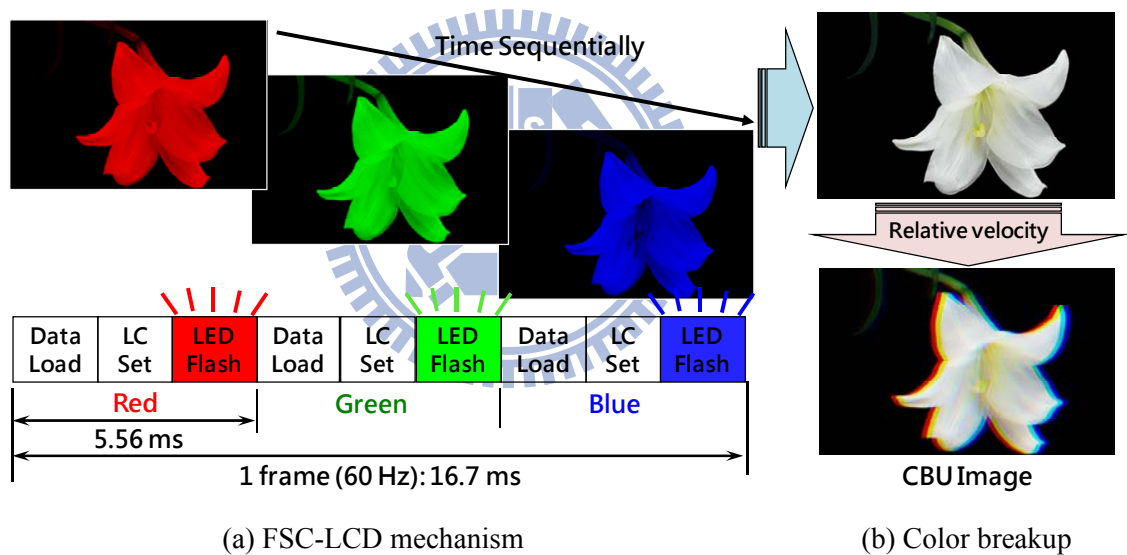
Fig. 1-11   (a) The field-sequential color (FSC) LCD mechanism: Displaying red, green, and blue field-images at 180Hz field rate. (b) Color breakup (CBU) occurring while relative velocity exists between the screen object and the human eye.

1.4 Motivations and Objectives

In creating a sustainable world, energy conservation and altering of our "consuming" live style is worthy to be practiced. This is a great incentive to reduce the power dissipation of state-of-the-art LCDs. In addition, as people always admire beautiful scenes; higher image

qualities (e.g. image resolution, contrast ratio, color saturation) are required. Hence, LCD manufacturing is working hard on enhancing image quality and lowering power consumption.

An LED-based backlight LCD opens up an alternative way for creating a low power "Eco-Display." Particularly, the HDR- and FSC-related LCDs have an essential role to play in display manufacturing. To make them more feasible, some topics, such as HDR-LCD backlight determinations and FSC-LCD color breakup have to be developed and resolved. To effectively improve image quality and reduce power consumption, we study these topics in two stages, 1st stage: replacing a CCFL full-on backlight by a dynamic RGB-LED backlight; 2nd stage: removing color filters for the LC panel. Finally, these two stages are convolved together to reach a high image quality eco-LCD.
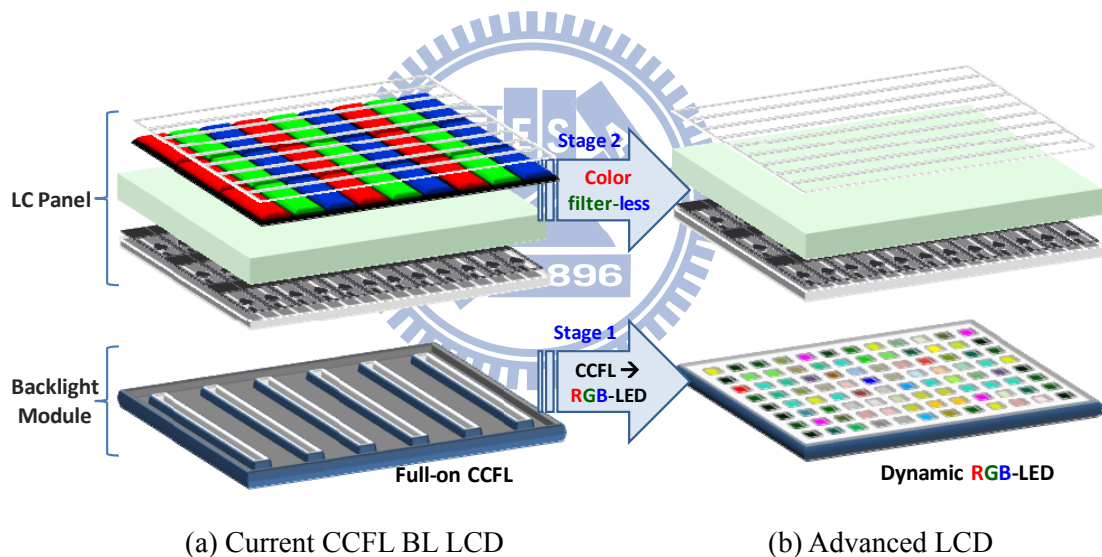
Fig. 1-12 Two stages for minimizing power consumption and enhancing image quality. (a) A current CCFL full-on BL LCD and (b) advanced LCD: color filter-less with dynamic RGB-LED BL LCD.

In the first stage, we propose an efficient method, "Inverse of a Mapping Function (IMF)," to optimize backlight signals [31][32]. The IMF method provides a dynamic gamma function for the backlight panel to not only maintain a high contrast ratio but also maintain maximum luminance and clear image detail. Additionally, power consumption and image distortion are also reduced. The detailed IMF method is described in Chapter 3.

In the second stage, local color-backlight dimming technology is ingeniously applied on an FSC-LCD to overcome the CBU issue and name "Stencil Field-Sequential-Color" (Stencil-FSC). The Stencil-FSC field rate is controlled at less than 240Hz (4 field-images), including the 240Hz (4-field) [33]-[35] and 180Hz (3-field) Stencil-FSC methods [36][37]. Stencil-FSC methods are consequently implemented on an FSC-LCD using a commercial OCB-mode [38][39] because of their low field rates. Using local color-backlight dimming technology, a high luminance multi-color image is generated on a color filter-less LCD. Therefore, the intensities of the residual primary-color images are greatly reduced and effectively suppress CBU. Utilizing a "multi-color" field in a single field-image to suppress CBU is an originality and much different from previous CBU suppression methods. The detailed Stencil-FSC methods are expressed in Chapters 4 and 5.

According to current specifications of 32-inch CCFL and RGB-LED backlight LCDs, the objectives of this dissertation are as follows: using a dynamic RGB-LED backlight system to enhance the image contrast ratio more than 20,000:1, save 50% power consumption, and increase the color gamut to more than 110% NTSC. Finally, using a 180Hz driving algorithm to render CBU imperceptible and maintain image fidelity (Table 1-1).

Table 1-1   The objectives of this dissertation.

Current 32-inch LCD			This Dissertation
CCFL BL	RGB-LED BL		
~1,500 : 1	~1,500:1	Static Contrast Ratio	> 20,000:1
110 (100%)	190 (172%)	Power Consumption (W)	< 55 (50%)
72	>105	Color Gamut (% NTSC)	> 110
$D \equiv \dfrac{\#\ of\ distorted\ pixels}{\#\ of\ total\ pixels} \times 100\%$		Color Breakup (CBU)	Imperceptible
		Field Rate (Hz)	180
		Image fidelity	D<5% or ΔE_{00}<3

1.5 Organization of this Dissertation

This dissertation is organized as follows: the fundamental HDR algorithm and basic color science principles are in Chapter 2. In this Chapter, the human eye movements and CBU mechanism are also presented. In Chapter 3, a dynamic backlight gamma curve, inverse of a mapping function (IMF) embedded into an HDR-LCD is proposed to enhance image contrast while simultaneously reduce power consumption. Following, HDR technology was applied on FSC-LCDs to suppress CBU. The 240Hz Stencil-FSC and 180Hz Stencil-FSC methods are consequently proposed in Chapters 4 and 5. In these two chapters, the algorithm, optimization of hardware parameters, simulations and experimental results are presented. Finally, Chapter 6 concludes the dissertation; current issues and future work are also discussed.
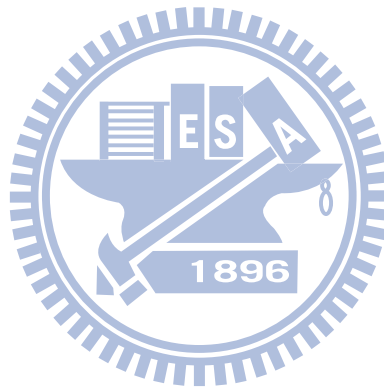
Chapter 2

PRINCIPLES

The fundamental algorithm of a high dynamic range (HDR) system is first discussed in this chapter, including determining backlight signals and compensating LC signals. Following, the physiological structure of the human eye and types of eye movements are presented to help develop a proper method to suppress the color breakup (CBU) issue. The CBU mechanisms caused by different eye movements are also discussed. In addition, the color difference of CIEDE2000 was utilized to evaluate the differences between simulated images and original images while using the proposed algorithm. Therefore, the definition of CIEDE2000 is presented.

2.1 Fundamentals of High Dynamic Range Displays

The dynamic range of real-world environments exceeds the capabilities of existing display technology by several orders of magnitude. To present a high dynamic range on an LCD, an LED-based backlight is utilized because of its point-like light source and individual control.

The HDR algorithm is expressed in Fig. 2-1 [10]. Each input image[1] is recalculated for the LED-based backlight[3] and LC panel[6]. The first step in this algorithm is to down-sample the input image resolution to the resolution of LED array. After that, taking the square root[2] of the reduced resolution image[2a] as the backlight signals, the LC signals are then compensated for the variation in the LED-based backlight. To correctly compensate the LC signal, the next step is to calculate the backlight intensity distribution[4] (p_1*I_L) generated by the LED-based backlight through summing up the contributions of each LED for this input image. It is important that the point spread function (p_1) used in this process accurately

reflects the effective light distribution of each LED, including any interaction with the optics and films used in the package. Moreover, the compensated LC signal can be generated through dividing the input image by the simulation of backlight intensity distribution[5], as shown in Eq. 2-1. Finally, the HDR-LCD shows a completed image.

$$I' = \frac{I}{p_1 \otimes I_L}$$

(2-1)

where I, I' represent original and compensated LC signals
$p_1 \otimes I_L$ *represents the backlight intensity distribution*

The LED is driven to the appropriate intensity, and the LED backlight creates a luminance distribution which is similar to backlight intensity distribution simulation. Then, the LC panel modulates this luminance distribution so that the final output image matches the input image, as illustrated in Fig. 2-2 [9].
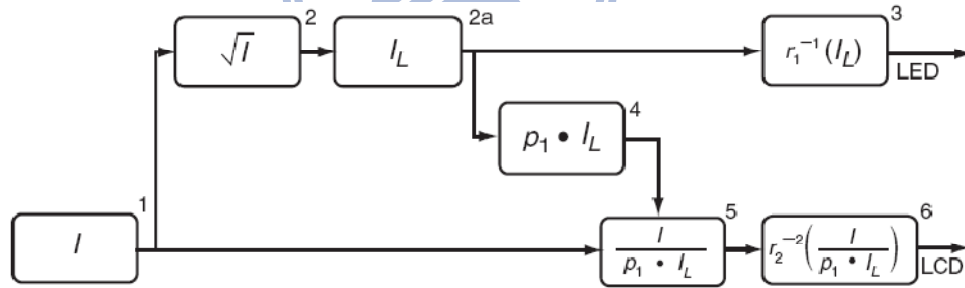
Fig. 2-1   The algorithm for an LED-based HDR display [10].

(a) Input image   (b) LED signals   (c) Compensated LC   (d) Final image
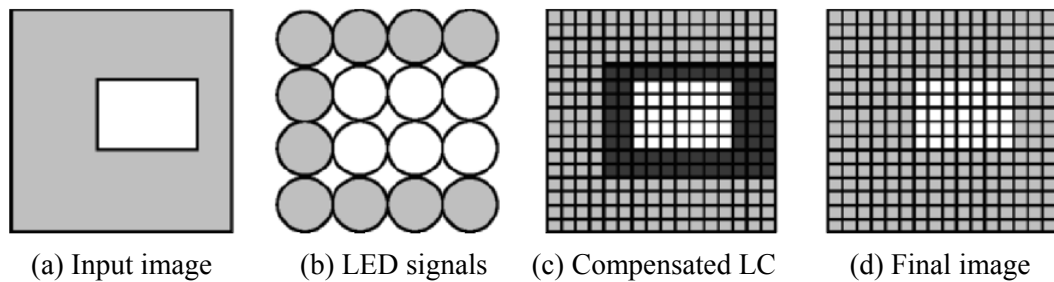
Fig. 2-2   Schematic HDR Display image processing steps: (a) desired image, (b) LED-based backlight signals, (c) LC compensated signals, and (d) final output image [9].

2.2 Structure of the Human Eye

The human eye is an adaptive lens. Fig. 2-3 shows the cross section of the human eye [40]. When light goes into the pupil of the eye and continues through the lens which acts the same as a camera focusing light onto the retina. The retina contains two types of photoreceptors, rods and cones, named for their shapes. The rods are more numerous, roughly 125 million, and are more sensitive than the cones to detect small amounts of light, such as starlight. However, they are unable to distinguish color. 6 to 7 million cones perform in bright light, giving detailed colored views, but they fail at low light levels [41]. Cones are much more concentrated in the central yellow spot known as the "macula." In the center of macula is the "fovea centralis," a 0.2 mm diameter rod-free area with very thin, densely packed cones. In addition, the fovea is the area of the eye responsible for sharpest vision.

The distribution of rods and cones in the retina is not uniform, as illustrated in Fig. 2-4 [42]. The density of cones falls rapidly to a constant level at about 10 to 15 degrees from the fovea. At about 15 to 20 degrees from the fovea, the density of the rods reaches a maximum. Because there is only one pigment type for rods, humans only see objects as shades of gray. In contrast, there are 3 types of cones which refer to as the short-wavelength (S-cone), middle-wavelength (M-cones) and long-wavelength (L-cones) sensitive cones (Fig. 2-5) [43]. This is why humans perceive vivid colors. While receiving light, the retina converts it into nerve signals, and then the nerve signals are sent through the optic nerve, at the back of the eye, to the brain. Hence, in the optical nerve region, there is no any receptor to sense light stimuli and is so-called "blind spot."
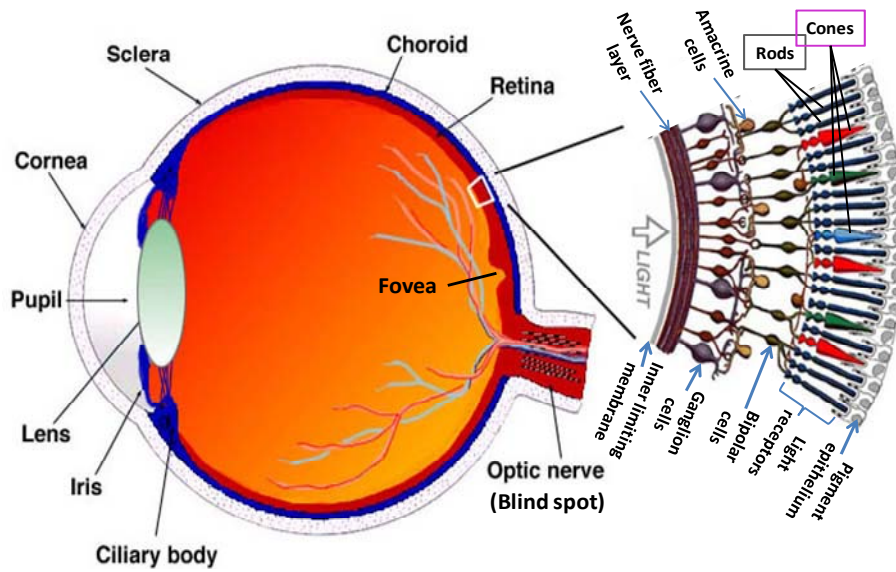
Fig. 2-3   A drawing of a cross section through the human eye with a schematic enlargement of the retina including rod and cone light receptors [40].
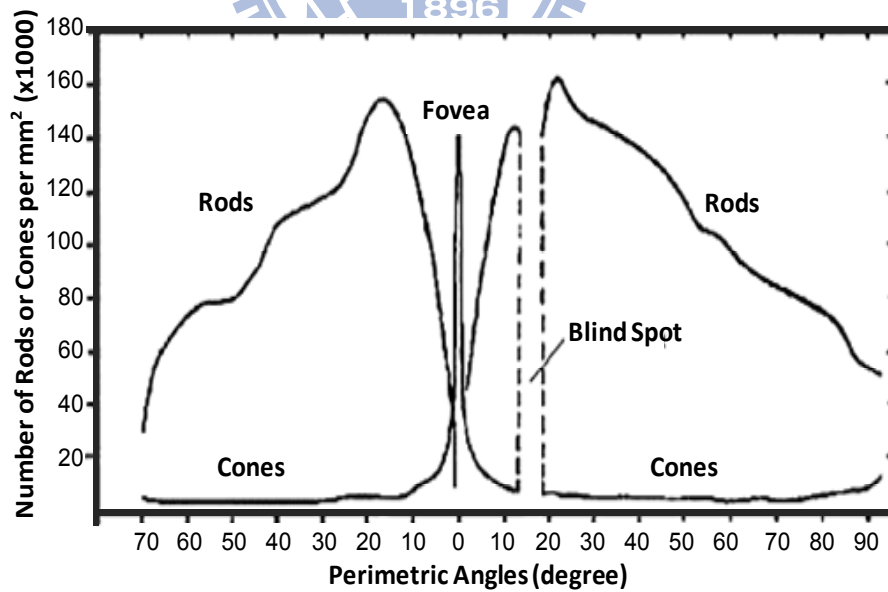
Fig. 2-4   Distribution of rods and cones in the retina [42].
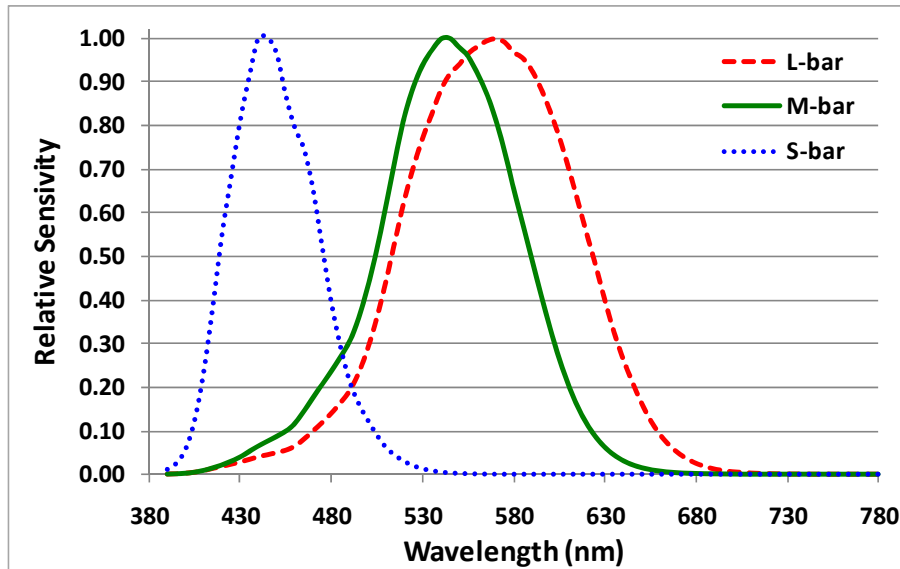
Fig. 2-5   Response sensitivity of three cone-types-- L-, M-, and S-cones [43].

2.3 Types of Eye Movements

Since only the fovea, which is around 10 degrees distribution of the retina (Fig. 2-4), is employed for distinct vision, the human eye perceives scenery by voluntarily or spontaneously moving. Most primates use two types of voluntary eye movement and fixation to track interesting objects: saccade and smooth pursuit.

2.3.1 Saccade and Fixation

Saccade is a rapid, random eye movement while perceiving static objects. The eye moves around the objects and locates interesting parts (fixation) to gather visual information. Saccade to an unexpected stimulus normally takes about 200 ms to initiate and lasts from about 20 to 200 ms, depending on amplitude. Fig. 2-6 is an example of saccadic movement. When a police wants to shoot terrorists in a shooting game, he has to move his eyes rapidly (saccade), gaze at objects (fixation) and then distinguish the terrorists from following officers. Generally, saccade is spontaneous when examining new targets, reaching a peak angular speed of 1000 degree/sec.
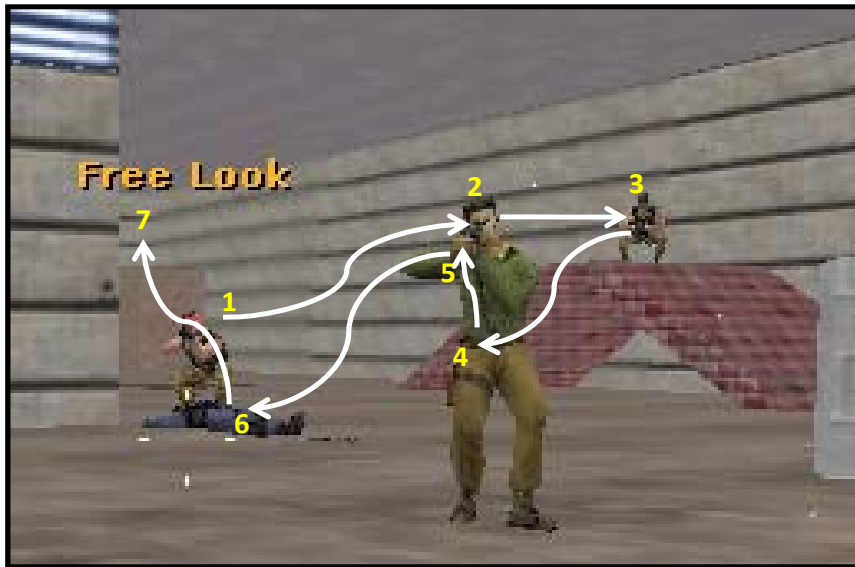
Fig. 2-6 An example of saccadic movement while playing a shooting game with tracing directions (white lines) and fixation points (yellow numbers). (Adopted from the on-line game of Counter Strike)
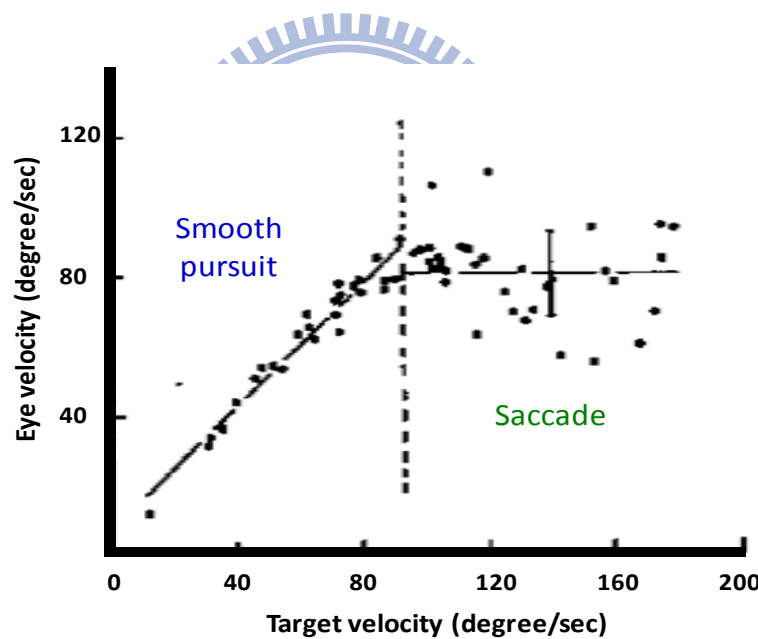
Fig. 2-7 Experiments of the human eye velocity in tracing a moving object [24].

2.3.2 Smooth Pursuit

Smooth pursuit is a predictable movement while following moving objects. When following a moving object, the human eye will trace at the same velocity as the object focusing on the fovea and catching clear images. Compared to saccade, pursuit velocity is

much slower, and research has proposed the velocity is about 90 degree/sec. If a target moves at a velocity faster than 90 degree/sec, the eye cannot pursue it, as shown in Fig. 2-7 [24].

Table 2-1   Two common types of eye movements for color breakup discussion.

Types of Eye Movements	Stimulus	Effect	Speed
Smooth Pursuit	Slowly moving objects	Track slowly moving objects	Slow, usually only up to 90 degree/sec
Saccade	Either peripherally detected motion or decision to change fixation	Examine new objects, visual search	Very fast, up to 1000 degree/sec

Eye movement is a natural response for human beings when perceiving the whole scenery (Table 2-1). Nevertheless, unconscious eye movement results in color breakup on FSC-related displays and prevents FSC-related applications.
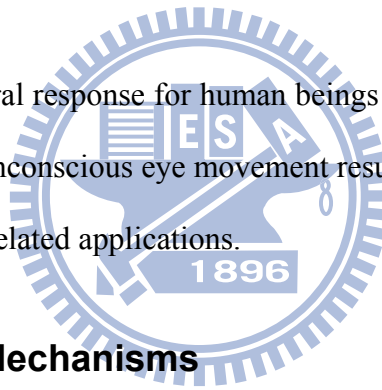
2.4 Color Breakup Mechanisms

The color breakup (CBU) phenomenon is perceived while the eye is moving. Therefore, CBU is strongly dependent on two main types of eye movements: saccade and smooth pursuit. Consequently, the CBU phenomenon is categorized into static CBU and dynamic CBU according to images and eye movements.

2.4.1 Static Color Breakup

Static CBU phenomenon happens when observing static images. While humans watch a static image, eyes will move around the image to gather details. During or after saccade, static CBU is perceived. The mechanism of static CBU is illustrated in Fig. 2-8 [25][26]. Fig. 2-8(a) shows three static white bars with a black background showing on an FSC-display. When perceiving the image, eyes sweep and gaze between white bars with

saccadic movement, like the white line in Fig. 2-8(a). In a conventional FSC-LCD using a RGB color sequence, the display shows red, green, and blue fields sequentially. When eyes move in saccade, the field images of different colors are projected onto the retina separately, and CBU is perceived, as illustrated in Fig. 2-8(b). The effective factors of static CBU are saccade velocity, image difference between objects and background, and display filed rate.

(a)   (b)
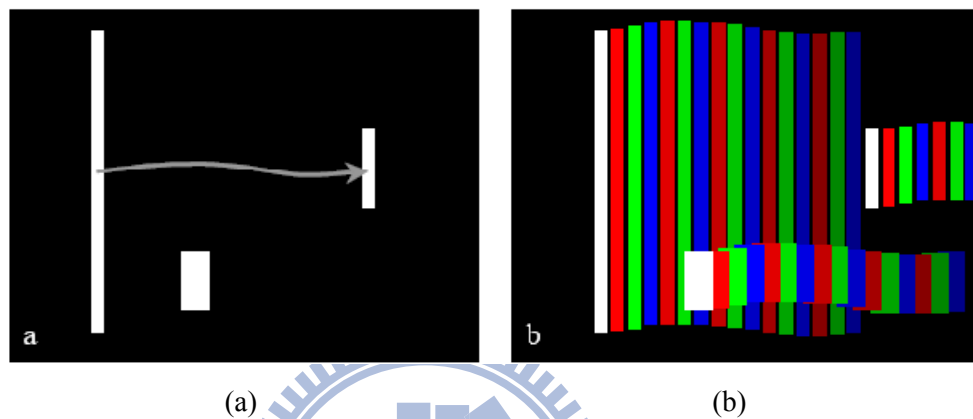
Fig. 2-8   Mechanism of the static CBU. (a) White bars on an FSC display and a saccade path and (b) observed color breakup during or just after saccade [25].

2.4.2 Dynamic Color Breakup

The other type of CBU, dynamic CBU, happens while perceiving dynamic images [27]. In order to focus on the fovea, human eyes will pursue the moving object at the same velocity (Fig. 2-9). When a white bar is moving from left to right on an FSC-LCD using a RGB color sequence, the observer perceives it through pursuit movement. Fig. 2-9(b) shows the spatial-temporal relation. The horizontal axis is the position of the FSC-LCD, the vertical axis is time, and the eye trace direction is indicated by oblique black lines. After eye integration, the three primary-colors are projected onto the retina separately and causes the colorful band appeared on the edge of the white bar. From the observing mechanisms of these two types of CBU, static CBU is more serious and troublesome than dynamic CBU because of faster eye velocity.
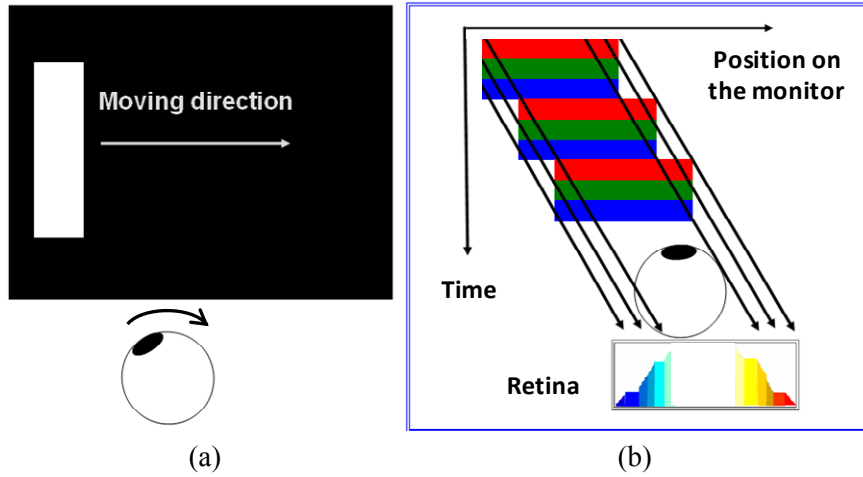
Fig. 2-9   Mechanism of the dynamic CBU. (a) Human eyes synchronized with the moving image and (b) the eye-trace integration on the retina. The extra color field will be observed at the bar edge.

2.5 Color Spaces and Color Differences

2.5.1 Color Matching Functions and Three Tristimulus

Color matching experiments was conducted in 1931 to describe the color that the human eye perceives, as illustrated in Fig. 2-10. Based on this study, a set of color matching functions (CMFs): $\bar{r}(\lambda)$, $\bar{g}(\lambda)$, and $\bar{b}(\lambda)$ was derived as shown in Fig. 2-11(a) [44]. To avoid the negative values appearing on the CMFs, the CMFs were transformed to $\bar{x}(\lambda)$, $\bar{y}(\lambda)$, and $\bar{z}(\lambda)$ using mathematics Fig. 2-11(b)). This is the well-know CIEXYZ color space established by the Commission Internationale de l'Éclairage (CIE) in 1931. Consequently, the color perceived can be quantified by the CIE as three tristimulus: *X, Y,* and *Z*. The color (*X, Y, Z*) is affected by three components: illuminant (*P*), a object's reflectance factor (*R*), and the CMFs of the human eye, ($\bar{x}(\lambda)$, $\bar{y}(\lambda)$, and $\bar{z}(\lambda)$), and is given in Eq. 2-2.

$$X = \int P(\lambda)R(\lambda)\bar{x}(\lambda)d\lambda$$
$$Y = \int P(\lambda)R(\lambda)\bar{y}(\lambda)d\lambda \qquad (2\text{-}2)$$
$$Z = \int P(\lambda)R(\lambda)\bar{z}(\lambda)d\lambda$$

| (a) Experimental setup | (b) Patterns on the screen |
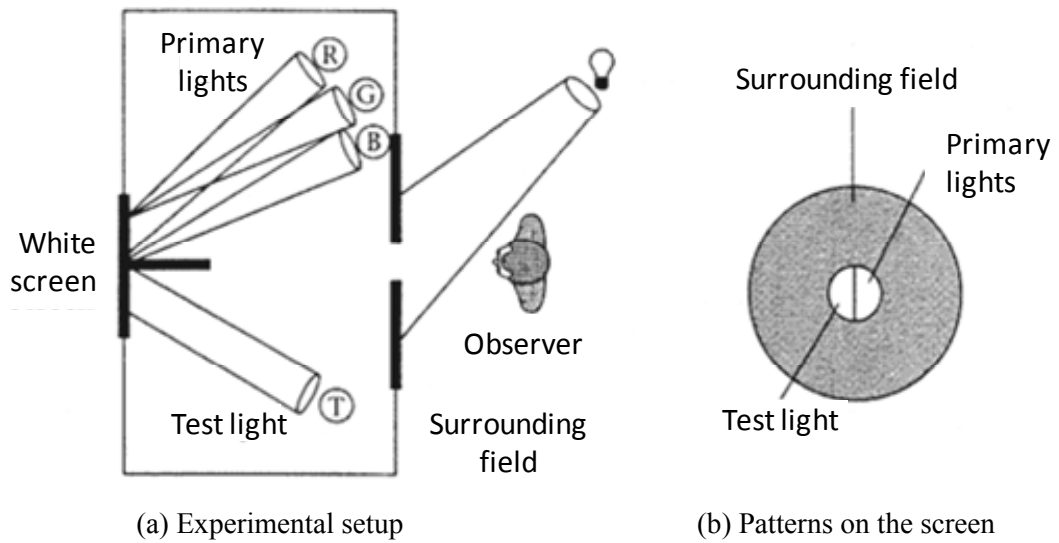
Fig. 2-10   Color matching experiment. (a) The observer sees a white screen divided into two halves, one half illuminated by a test light, the other half illuminated by a mixture of one or more primary lights (here three are shown). (b) The observer can adjust the intensity of the primary light(s) to try to make the two halves of the screen match [44].

| (a) | (b) |
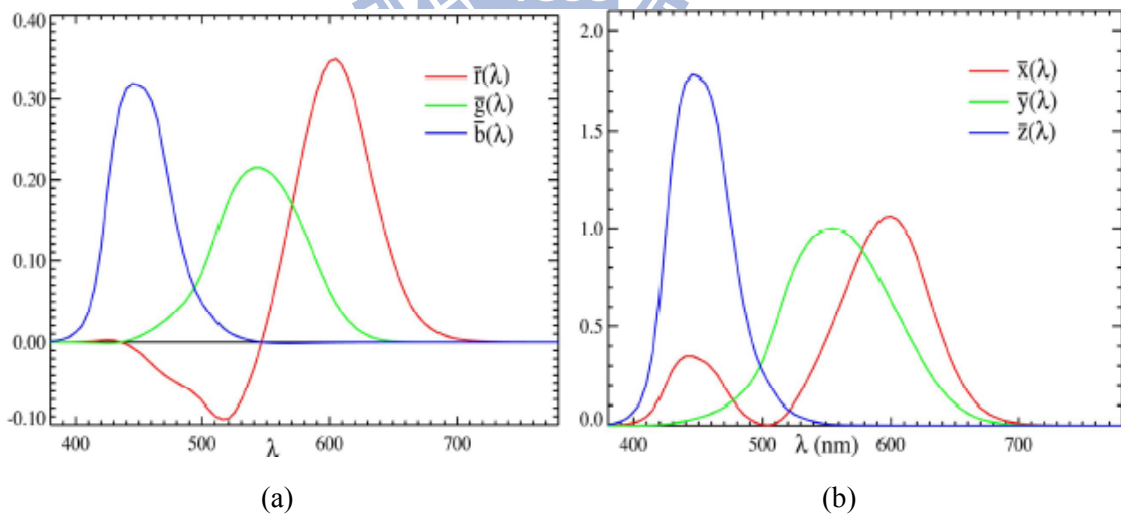
Fig. 2-11   Color matching functions from (a) human experiments and (b) transformation using mathematics [45].

2.5.2 CIELAB Color Space and Color Difference of ∆E*_ab

However, the CIEXYZ causes arguments since it is not uniform enough to describe the color difference, especially for green and blue colors [46][47]. Therefore, the CIE recommended two color-difference formulas for industrial applications, the CIELAB and CIELUV in 1976. The non-linear transformations from CIEXYZ to CIELAB are described in Eqs. 2-3~2-7. In these equations, X_n, Y_n, and Z_n are the tristimulus values of the reference white. L^* represents lightness, a^* approximate redness-greenness, and b^* approximate yellowness-blueness. A more uniform color difference formula of ΔE^*_{ab} is consequently given in Eq. 2-8. The CIELAB provided a uniform chromaticity diagram so that most of color-difference formulas were established based on the CIELAB color space, including CIE94 [47] and CIEDE2000 [48]-[50].

$$L^* = 116(Y/Y_n)^{1/3} - 16 \qquad \text{for } Y/Y_n > 0.008856$$
$$L^* = 903.3(Y/Y_n) \qquad \text{for } Y/Y_n \leq 0.008856 \tag{2-3}$$

$$a^* = 500 \, [f(X/X_n) - f(Y/Y_n)] \tag{2-4}$$

$$b^* = 200 \, [f(Y/Y_n) - f(Z/Z_n)] \tag{2-5}$$

$$C^*_{ab} = \sqrt{(a^*)^2 + (b^*)^2} \tag{2-6}$$

$$H^*_{ab} = \tan^{-1}(b^*/a^*) \tag{2-7}$$

where

$$f(Y/Y_n) = (Y/Y_n)^{1/3} \qquad \text{for } Y/Y_n > 0.008856$$
$$f(Y/Y_n) = 7.787(Y/Y_n) + \frac{16}{116} \qquad \text{for } Y/Y_n \leq 0.008856$$
$$f(X/X_n) \text{ and } f(Z/Z_n) \text{ are similar defined.}$$

$$\Delta E^*_{ab} = \sqrt{(\Delta L^*)^2 + (\Delta a^*)^2 + (\Delta b^*)^2} \tag{2-8}$$

2.5.3 Color Difference of CIEDE2000

In the past three decades, color scientists have found that the 1976 CIELAB is more uniform than the CIEXYZ color space. However, the CIELAB is unable to describe large color differences precisely, particular in the blue color region. Therefore, the CIE modified the formula to describe all color-difference ranges and proposed the CIEDE2000. In 2001, the CIEDE2000 formula was published and is expressed in Eq. 2-9 [48][49]. The methodology used for developing the formula from experimental color difference data was described by Luo, Cui, and Rigg [50]. The formula provides an improved procedure for the computation of industrial color differences. In Eq. 2-9, the parameters S_L, S_C, and S_H are the weighting functions for lightness, chroma, and hue differences, respectively (Eq. 2-10). k_L, k_C, and k_H values are the parametric factors adjusted according to different viewing parameters, for the lightness, chroma, and hue components, individually. R_T function is intended to improve the performance of the color-difference equation for describing chromatic differences in the blue region. The color difference of CIEDE2000 considers more color conditions. Therefore, this dissertation utilizes CIEDE2000 to evaluate the color difference between original images and simulated images which are processed by the proposed methods.

$$\Delta E_{00} = \sqrt{\left(\frac{\Delta L^*}{K_L S_L}\right)^2 + \left(\frac{\Delta C_{ab}^*}{K_C S_C}\right)^2 + \left(\frac{\Delta H_{ab}^*}{K_H S_H}\right)^2 + R_T\left(\frac{\Delta C_{ab}^*}{K_C S_C}\right)\left(\frac{\Delta H_{ab}^*}{K_H S_H}\right)} \qquad (2\text{-}9)$$

$$S_L = 1,\ S_C = 1 + 0.045 C_{ab}^*,\ and\ S_H = 1 + 0.015 C_{ab}^* \qquad (2\text{-}10)$$

where

ΔL^*, ΔC_{ab}^*, ΔH_{ab}^*: *Differences of luminance, chroma, and hue*
K_L, K_C, K_H: *Parametric factors of luminance, chroma, and hue*
S_L, S_C, S_H: *Weighting functions of luminance, chroma, and hue*
R_T: *Rotation function*

Chapter 3

DYNAMIC BACKLIGHT GAMMA ON HIGH DYNAMIC RANGE LCDS

A high dynamic range liquid crystal display (HDR-LCD) enhanced the image contrast ratio and lowered power consumption by utilizing local backlight dimming technology. This dissertation studied an HDR-LCD as a dual-panel display composed of a backlight module and a liquid crystal (LC) cell. In the first stage of backlight panel optimization, as an optimized gamma of LC signals to enhance the final image, the backlight module was similarly given with a dynamic gamma function to control the contrast ratio of an HDR image (Fig. 3-1). The inverse of a mapping function (IMF) method, proposed as a dynamic gamma mapping curve for the backlight module, has been demonstrated to further improve HDR image quality. By implementing the IMF method on a 37-inch HDR-LCD with 8×8 backlight divisions, the image contrast ratio was enhanced by ~20,000:1 while maintaining high brightness, clear image detail, and an average power reduction of 30% compared to a 37-inch LED LCD without using local backlight dimming technology.
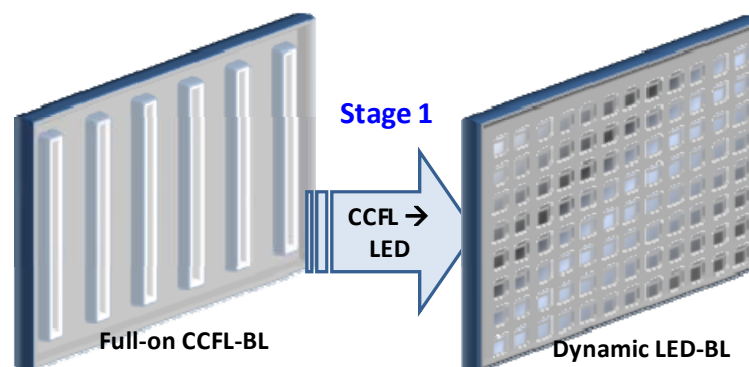
Fig. 3-1   The first stage of this dissertation. Using a dynamic LED-BL enhances image contrast and lowers power consumption.

3.1　Dual-Panel Display for HDR Images

To enhance HDR-LCD image quality, a dual-panel LCD was created from a backlight module and an LC panel (Fig. 3-2). The backlight module was a low resolution panel to control the image contrast ratio. The second panel, the LC cell, was a high resolution panel to maintain image details according to the backlight intensity distribution.

Low resolution　　　　　　　　　　　　　　　　　　　　　**High resolution**

(a) Backlight image　　　　(b) HDR-LCD structure　　　　(c) LC panel
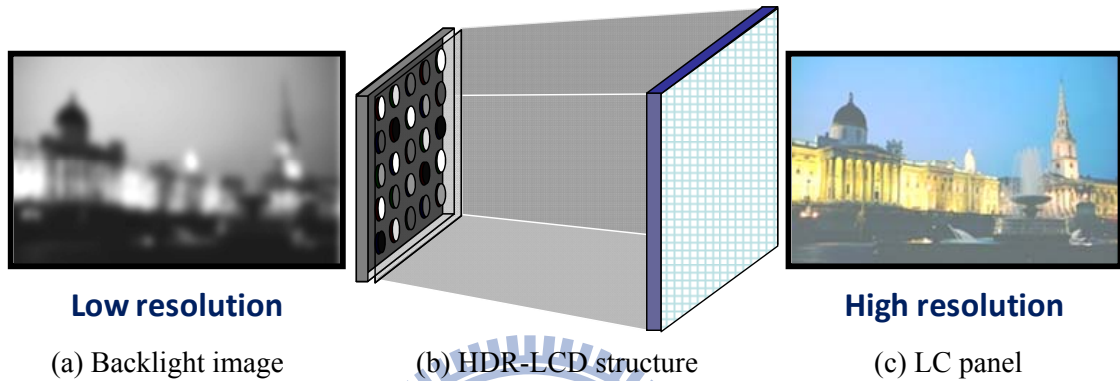
Fig. 3-2　Schema of a dual-panel display with a low resolution backlight and a high resolution LC panel.

In HDR-LCDs, two conventional methods, "Average" and "Square-Root," were used to determine backlight signals [9][10]. The Average method averaged the gray levels of all sub-pixel values in each backlight division. The mapping function of original and modified backlight levels is an oblique line with a slope of one (Fig. 3-3). On the other hand, the Square-Root method calculated the average value in each backlight division first, and then took its square root after normalizing the average value. Thus, the Square-Root method enhanced the backlight signal and maintained final image brightness.

For practical applications, the number of backlight divisions in the HDR-LCD was reduced to lower IC driver usage and simplify hardware computation complexity. However, due to the decrease of backlight resolution, many image details were lost through applying the Average method because of low backlight brightness. Using the Square-Root method, image

details were much clearer than that of the Average method, but the contrast ratio (CR) decreased substantially because of "over-enhancement" in darker backlight zones. Additionally, both of these methods used fixed backlight mapping curves (Fig. 3-3) that might be not suitable for diverse types of images, such as high and low CR images.

Consequently, we proposed an efficient method, the inverse of a mapping function (IMF), to control backlight signals. The IMF method was decided by inverting the mapping function of each image; in other words, the IMF method provided the backlight signal with a dynamic gamma to optimize the backlight "image." Thus IMF maintained not only a high contrast ratio but also maximum luminance and clear image detail. Additionally, power consumption and image distortion were also reduced.
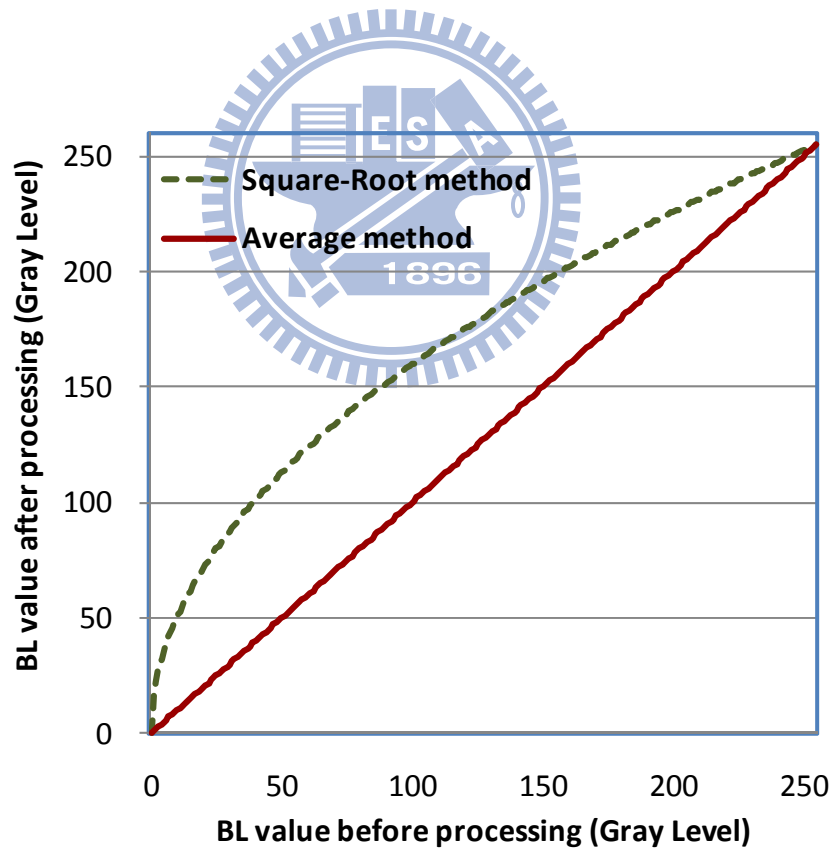
Fig. 3-3 The mapping functions of two conventional backlight determination methods, the Average and Square-Root methods [9][10].

3.1.1 Backlight Determination-- Inverse of a Mapping Function Method

Several mapping methods have been proposed to successfully enhance image performance [51]-[55]. In this dissertation, histogram equalization [51] was utilized as the mapping function. The basic procedure of the IMF method was first to compute the global histogram of a target image to get a probability density function (PDF). Then the PDF from the lowest to the highest gray level was accumulated to obtain the mapping function (also called the cumulative distribution function, CDF) of the traditional histogram equalization. Finally, inverting the CDF of a target image with the oblique line y=x generated a new curve for backlight modulation called the "Inverse of a Mapping Function (IMF) [31][32]."

Before IMF processing, a zone-value of each backlight division was first decided. To optimize the image quality and power consumption, a weighting, n ($0 \leq n \leq 1$), was taken for the average (Avg) and maximum (Max) values in each backlight division. The zone-value is given in Eq. 3-1. In this work, n=0.9 was the optimized weighting for the IMF method.

$$Zone-Value = n \times Max. + (1-n) \times Avg. \tag{3-1}$$

A significant feature of the IMF method was the optimization of backlight signals based on each input image, i.e. backlight signals with a dynamic gamma were controlled frame by frame to produce high quality images in high and low CR images. For example, in a high CR image (Fig. 3-4(a)), the CDF curve has steep slopes in high and low gray-level areas; in contrast, the IMF curve has gentle slopes in these two areas. Therefore, backlight signals for dark regions distributed to the lower IMF area, and backlight signals for bright regions distributed to the higher IMF area. Hence, the backlight panel showed a high CR image using the IMF method. Additionally, IMF also maintained the brightness of the target image showing less distortion image details. Fig. 3-5 shows a high CR target image_ *Lily,* and its backlight image obtained using the IMF method.

Excluding high CR images, Figs. 3-4(b)-(d) show the CDF and IMF curves of low CR images, i.e. dark, bright, and medium gray-level images. Most backlight signals were distributed to a particular area with uniform values, thus eliminating the visible boundaries of each LED backlight block. For example, most backlight signals of the bright image, *Yushan* (Fig. 3-6), distributed to the higher IMF area (with gray levels between 220 and 250). Likewise, dark and medium gray-level images were also modulated with a uniform brightness distribution. So the LC signals were easily compensated and produced a high-quality image.

(a) High CR image   (b) Dark image   (c) Bright image   (d) Medium GL image
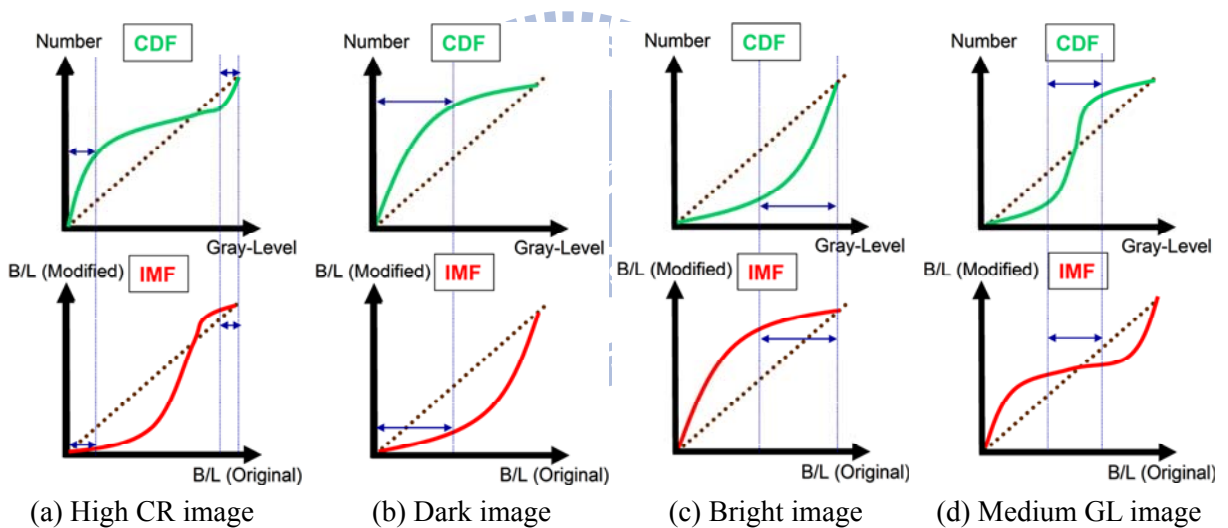
Fig. 3-4   The cumulative distribution function (CDF) and inverse of a mapping function (IMF) curves of backlight signals for (a) high CR, (b) dark, (c) bright, and (d) medium gray-level images.
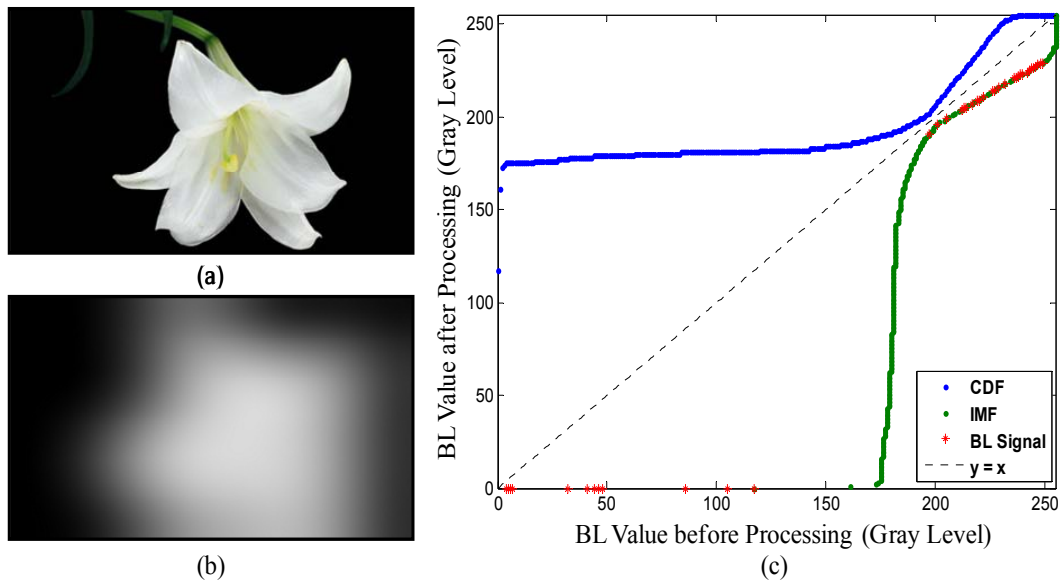
Fig. 3-5   An example of using the IMF method. (a) High CR target image – Lily, (b) BL image of Lily, and (c) the mapping curves of CDF and IMF.
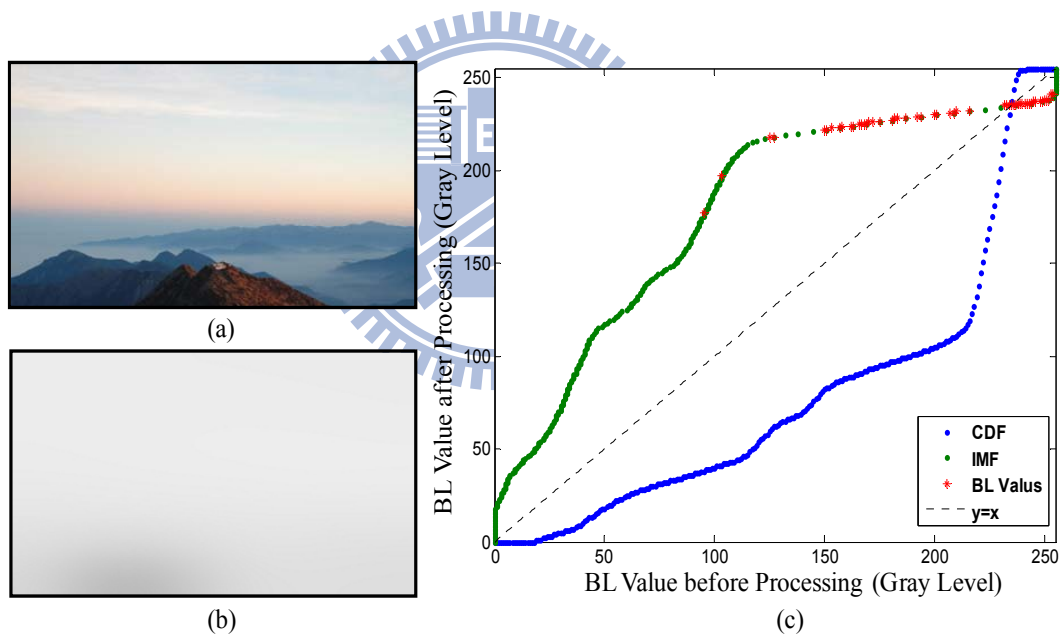
Fig. 3-6   An example of using the IMF method. (a) Low CR target image (bright image) – Yushan, (b) BL image of Yushan, and (c) the mapping curves of CDF and IMF.

3.1.2 LC Signal Compensation

After determining backlight signals, the backlight image was obtained through convolving the backlight signals with a point spread function (PSF) which represents the spatial intensity distribution of each backlight division (Fig. 3-7) [56][57]. The backlight

images using the Average, Square-Root, and IMF methods are shown in Figs. 3-8(b)-(d). These convolution results (BL_{HDR}) were ideally simulated for distribution of backlight illumination. Based on brightness preservation, the compensation signals of liquid crystal (GL_{HDR}) were obtained through Eq. 3-2 [22].

$$GL_{HDR} = (\frac{BL_{full}}{BL_{HDR}})^{1/\gamma} \times GL_{Target}$$

(3-2)

where BL_{full} and BL_{HDR} denote intensities of the conventional (full-on) backlight and the HDR backlight, respectively and GL_{Target} denotes the original signals of the target image. Finally, an HDR image was created through combining the backlight convolution result and LC compensation signals considering the gamma effect. However, if gray levels of LC compensation signals, GL_{HDR}, exceed 255, the HDR system cannot show the signal correctly, thus the "clipping effect" is observed [22]. The clipping effect reduces image luminance and details degrading image quality.

(a) BL signal   (b) LSF   (c) BL image
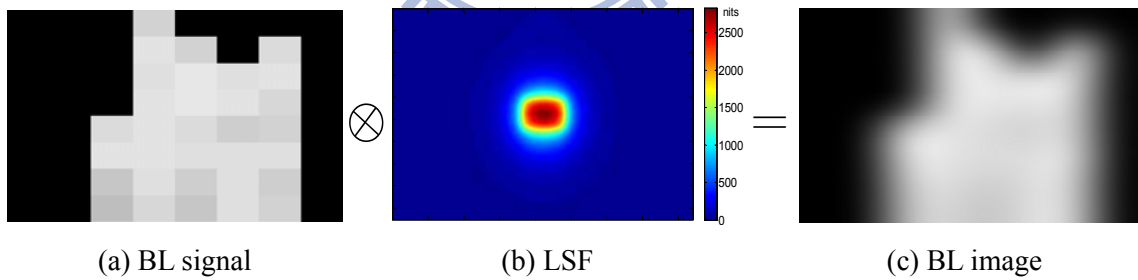
Fig. 3-7   *The processing of convolution. (a) BL signal, (b) light spread function, and (c) BL image.*

(a) Target image   (b) Average method   (c) Square-Root method   (d) IMF method
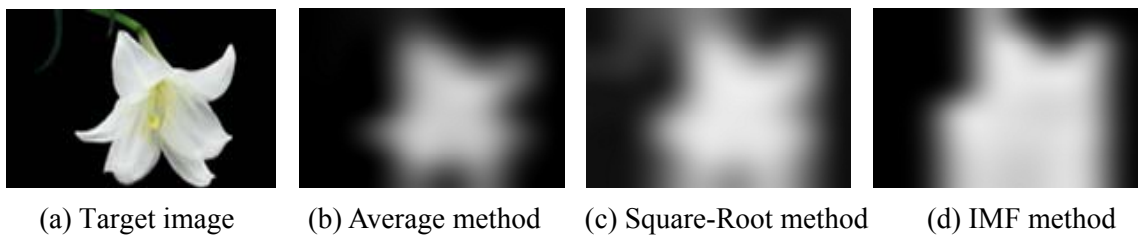
Fig. 3-8   *(a) Target image; Convolution results of backlight signal determined by the (b) Average, (c) Square-Root, and (d) IMF methods.*

3.2 Verification on a 37-inch HDR-LCD

3.2.1 Target Images and Hardware

The main objectives of an HDR system are to achieve a high contrast ratio (CR) image to match the human vision range in the real world (high dynamic range) [22] while simultaneously reducing power consumption. A high CR target image, *Lily*, and three low CR images, *Robot* (dark image), *Shore* (medium GL image), *and Yushan* (bright image) shown in Fig. 3-9 were simulated and then implemented on a 37" 1920×1080 resolution HDR-LCD with 8×8 backlight divisions (the panel was provided by AU Optronics, Taiwan). The CR was measured using a luminance analyzer, CA-210 [58], with a measuring area of 27 mm in diameter (covering about 12,834 pixels); the positions of maximum luminance (L_{max}) and minimum luminance (L_{min}) are respectively marked with a solid-blue circle and a dotted-pink circle in Fig. 3-9. Areas within the red rectangle parts in Figs. 3-9(a)(b) are magnified for image detail comparison and shown in Figs. 3-10 and 3-11.

(a) Lily (high CR image)   (b) Robot (dark image)

(c) Shore (medium GL image)   (d) Yushan (bright image)
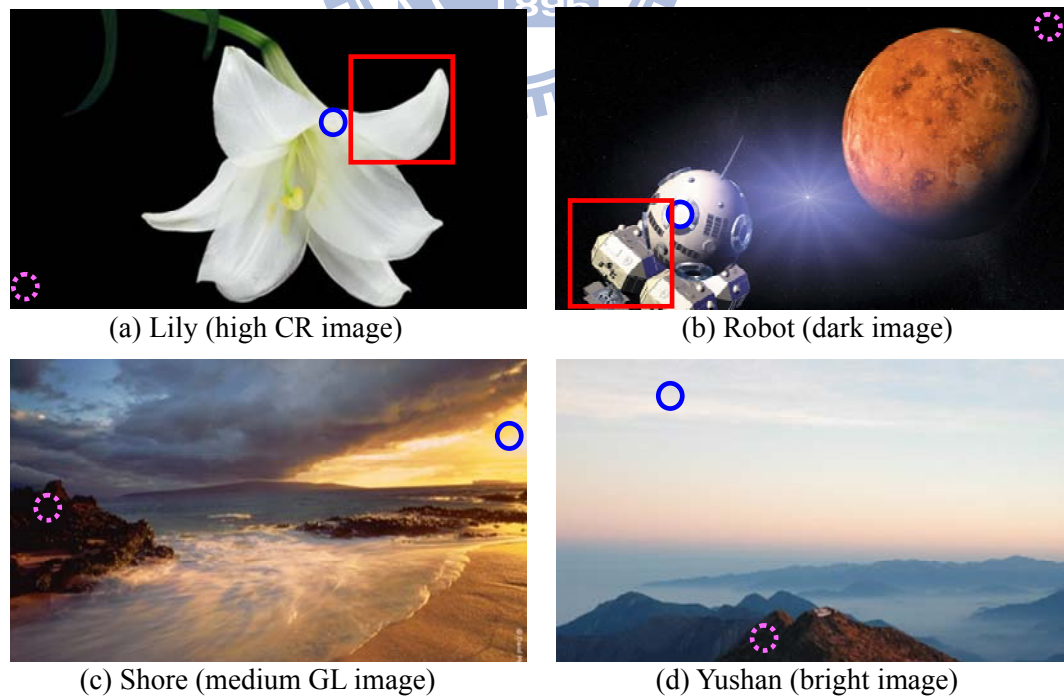
Fig. 3-9   Target images with their CR measuring points; L_{max} and L_{min} are respectively marked with a solid-blue circle and a dotted-pink circle. Areas within the red rectangles in Figs. (a) and (b) are magnified, shown in Figs. 3-10 and 3-11.

(a) Average method   (b) Square-Root method   (c) IMF method   (d) Target image
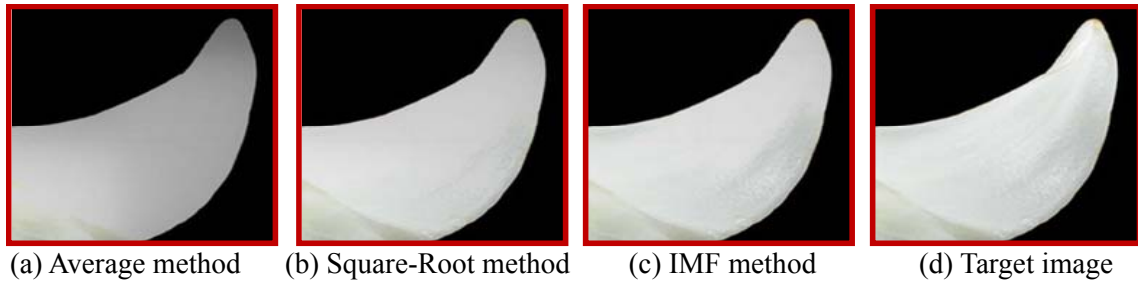
Fig. 3-10   The results of the magnified section in the test image- Lily. (a), (b), and (c) are produced using the Average, Square-Root, and IMF methods, respectively. (d) The target image.

(a) Average method   (b) Square-Root method   (c) IMF method   (d) Target image
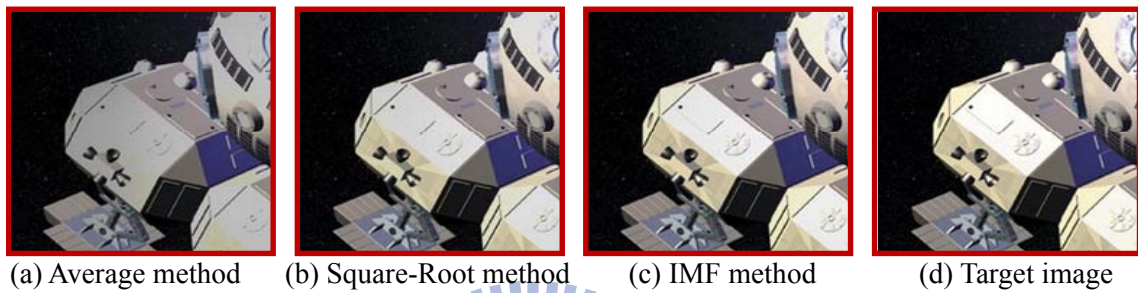
Fig. 3-11   The results of the magnified section in the test image- Robot. (a), (b), and (c) are produced using the Average, Square-Root, and IMF methods, respectively. (d) The target image.

3.2.2 Target Parameters

In the first stage of backlight module optimization, based on the dual-panel display concept, the target contrast ratio of high CR images must be enhanced more than 20,000:1 with a 30% average power reduction compared to an LED backlight LCD. Additionally, using the LC panel control, the maximum luminance (L_{max}) must be maintained to close to that of the target image with low distortion of less than 5%.

A distortion ratio, D, quantifying the clipping distortion of final HDR images is given in Eq. (3-3)

$$D \equiv \frac{N_c}{N_t} \times 100\% \tag{3-3}$$

where N_c and N_t are the total number of clipped sub-pixels and the total number of sub-pixels (1920×1080×3) in an HDR image. The D value denotes the distortion severity

due to the limited LC's maximum transmittance (100%). An HDR image with a smaller D value implies the HDR system produces a more detailed image and gets a higher quality image. Therefore, four parameters: contrast ratio (CR), power consumption (P), maximum luminance (L_{max}), and distortion value (D) were utilized to evaluate and optimize HDR-LCDs.

3.2.3 Results and Discussions

The experimental results of the four target images, *Lily*, *Robot*, *Shore*, and *Yushan*, are listed in Table 3-1, Figs. 3-12 and 3-13. For the high CR image, *Lily*, the D values were 16.97%, 5.70%, and 3.17% using the Average, Square-Root, and IMF methods, respectively. From D values and the partly magnified image sections shown in Fig. 3-10, image details in the high brightness region almost disappeared while using the Average and Square-Root methods. Conversely, image details were well preserved in the IMF method with a distortion of 3.17% (Fig. 3-10(c)). Although the Average method had the highest CR of 32,150:1, the distortion of 16.97% was the largest (Fig. 3-10(a)) and the brightness (321.5 nits) was much lower than that of the conventional full-on backlight (401.4 nits). Comparing L_{max} and CR values of the IMF and Square-Root methods, L_{max} values were close to the conventional full-on backlight, and the CR of the IMF method (19,695:1) was much higher than that of the Square-Root method (9,855:1) in this high CR image.

For the low CR image, *Robot*, the IMF method also preserved most image details with 2.45% of D value (shown in Fig. 3-11 and Table 3-1), and consumed less power than the Square-Root method. The 4,278:1 of the CR value was also higher than that of the Square-Root method (2,557:1). For the other two low CR images, *Shore* and *Yushan*, the IMF method also maintained good image details with high maximum brightness.

From experimental results, the Average method achieved the lowest power consumption and the highest image contrast ratio. However, it sacrificed image luminance and too many

details. The Square-Root method reduced power consumption and maintained the image maximum brightness. Nevertheless, the image contrast enhancement was limited because backlight signals were over enhanced in dark regions. In contrast, the IMF method efficiently lowered power consumption while simultaneously enhancing the image contrast ratio and maintaining image quality because of its dynamic backlight gamma.

Table 3-1   The distortion ratio (D), luminance (L_{max} and L_{min}), contrast ratio (CR), and power consumption (P) of Lily, Robot, Shore, and Yushan using the conventional method (full-on) and three different backlight determination methods.

B/L / Image	Full-on				Average				Square-Root				IMF			
	D(%)	L_{max} (nits) / L_{min} (nits)	CR	P (W)	D(%)	L_{max} (nits) / L_{min} (nits)	CR	P (W)	D(%)	L_{max} (nits) / L_{min} (nits)	CR	P (W)	D(%)	L_{max} (nits) / L_{min} (nits)	CR	P (W)
Lily	0	401.4 / 0.30	1338	190	16.97	321.5 / 0.01	32150	60	5.70	394.2 / 0.04	9855	94	3.17	393.9 / 0.02	19695	93
Robot	0	480.1 / 0.34	1412	190	6.54	278.4 / 0.04	6960	68	3.78	383.6 / 0.15	2557	124	2.45	385.0 / 0.09	4278	120
Shore	0	326.4 / 0.67	487	190	5.16	335.9 / 0.34	988	112	3.08	335.5 / 0.46	729	143	3.18	343.2 / 0.47	730	133
Yushan	0	412.1 / 1.36	303	190	4.14	435.2 / 1.63	267	149	0.31	444.0 / 1.43	310	176	1.91	446.2 / 1.45	308	176

(a) Conventional LCD BL (Full-on)   (b) IMF method

(c) Square root method   (d) Average method

Fig. 3-12   Lateral pictures of a 37 inch HDR-LCD while using the (a) the full-on backlight, (b) IMF, (c) Square-Root, and (d) Average methods. (The panel was provided by AU Optronics, Taiwan)

(a) D-value   (b) CR

(c) L$_{max}$ (nits)   (d) Power (Watt)
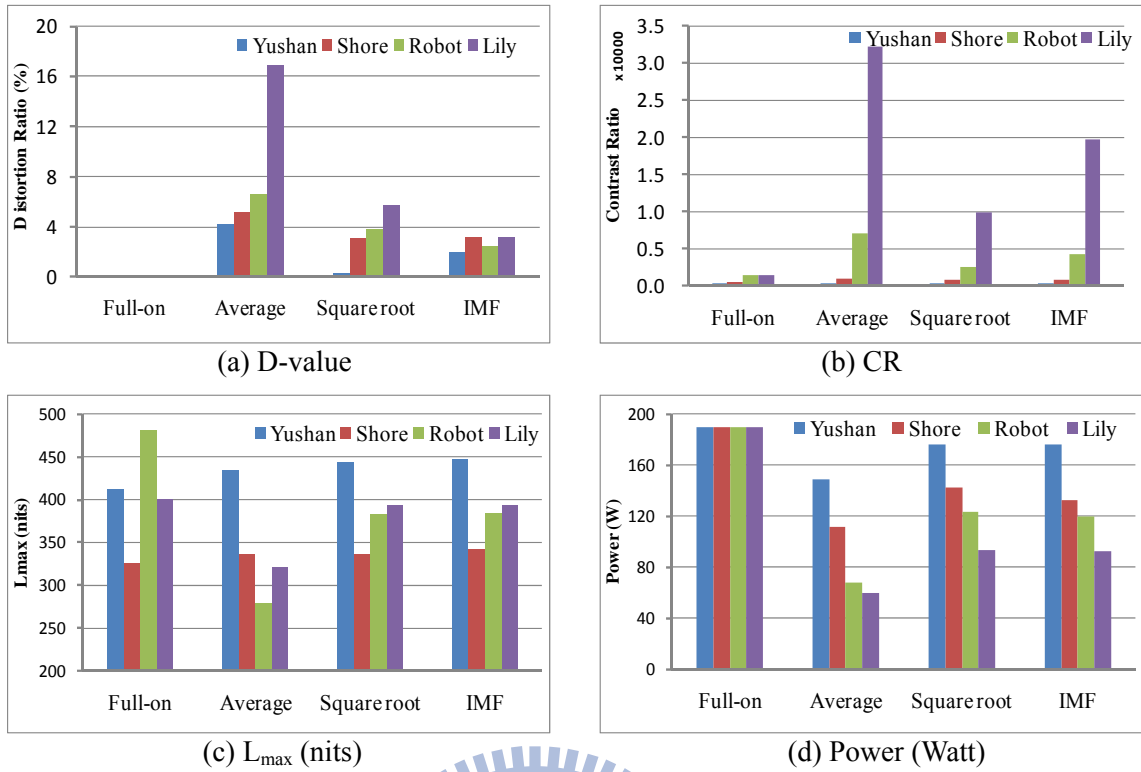
Fig. 3-13 Image characteristics of different images using different methods. (a) Distortion ratio, (b) contrast ratio, (c) maximum luminance, and (d) power consumption.
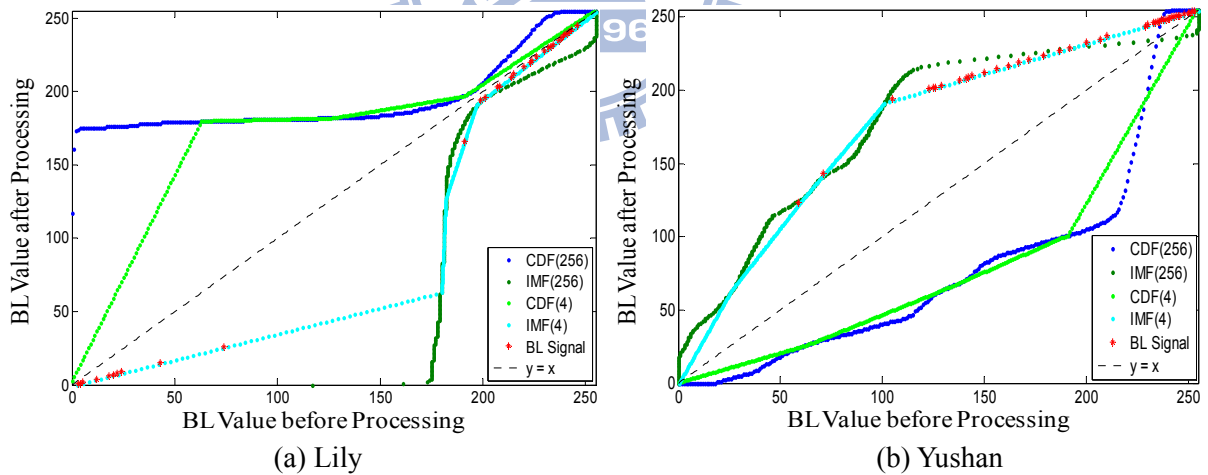
(a) Lily   (b) Yushan

Fig. 3-14 Comparisons of mapping curves using 256 and 4 registers in computing histogram. (a) Lily and (b) Yushan.

Considering computational complexity of the IMF method, a mapping function for image enhancement in each LC panel was provided in conventional LCDs. Therefore, inversing this mapping function was the only step to get an IMF curve. On the other hand,

the histogram equalization method was chosen as our mapping function. To further reduce computational complexity, the registers in the computing histogram were reduced from 256 to 4 units. The simulation results shown in Fig. 3-14 indicate that a 4-register can also reach similar results to a 256-register. Therefore, the IMF method can be easily implemented.

3.3 Summary

The HDR-LCD was studied as a dual-panel display composed of a backlight module and an LC cell. The backlight module was a low resolution panel which controlled the HDR image contrast ratio, and the LC cell was a high resolution panel which preserved image details. In the first stage of this dissertation, we proposed the Inverse of a Mapping Function (IMF) method to determine backlight signals for high dynamic range (HDR) displays based on this dual-panel concept. The extraordinary feature of IMF was to provide an optimized dynamic gamma for a backlight panel to produce high quality images, including high/low contrast images. The IMF method was demonstrated on a commercial 37" HDR-LCD to achieve a high contrast ratio (~20,000:1) image, and to preserve clearer image details with low distortion (D=3.17%). Furthermore, the IMF method still maintained high brightness and showed a more active image using an average power reduction of 30% compared to the same size LED backlight LCD.

Although reducing average power consumption by 30% is significant, the LCD still requires 130 Watts which is equivalent to that of a conventional 37-inch CCFL backlight LCD. In the next chapter, the power consumption is further reduced using field-sequential color technology. To increase manufacturing feasibility and suppress color breakup, the Stencil Field-Sequential-Color (Stencil-FSC) method is proposed and expressed in the following chapters.

Chapter 4

CBU Suppression and Low Power Consumption by Stencil-FSC Method

Field-sequential color (FSC) is a potential technique for future green liquid crystal displays (LCDs). The second stage of this dissertation was to remove color filters to further reduce power consumption and larger the display color gamut. However, a lethal issue, color breakup (CBU), was perceived when relative velocities exist between the screen image and the human eye. We proposed the Stencil Field-Sequential-Color (Stencil-FSC) method with a 240Hz field rate to make CBU imperceptible. Given the Stencil-FSC method, the hardware parameters were optimized to reduce hardware complexity while maintaining sufficient CBU suppression. After implementing Stencil-FSC on a 32-inch FSC-LCD, the image contrast ratio was shown to be 10 times more than that of a conventional CCFL LCD, and the average power consumption was reduced to less than 35 Watts-- a 68% savings in power consumption.
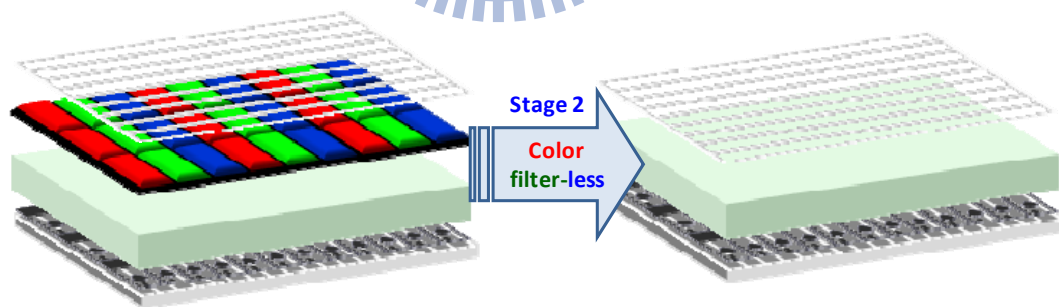
Fig. 4-1   The second stage of this dissertation. Removing color filters lowers power consumption.

4.1 Prior Color Breakup Suppressions for FSC-LCDs

Color breakup (CBU) suppression has been implemented on digital light processing (DLP) projectors by inserting additional mono-color fields [59] or increasing the field rate to 540Hz or more [60]. Hence, most traditional CBU solutions for FSC-LCDs involved either

increasing the field rate (Fig. 4-2(a)) or inserting additional mono-color fields (RGBY or RGBCY) (Fig. 4-2(b)). The black-fields insertion method (360Hz-RGBKKK) was reported to further narrow the CBU width to be less perceptible [61]-[65], as illustrated in Fig. 4-2(c). Among these three methods, 360Hz-RGBKKK was concluded as the best CBU suppression method. Although LED backlights can be switched on and off very rapidly, LC response time prevents the implementation of many of the above methods (e.g. field rate > 300Hz) in large-sized FSC-LCDs. Consequently, we proposed Stencil-FSC method using a 240Hz field rate to suppress the CBU issue [33]-[35].

(a) Double field rate (360Hz-RGBRGB)

(b) Mono-color field insertion (300Hz-RGBCY)

(c) Black-fields insertion (360Hz-RGBKKK)
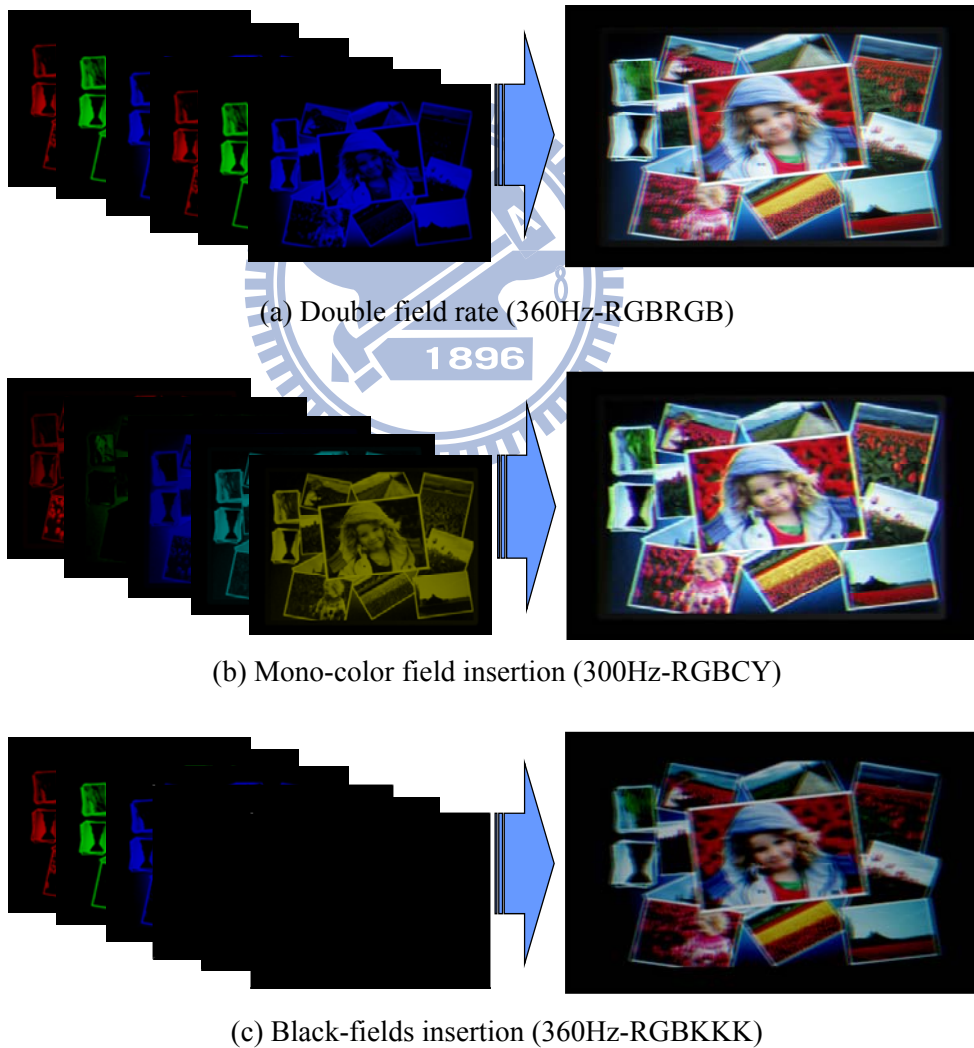
Fig. 4-2 Prior color breakup suppression methods. (a) Double field rate, (b) mono-color field insertion, and (c) Black-fields insertion.

4.2 Stencil Field-Sequential-Color Method

4.2.1 Concept

CBU is perceived because three high luminance primary-color images are not projected onto the retina at the same position. When R, G, and B image intensities are reduced, the CBU phenomenon caused by smooth pursuit (in dynamic videos) or saccadic movement (in static pictures) is noticeably suppressed even though the three images are not overlapped well onto the retina. Therefore, using this concept, instead of "mono-color" images, a "multi-color" image was used in the first field to display high luminance and rough color; the residual three dimmer primary-color fields were then used to only modify color details (Fig. 4-3). Displaying these four field-images at 240Hz, a vivid color image with less perceptible CBU was created on an FSC-LCD. Using a "multi-color" image in a color filter-less LCD to suppress CBU is unprecedented in FSC-related technologies. This idea came from the recreation of "Stencil," like a kid who painted an undertone on his "Peter Pan" first, and then painted other colors over it to complete a vivid, colorful Peter Pan (Fig. 4-3(bottom)). Therefore, we named the method Stencil Field-Sequential-Color or Stencil-FSC because its process was similar to "stencil" painting.
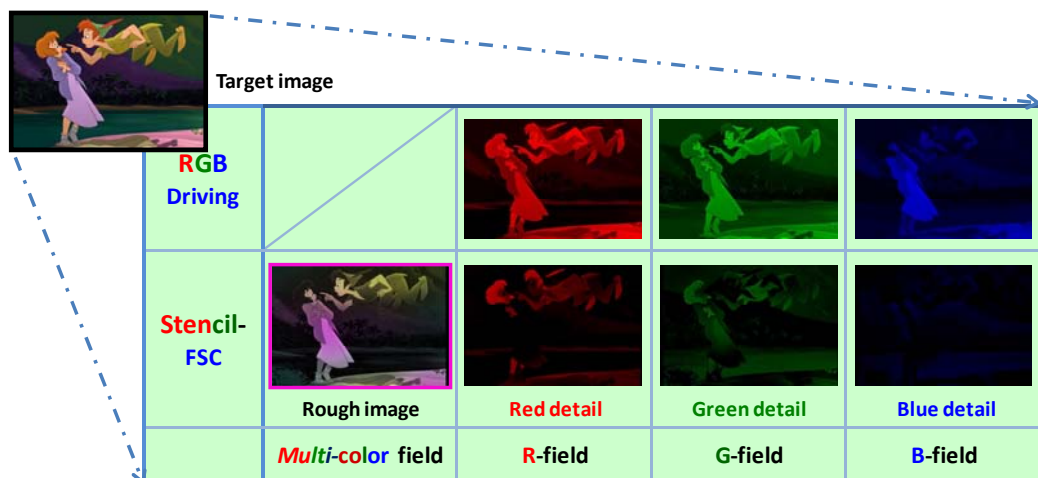
Fig. 4-3   Target image_ Peter Pan (©Disney) and field images using the conventional FSC-LCD and Stencil-FSC method.

Local color-backlight dimming technology [9]-[15] was utilized to produce a multi-color image on a color filter-less FSC-LCD, as illustrated in Fig. 4-4. An LC-TV with a local backlight control comprised the superposition of two displays with different spatial resolutions: a low resolution controllable RGB-LED backlight and a high resolution LC panel. The backlight module provided a low resolution colorful image, and the color filter-less LC cell preserved high resolution monochrome image details. In applying the Stencil-FSC method to suppress CBU, there were two main features that necessitated local color-backlight diming technology: high image contrast ratio and low power consumption when compared to conventional LCDs and traditional FSC-LCDs.
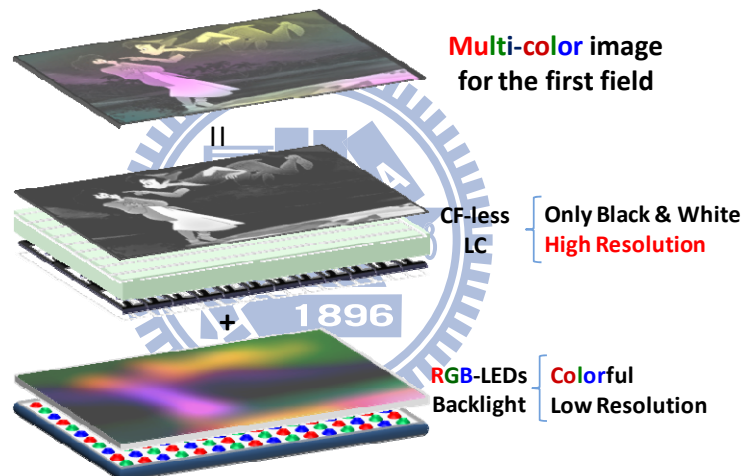
Fig. 4-4   A "multi-color" image is yielded by a low resolution controllable RGB-LED backlight and a high resolution color filter-less LC cell.

The Stencil-FSC algorithm is derived and illustrated in Fig. 4-5. Using local color-backlight dimming technology, a set of three primary-color backlight signals was obtained using a color-backlight determination method (BL_R, BL_G, and BL_B) [34]. Accordingly, the corresponding LC compensation transmittances were determined (T_R, T_G, and T_B). In this dissertation, the image was evenly divided into non-overlapping rectangles corresponding to the number of backlight divisions. To reduce more power consumption, the Average method was utilized for determining three primary-color backlight signals. We

directly averaged the all three primary-color pixel values that subtended the rectangular region in front of each given backlight division independently as color-backlight signals (BL_R^o, BL_G^o, BL_B^o). The detailed local color-backlight dimming algorithm is illustrated in Fig. 4-6 and explained in section 4.2.2.
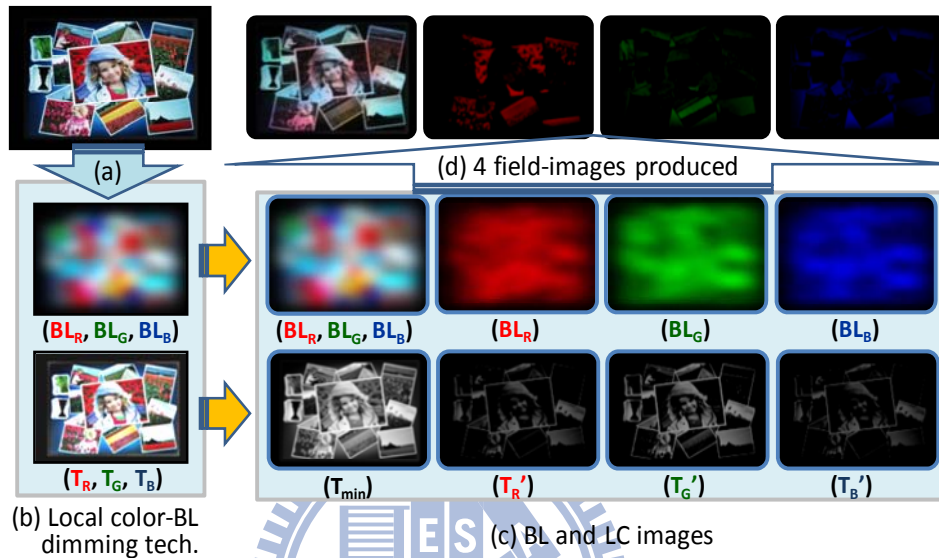
Fig. 4-5   Stencil-FSC algorithm processing. (a) Input image_ Girl (b) local color-backlight dimming technology, (c) backlight and LC images, and (d) 4 field-images produced. (Girl ©Microsoft, http://www.microsoft.com/surface/index.html)
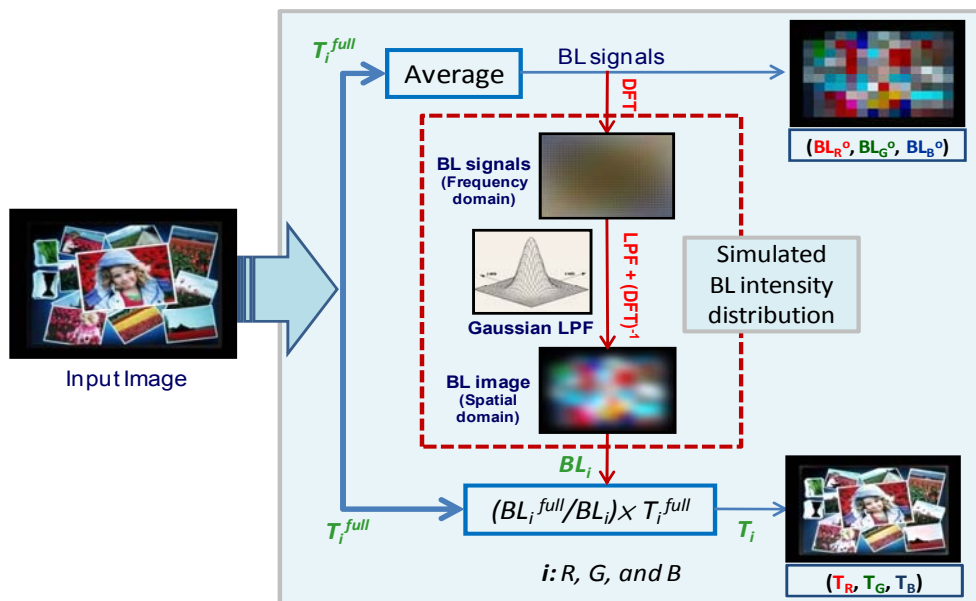
Fig. 4-6   Processing of local color-backlight dimming algorithm.

4.2.2 Backlight Intensity Distribution

After determining color-backlight signals, the crosstalk between LED backlight divisions was considered when compensating LC signals [56][57][59][67]. Convolving the backlight signal with the point spread function (PSF) of each backlight division is a traditional method for obtaining backlight intensity distribution. A broader PSF results in visible crosstalk and produces a blurrier backlight image. When convolution is used, computational complexity makes real-time demonstrations prohibitively difficult. To reduce computational complexity, we utilized the Discrete Fourier Transformation (DFT) and a Gaussian low pass filter (GLPF) to simulate three primary color-backlight intensity distributions (BL_R, BL_G, and BL_B), as illustrated in Fig. 4-6. First, the color-backlight signals of each backlight division were determined (BL_R^o, BL_G^o, and BL_B^o). Second, the DFT process transferred the backlight signals from the spatial domain to the frequency domain. When utilizing a GLPF, the high frequency information (the boundary area) was filtered out. Finally, a light spread backlight image was simulated by using the inverse of the DFT process (BL_R, BL_G, and BL_B). Let $G(u,v)$ denote the Gaussian filter in the frequency domain, and its function is given in Eq. 4-1

$$G(u,v) = e^{-D^2(u,v)/2D_0^2} \tag{4-1}$$

where $D(u,v)$ is the distance from the Fourier transform origin and D_o is the cutoff frequency. The (u,v) represents the position in the frequency domain [68]. Moreover, D_o is directly related to backlight spread. For example, a smaller D_o value allows lower frequency content and results in a blurrier backlight image, as illustrated in Fig. 4-7. Therefore, we can simulate the backlight intensity distribution in arbitrary PSFs by controlling D_o. To suggest hardware design of backlight systems, the cutoff frequencies were finally transferred back to spatial domain and described by Eq. 4-2, where σ_x and σ_y are two directional standard deviations (S.D.) of the Gaussian distribution.

$$g(x,y) = e^{-\left(\frac{x^2}{2\sigma_x^2} + \frac{y^2}{2\sigma_y^2}\right)}$$

(4-2)

| D_o =0.015 | D_o =0.009 | D_o =0.003 |
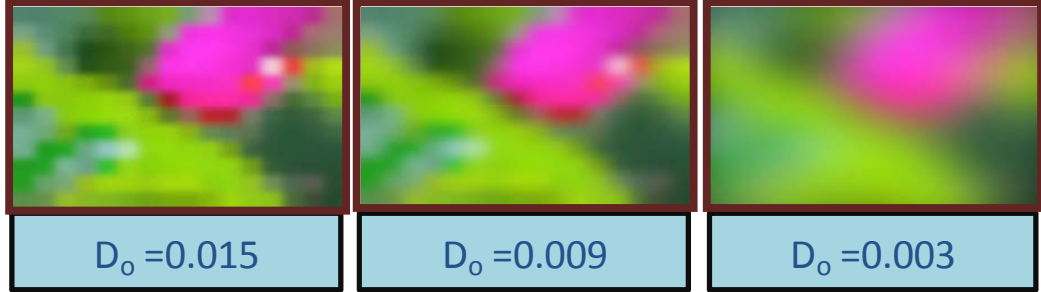
Fig. 4-7   Simulated backlight intensity distribution of Lotus in various cutoff frequency:D_o=0.015, 0.009, and 0.003 at 16x12 backlight division combination.

4.2.3 Production of Four Field-Images

After obtaining the backlight intensity distribution (BL_i) through the DFT and a GLPF, the LC transmittance values of R, G, and B sub-frames, T_R, T_G, and T_B, were compensated for using Eq. 4-3, where I_i^{full} and I_i denote image luminance; BL_i^{full} and BL_i denote intensities of the traditional full-on backlight and blurred backlight images while using local color-backlight dimming technology. Then, T_{min} was calculated by taking the minimum transmittance value across T_R, T_G, and T_B for each LC pixel to generate the LC signal for the first sub-frame. The new LC signals for the R, G, and B sub-frames, T_R', T_G', and T_B', were determined using Eq. 4-4.

$$I_i^{full} = I_i \Rightarrow BL_i^{full} \times T_i^{full} = BL_i \times T_i \qquad i = R, G, B$$

$$\Rightarrow \begin{bmatrix} T_R \\ T_G \\ T_B \end{bmatrix} = \begin{bmatrix} BL_R^{full} / BL_R & 0 & 0 \\ 0 & BL_G^{full} / BL_G & 0 \\ 0 & 0 & BL_B^{full} / BL_B \end{bmatrix} \begin{bmatrix} T_R^{full} \\ T_G^{full} \\ T_B^{full} \end{bmatrix}$$

(4-3)

$$\begin{bmatrix} T_R^{'} \\ T_G^{'} \\ T_B^{'} \end{bmatrix} = \begin{bmatrix} T_R \\ T_G \\ T_B \end{bmatrix} - T_{\min}, \quad where \quad T_{\min} = \min(T_R, T_G, T_B) \qquad (4\text{-}4)$$

Once the backlight and LC signals were determined, the three primary-color backlight signals (BL_R, BL_G, and BL_B) and the minimum LC signal (T_{min}) were combined to display high luminance with rough color information in the first sub-frame image. Likewise, combining the BL_R with T_R', BL_G with T_G', and BL_B with T_B', created three other primary-color images as shown in Figs. 4-5(c)(d). Displaying these four field-images at 240Hz generated a vivid color image. This allowed the image energy to be concentrated in the first field, thus reducing the intensities of the red, green, and blue fields which ultimately suppressed CBU.

On the other land, a clipping effect was easily observed while using the Average method to determine the backlight signals, as mentioned in section 3.1.2 [22]. Nevertheless, when using the Stencil-FSC method, each primary color had two sub-frames displaying its luminance and color (the multi-color field and the primary-color field); therefore, the clipping effect was not obvious. Accordingly, the Stencil-FSC method also increased the dynamic contrast and lowered power consumption because local color-backlight dimming technology was used.

4.3 Optimization of the Stencil-FSC Method

In CBU suppression and hardware implementation, three parameters were optimized to suppress CBU more efficiently: one for algorithm-- a backlight dimming ratio (section 4.3.2); two for hardware-- the point spread function and the number of backlight divisions.

4.3.1 Relative CBU value for CBU Evaluation

The color difference of the CIEDE2000 (ΔE_{00}) [48]-[50] was calculated to evaluate

CBU reduction (ΔE_{00} is given in Eq. 2-9). To simulate a relative velocity between the screen object and human eyes, a CBU image was produced by composing the four field-images with 60 total pixel shifts which is equivalent to a velocity of about 180 cm/sec. By summing up the color difference between the original image and the CBU image ($\Sigma\Delta E_{00}$), CBU was evaluated. A lower $\Sigma\Delta E_{00}$ corresponded to less CBU.

$$\Delta E_{00} = \sqrt{\left(\frac{\Delta L^*}{K_L S_L}\right)^2 + \left(\frac{\Delta C_{ab}^*}{K_C S_C}\right)^2 + \left(\frac{\Delta H_{ab}^*}{K_H S_H}\right)^2 + R_T \left(\frac{\Delta C_{ab}^*}{K_C S_C}\right)\left(\frac{\Delta H_{ab}^*}{K_H S_H}\right)} \tag{2-9}$$

4.3.2 Backlight Dimming Ratio—Optimizing for Multi-Color Field Image

According to the Stencil-FSC algorithm, the first field LC signal (T_{min}) chose the minimum LC transmittance among three primary LC signals (T_R, T_G, T_B). If the color of an object was close to yellow, magenta, or cyan, it resulted T_{min} was not large enough to form a colorful image (Fig. 4-8). Hence, CBU reduction was limited. Therefore, enlarging the T_{min} to colorize first field-image was required. From Eq. 4-5, based on the same light luminance (I) perceived by human eyes, lower BACKLIGHT intensity (I_{BL}) could generate a larger LC transmittance value (T_{LC}). Therefore, after determining color-backlight signal, minimum backlight value of each backlight division was taken and then dimmed using a dimming ratio (DR) ranging from 0~100% to get a higher saturated backlight image (Fig. 4-9). By using the HDR tech, T_{min} was enlarged and become a colorful first field-image (Fig. 4-10(b)). The lower DR resulted in more colorful backlight and generated higher T_{min} in the first field, thus the brightness of R, G, and B fields were reduced to further suppress CBU. However, if DR was excessively low, the clipping effect might be appeared and resulted in image distortion.

$$I = I_{BL} \times T_{LC} \tag{4-5}$$

(a) Test image_ *Maple*　　　　(b) LC signal (T_{min})　　　　(c) first field image
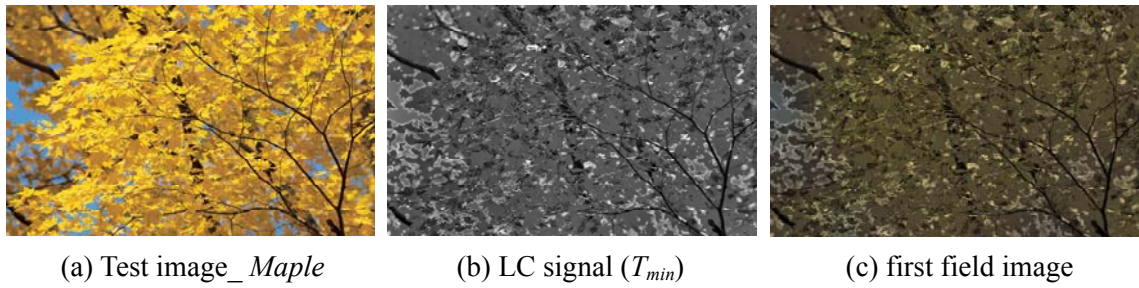
Fig. 4-8　Insufficiently colorful first field-image (a) Test image_ Maple, (b) LC signal, and (c) the first field-image.

(152,135,<u>89</u>)

DR=10%

(152,135,<u>9</u>)

(a) Original BL signal　　　　(b) DR applied　　　　(c) Colorized BL signal
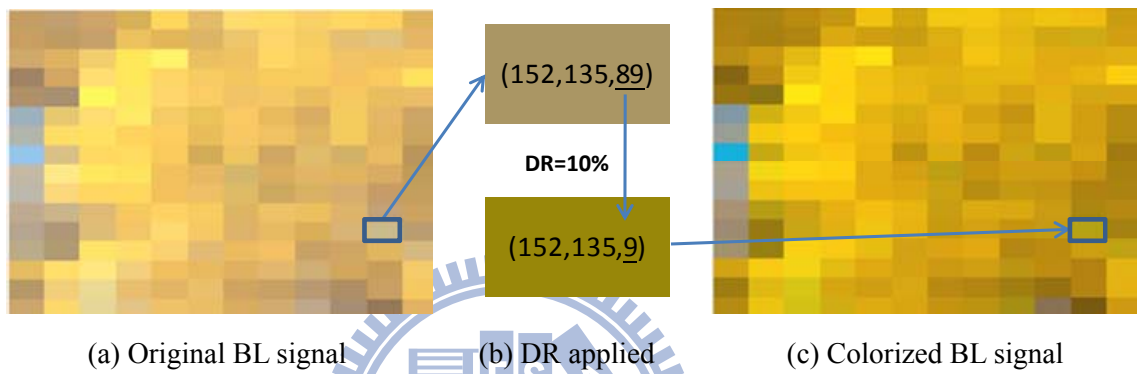
Fig. 4-9　Processing of colorized backlight image. (a) Original backlight signal, (b) applying the dimming ratio (DR=10%), and (c) the final colorized backlight signal.

(a)

(b)
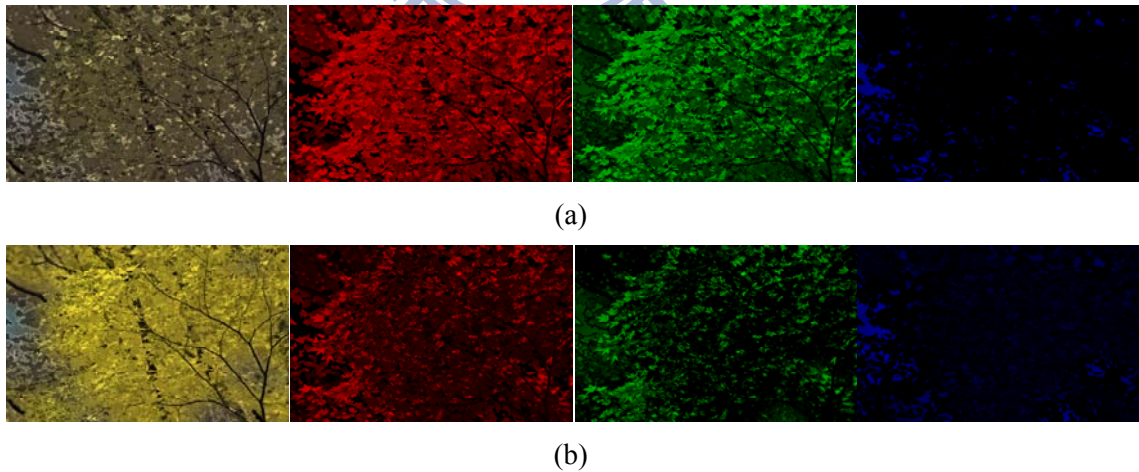
Fig. 4-10　Four Stencil-FSC sub-frame images using the (a) original color backlight and (b) colorized backlight with DR=10%.

Accordingly, the DR vs. CBU reduction and image distortion were simulated, and the *relative CBU$_{DR}$* index (given by Eq. 4-6) and distortion ratio (D) (given by Eq. 3-3, section

3.2.2) were used as evaluation indexes. Using four particular color test images, *Cyan-moon* (cyan color), *Maple* (yellow color), *Blossom* (magenta color), and *Lotus* (magenta-green color) (Fig. 4-11), the simulation results of DR vs. *relative CBU$_{DR}$* and DR vs. distortion ratio are shown in Fig. 4-12. In Fig. 4-12 (a), a smaller DR ratio generates a lower *relative CBU$_{DR}$* which implies less CBU. However, a smaller DR ratio results in a higher image distortion particularly when DR is smaller than 10%, as shown in Fig. 4-12 (b). Therefore, DR=10% was optimized according to the imperceptible clipping effect and efficient CBU suppression.

$$relative\ CBU_{DR} \equiv \frac{(\sum \Delta E_{00})_{DR=i}}{Max(\sum \Delta E_{00})_{DR=i}} \qquad i = 1,\ 5,\ 10,\ 20,\ 40,\ 60,\ 80,\ 100\ \% \qquad (4-6)$$

(a) Cyan-moon   (b) Maple   (c) Blossom   (d) Lotus
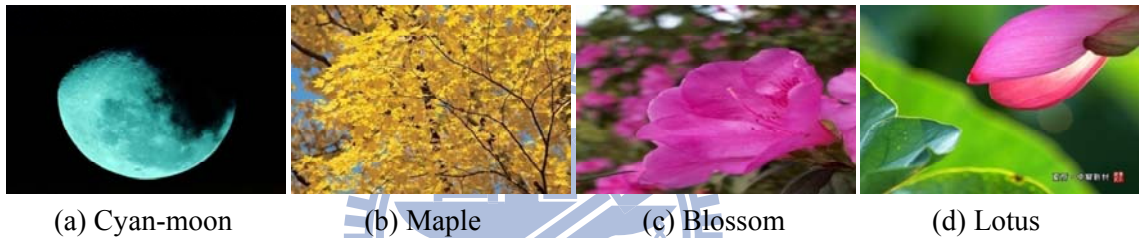
Fig. 4-11   Four particular color test images. (a) Cyan-moon, (b) Maple, (c) Blossom, and (d) Lotus.

(a) Relative CBU$_{DR}$ (b) Distortion ratio
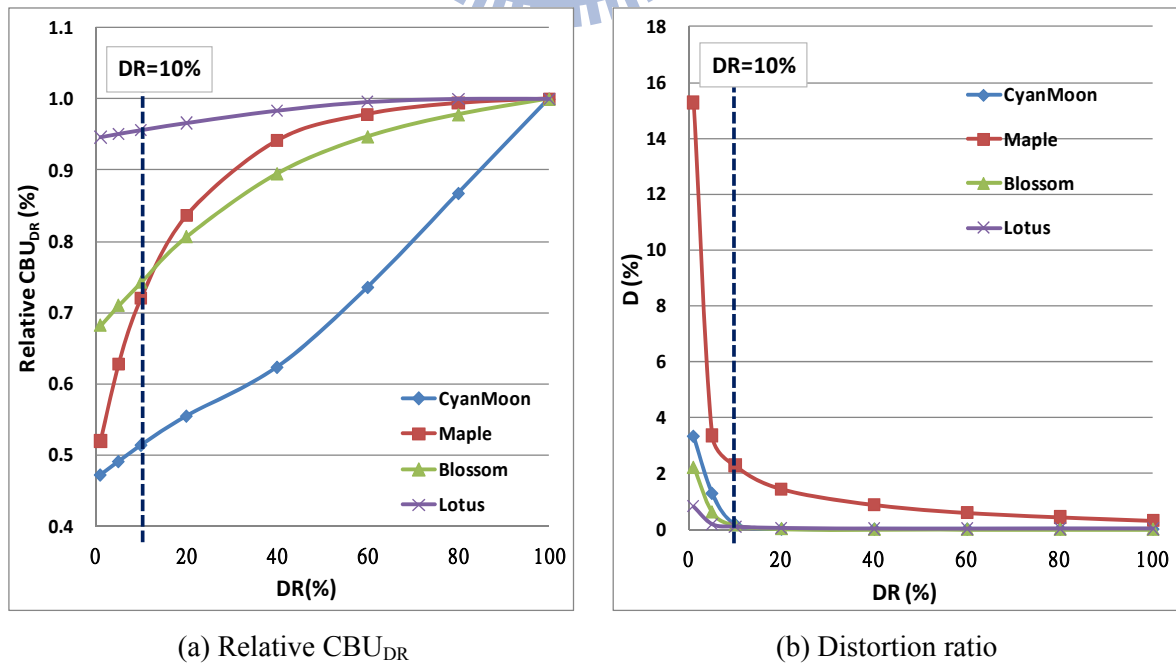
Fig. 4-12   Simulation results for the dimming ratio (DR) vs. (a) the relative CBU$_{DR}$ and (b) the distortion ratio (D) in the four test images.

4.3.3 Optimization for point spread function (PSF) and Backlight Divisions

For hardware implementations, two parameters were optimized to suppress CBU more efficiently: the cutoff frequency (D_o) of the GLPF and the number of backlight divisions. Nine images with different levels of detail and color complexity as shown in Table 4-1 were chosen as test images.

Table 4-1   Nine test images with different levels of color and detail complexity.

(*: taken by Jacky Lee, http://jac3158.com/blog)

Typically, a greater number of backlight divisions suppresses CBU more effectively. On the other hand, a greater number of backlight divisions uses more IC drivers and results in greater hardware computational complexity. To help determine the optimal arrangement of backlight divisions, nine different configurations were formed by variable subdividing the total set of LEDs in an existing backlight (48 horizontal $\times$ 24 vertical). Moreover, for the

expansion number of LEDs in future LED-based backlights, we added another three backlight combinations-- 32×24, 48×48, and 64×48 in the simulation optimization (Fig. 4-13). In addition, the point spread function (PSF) was also optimized using different backlight division combinations. As mentioned in section 4.2.2, PSF is directly related to D_o in the frequency domain. Therefore, 0.001, 0.003… and 0.019 were ten D_o values used in each backlight division combination to get the minimum total color difference ($\Sigma\Delta E_{00}$).

p	**4**	8	8	12	12	**16**	24	24	32	**48**	48	64
q	**4**	4	8	8	12	**12**	12	24	24	**24**	48	48
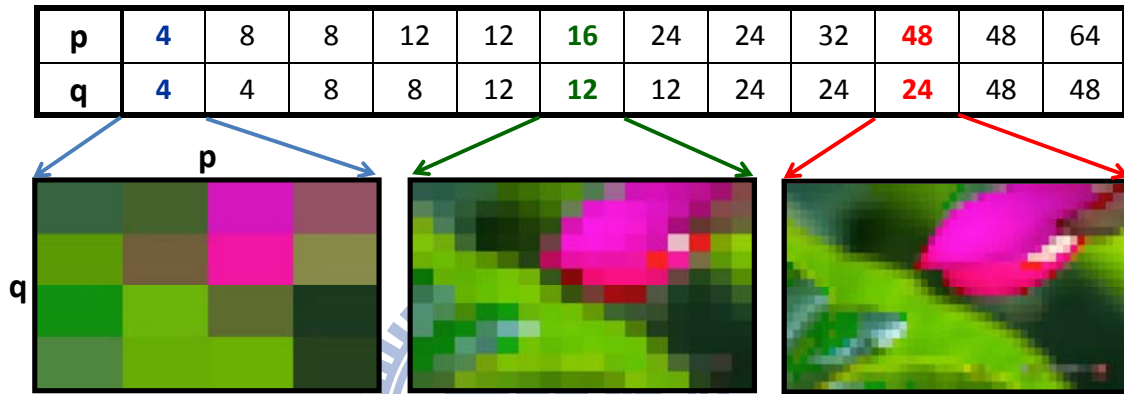
Fig. 4-13   Simulation backlight division combinations with three corresponding backlight signals for image_ Lotus. (p is the column number and q is the row number)

The *relative CBU*$_{RGB}$ index was defined as the ratio of total color difference between p×q backlight division while using the Stencil-FSC method and that of the conventional RGB-driving as given in Eq. 4-7, where p and q are the numbers of column and row backlight divisions. A smaller *relative CBU*$_{RGB}$ denotes less CBU in its backlight divisions when compared to the conventional RGB-driving.

$$relative\ CBU_{RGB} \equiv \frac{\sum \Delta E_{00}(Target, Stencil)_{p*q}}{\sum \Delta E_{00}(Target, RGB\_driving)} \times 100\% \quad p,q: division\ number \quad (4\text{-}7)$$

The nine test images, as shown in Table 4-1, were used to test the number of backlight divisions vs. D_o values which caused the minimum $\Sigma\Delta E_{00}$ and is shown in Fig. 4-14. In

addition, the frequency domain PSF was transferred to the spatial domain and is shown in Fig. 4-15. The number of backlight divisions vs. *relative CBU_{RGB}* is shown in Fig. 4-17. In Fig. 4-14, a larger number of divisions using a larger D_o value can get the minimum $\Sigma\Delta E_{00}$. Therefore, when the number of backlight divisions is larger, the PSF became more localized. This trend is also presented in Fig. 4-15. From Fig. 4-17, as the number of backlight divisions increases, *relative CBU_{RGB}* decreases till 24×24 when *relative CBU_{RGB}* is insensitive to the number of backlight divisions. When taking into account CBU suppression and hardware implementation, 24×24 might be the optimal number of backlight divisions. Finally, to suggest hardware design of backlight systems, the optimized cutoff frequency of 0.07 for 24×24 backlight divisions was transferred back to spatial domain. From Fig. 4-15, the two directional standard deviations of the Gaussian point spread function are σ_x=54 pixels and σ_y=32 pixels, as illustrated in Fig. 4-16.
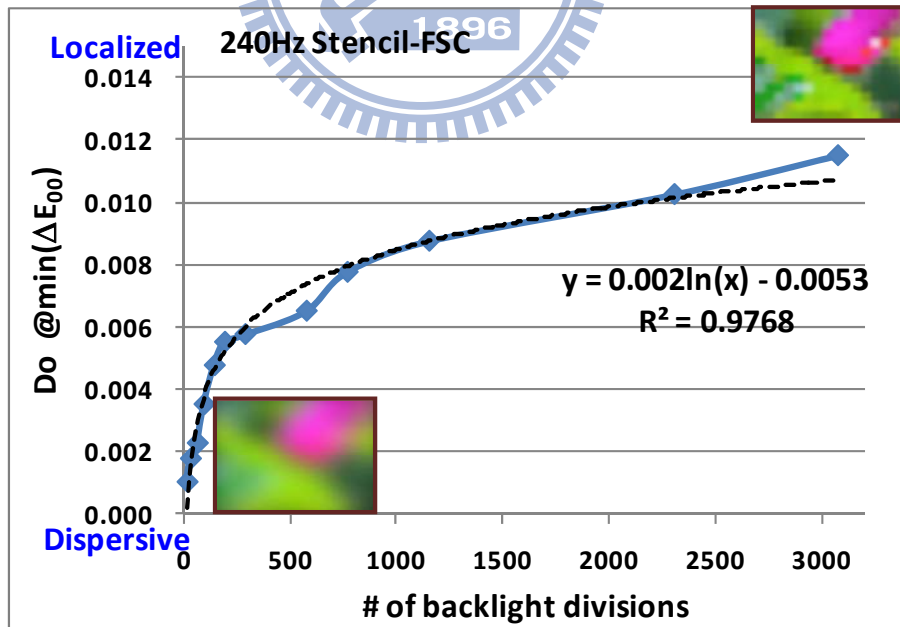
Fig. 4-14   Point spread function (PSF) in frequency domain. Relation between the number of backlight divisions and the cutoff frequency (D_0) value when creating minimum $\Sigma\Delta E_{00}$.
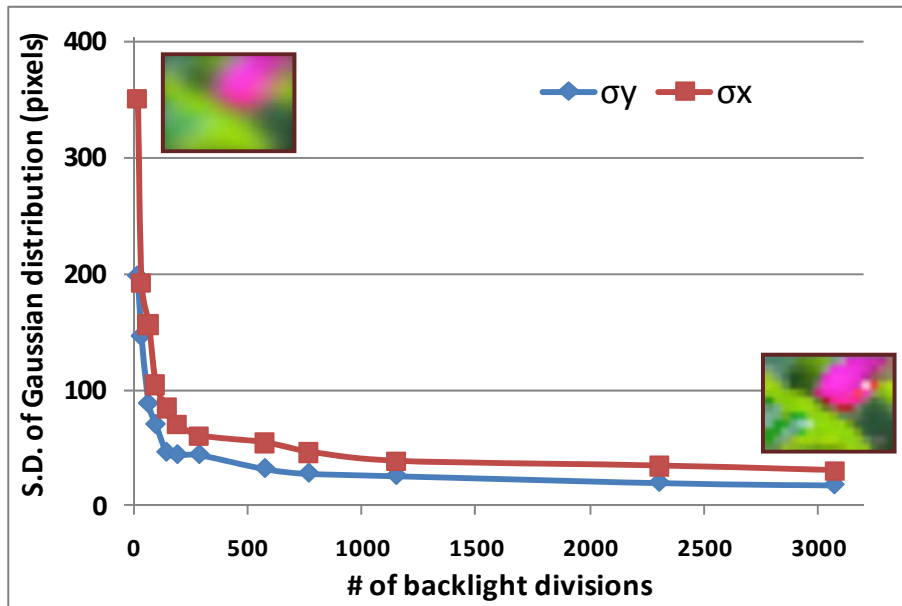
Fig. 4-15   Point spread function (PSF) in spatial domain. Relation between the number of backlight divisions and S.D. (σ_x and σ_y) of a Gaussian PSF when creating minimum $\Sigma\Delta E_{00}$.
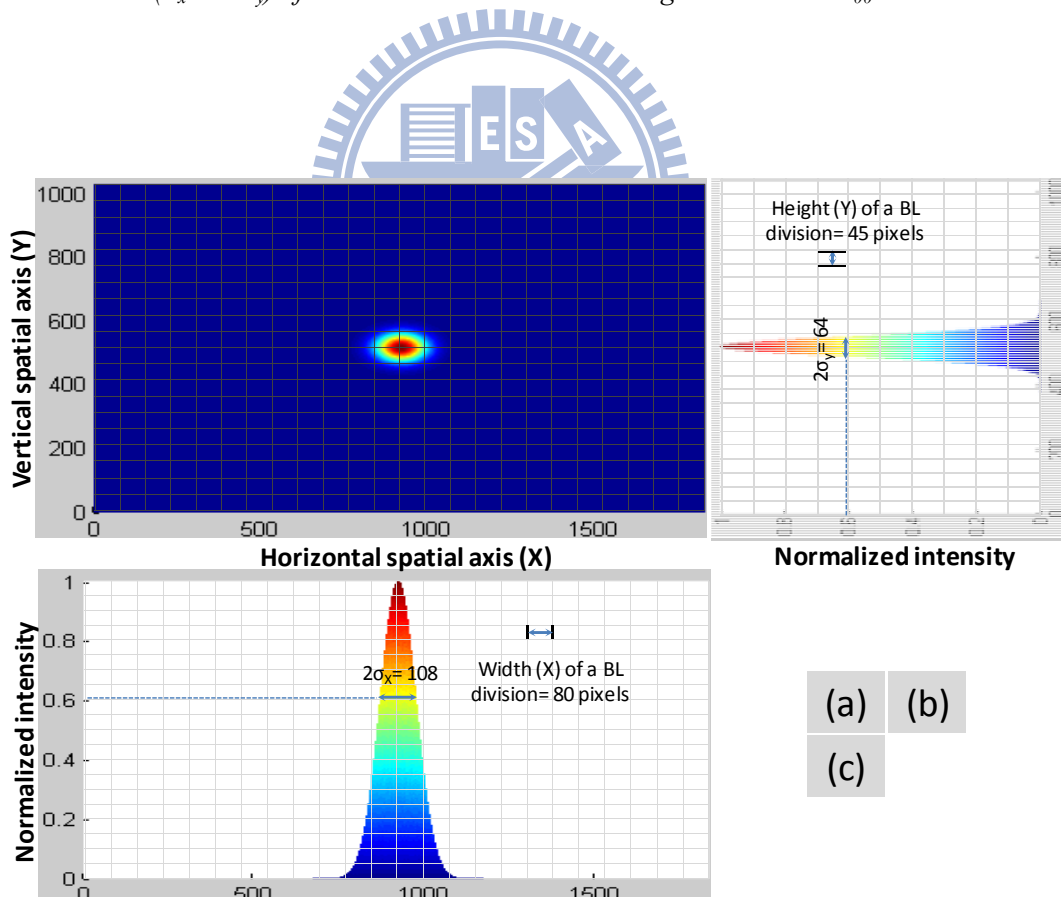
Fig. 4-16   The optimized Gaussian PSF with $\sigma_x=54$ pixels and $\sigma_y=32$ pixels in the 24×24 backlight division combination. PSF views from (a) vertical, (b) lateral (y-direction), and (c) bottom (x-direction).
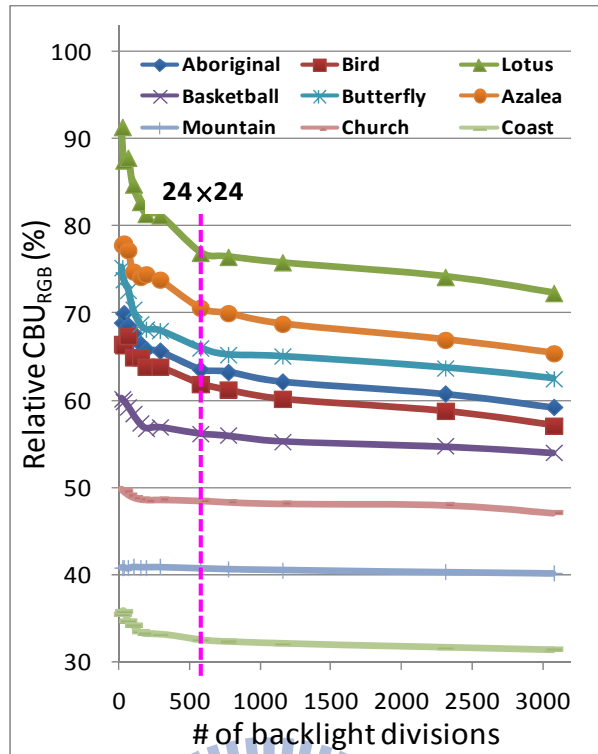
Fig. 4-17   Simulation results of the number of backlight divisions vs relative CBU$_{RGB}$ in the nine test images.

4.4 Simulations and Experiments

4.4.1 Simulations of CBU Suppression

Comparing the optimized number of backlight divisions and D_o value, we chose 24×24 backlight divisions with D_o=0.007 as the optimized hardware parameter combination to simulate CBU suppression while using a 10% dimming ratio for backlight optimization. Using *relative CBU$_{RGB}$* index (defined in Eq. 4-7) to evaluate the percentage of CBU was suppressed by optimized 240Hz Stencil-FSC method. According to Fig. 4-18, Stencil-FSC suppressed CBU by 33~79% when related to RGB-driving, and the average *relative CBU$_{RGB}$* was 57.9% for the nine test images. The 240Hz Stencil-FSC method effectively suppressed CBU particularly for the low color complexity images, such as *Mountain*, *Church*, and *Coast*. Because the first LC transmittances are large, 240Hz Stencil-FSC effectively accumulates image energy into the first field multi-color image.
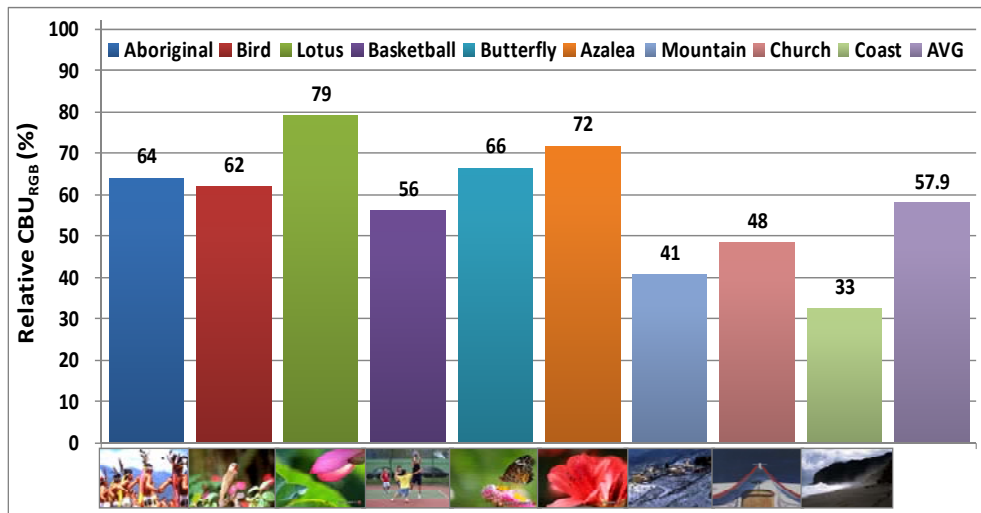
Fig. 4-18   Relative CBU$_{RGB}$ in the nine test images while using 240Hz Stencil-FSC.

4.4.2 Experiments on a 32-inch FSC-LCD

The Stencil-FSC method was implemented on a 32-inch OCB-mode FSC-LCD with 1366×768 image resolution. The backlight module was composed of 1152 (48×24) LEDs, as illustrated in Fig. 4-19 (the panel was provided by CPT, Taiwan) [28]. In Fig. 4-20(a), the first sub-frame photo presents a multi-color image with high luminance and rough color information. The red, green, and blue residuals in the remaining fields completed a full color image. This allowed the image energy to focus in the first field, and reduce the red, green, and blue field intensities and suppressed CBU.

(a) BL photo of 16x12 divisions   (b) Stencil-FSC TV
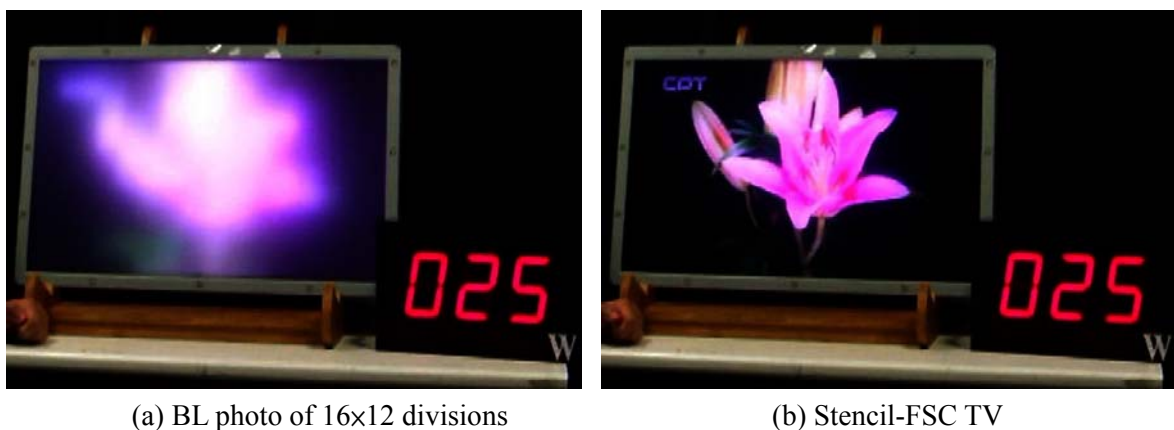
Fig. 4-19   Implemented Stencil-FSC on a 32-inch FSC-LCD TV with 25 W power consumption. (a) Backlight photo and (b) Stencil-FSC LCD TV. (The panel was provided by CPT, Taiwan)

| (a) Four field-images | (b) backlight image |
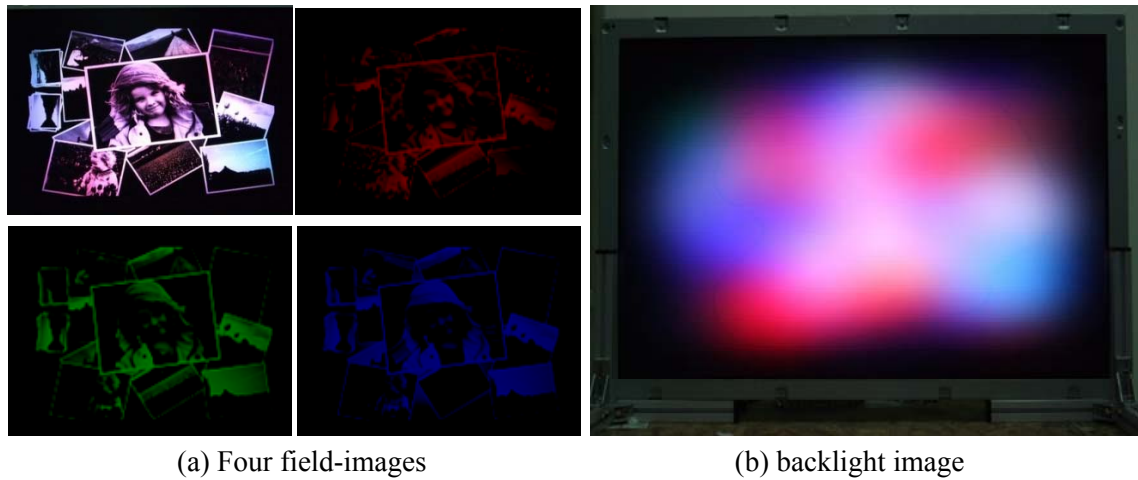
Fig. 4-20   (a) Four field-image demo photos of Girl on a 32-inch FSC-LCD using the Stencil-FSC method. (b) Backlight image on a Stencil-FSC LCD.

To capture the CBU image, a digital still camera (Fujifilm-F50) was set up 2 meters from the FSC-LCD on a moving stage with a horizontal velocity of 200 cm/sec to simulate eye movement (about 53 deg/sec), as illustrated in Fig. 4-21. The camera exposure time was 1/60 sec. Two pictures, *Girl* and *Lily*, were used as test images. The experimental CBU photos in Figs. 4-22 and 4-23 demonstrate the Stencil-FSC method suppresses CBU effectively. In addition, utilizing a locally controlled RGB-LED backlight, the dynamic contrast ratio (CR) of *Girl* was enhanced to 6,544:1 at 35 Watts power consumption. For the other high CR image, *Lily*, the CR was also enhanced to 26,335:1 using only 28 Watts. As a result, using the Stencil-FSC method, not only was CBU suppressed, but also reached high contrast with low power consumption in a 32-inch FSC-LCD. The contrast ratio (CR), power consumption (P), CBU, and color gamut (NTSC ratio) of the three 32-inch LCDs (commercial IPS-CCFL, conventional RGB driving FSC, and Stencil-FSC) displaying two test images were measured and are shown in Table 4-2.

Fig. 4-21 Experimental setup for capturing CBU images.
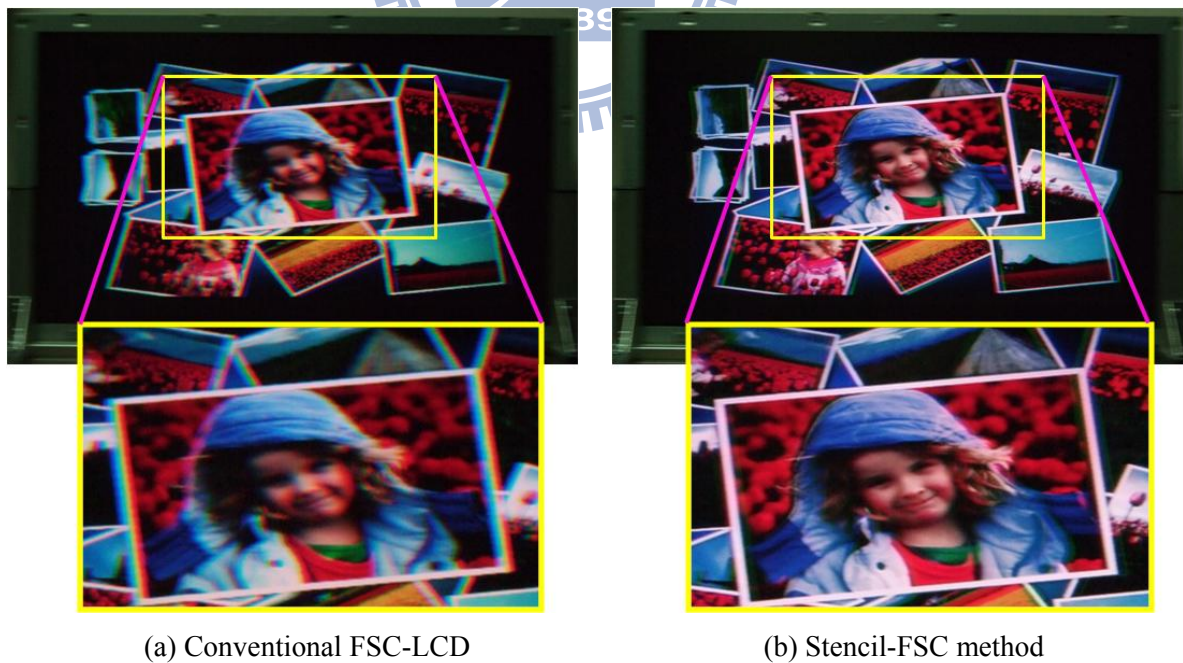
(a) Conventional FSC-LCD   (b) Stencil-FSC method

Fig. 4-22 CBU experimental results for Girl using the (a) conventional FSC-LCD and (b) the Stencil-FSC method.
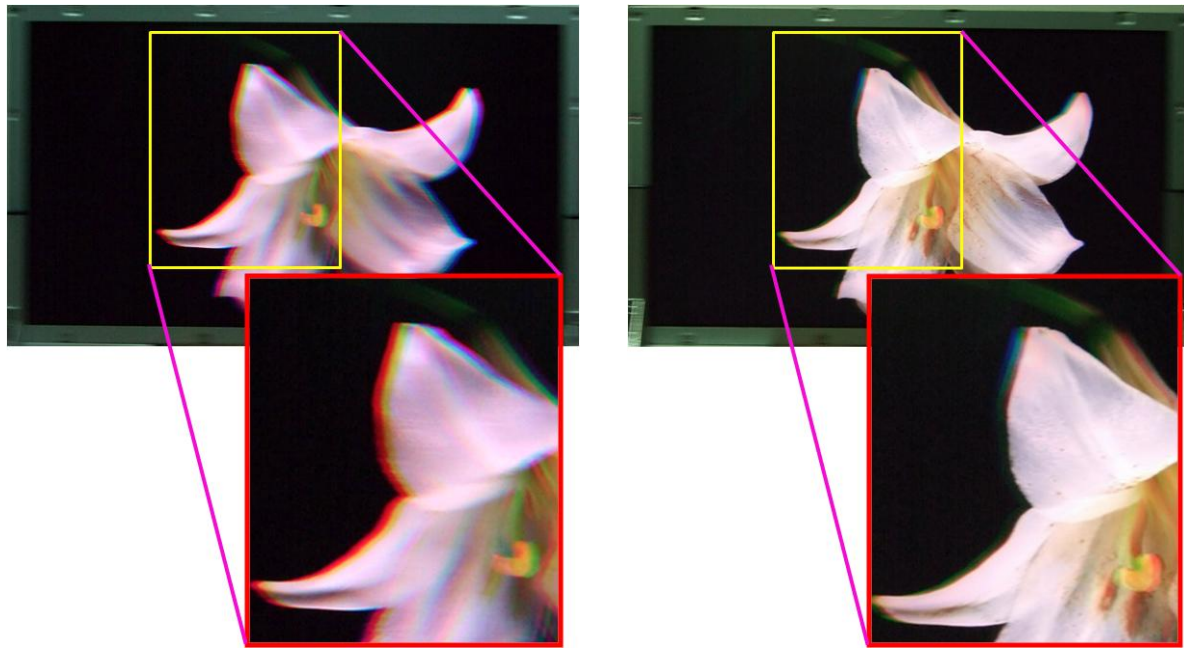
(a) Conventional FSC-LCD   (b) Stencil-FSC method

Fig. 4-23   CBU experimental results for Lily using the (a) conventional FSC-LCD and (b) the Stencil-FSC method.
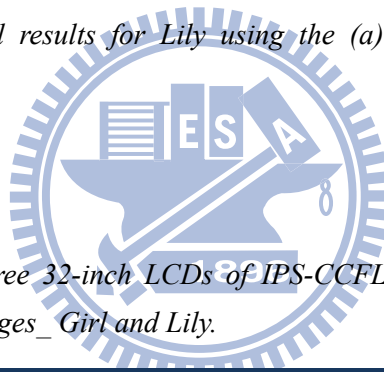
Table 4-2   Comparison of three 32-inch LCDs of IPS-CCFL, conventional FSC, and Stencil-FSC method displaying two test images_ Girl and Lily.

		IPS-CCFL	OCB-mode FSC (Conventional RGB-driving)	Stencil-FSC
Girl	**CR**	692 : 1	442:1	6,544:1
	P (W)	105	68	35
	CBU	--------	Fig. 4-22(a)	Fig. 4-22(b)
Lily	**CR**	766：1	512：1	26,335：1
	P (W)	105	68	28
	CBU	--------	Fig. 4-23(a)	Fig. 4-23(b)
Color Gamut* (% of NTSC)		72 %	114 %	114 %
➤ Power consumption of a 32" conventional LED-based TV: ~190W (*: The maximum NTSC ability of the LCD)				

4.5 Summary

Using a multi-color field image instead of a conventional single-color field, the Stencil-FSC method substantially suppressed the CBU phenomenon. The RGB-LED based backlight module was treated as a low resolution panel. Using local color-backlight dimming technology, the low resolution color image created by the LED backlight enabled the generation of a full color RGB image on a color filter-less LCD with an increased contrast ratio and color gamut. The multi-color sub-image provided high luminance and rough color content in the first field; the intensities of three other primary-color sub-images were greatly reduced and effectively suppressed CBU caused by smooth pursuit (in dynamic videos) and saccadic movement (in static images).

In order to balance hardware complexity and CBU suppression, the number of backlight divisions were reduced to 24×24 with σ_x=54 pixels and σ_y=32 pixels standard deviations of a Gaussian point spread function. CBU was suppressed by more than 40% and became almost imperceptible. The Stencil-FSC method was implemented on a 32-inch FSC-LCD TV to yield a high dynamic contrast of 26,000:1 for test image, *Lily*, average power consumption of less than 35 Watts, and a wide color gamut of 114% NTSC. Among the most important finding is that Stencil-FSC successfully suppressed CBU in an OCB-LC panel with a limited response time (240Hz). Using the 240Hz Stencil-FSC method, a color filter-less LCD TV has been successfully realized and demonstrated.

4.6 Discussion

Stencil-FSC efficiently suppressed CBU while heightening the image contrast ratio with low power consumption, however, the 240Hz Stencil-FSC method still faced some issues. First, because of a limited LC response time, a 240Hz large-sized LCD has not been well developed in current LCD manufacturing. In addition, 240Hz Stencil-FSC required one more field and resulted in the compression of available time. Eq. 4-8 explains each required time in

an FSC-LCD, where f is frame rate (60Hz at NTSC standard), N and n are the number of fields and effective scanning backlight divisions respectively [69]. t_{TFT}, t_{LC}, and t_{LED} are the data addressing time, LC response time, and LED-BL flashing time.

$$\frac{1}{Nf} = \frac{t_{TFT}}{n} + t_{LC} + t_{LED}$$ (4-8)

We assumed a case that the addressing time for each gate-line was 5 μs, LED-BL flashing time was 1.5 ms, and there were 5 (n=5) effective scanning backlight divisions in the Stencil-FSC system. Therefore, the LC response time for a full-HD resolution (1920×1080) LCD should be much shorter to 1.6 ms [70]. If LC response could not be speeded up, thus, LC would not rotate to correct orientation which yielded the color shift. Otherwise, the LED-BL response time would be compressed and decreased image brightness. Hence, we further reduced the Stencil-FSC field rate from 240Hz (4-field) to 180Hz (3-field). The objective was to make a high optical throughput color filter-less LCD more feasible. The detailed 180Hz Stencil-FSC method is presented in the next chapter.

Chapter 5

CBU SUPPRESSION--180Hz STENCIL-FSC

For practical applications, the field rate of CBU solutions should be controlled less than 240Hz (4 field-images). Afterward, we proposed the 180Hz (3-field) [36][37] Stencil Field-Sequential-Color (180Hz Stencil-FSC) method to suppress CBU, as illustrated in Fig. 5-1(d). By applying local color-backlight dimming technology to FSC-LCDs, a "green-based multi-color" field-image showed the most image luminance in the first field. Therefore, residual red and blue field-image intensities were reduced and effectively suppressed CBU. In addition, to further implement hardware, the number of backlight divisions and a proper Gaussian point spread function profile were optimized through simulations while considering CBU reduction and image fidelity.

(a) Target image

(b) RGB-driving   (c) 240Hz Stencil-FSC   (d) 180Hz Stencil-FSC
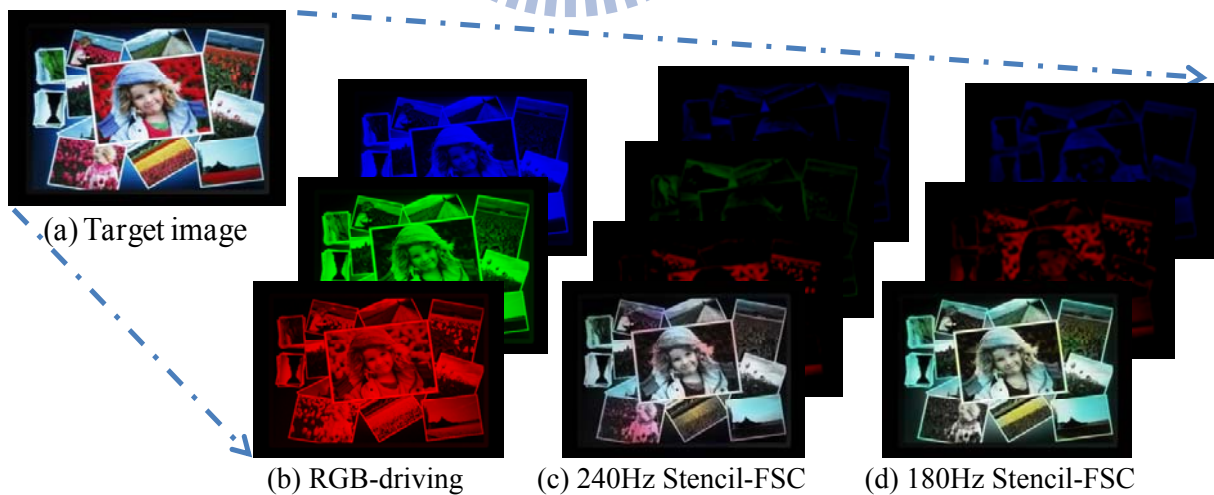
Fig. 5-1   (a) Target image_ Girl (Girl ©Microsoft) and each field-image using the conventional (b)RGB-driving, (c) 240Hz Stencil-FSC, and (d) 180Hz Stencil-FSC methods

5.1 180Hz Stencil-FSC Method

5.1.1 Concept and Algorithm

Concentrating the image intensity on a single field-image can reduce the human sensitivity to CBU. Additionally, the human eye is most sensitive to green color, the red and blue signals are therefore redistributed into the green field to create a "green-based field-image." When the separated colors do not contain green information, the CBU phenomenon is reduced [46].

Similar to 240Hz Stencil-FSC concept, local color-backlight dimming technology was applied to FSC-LCDs, a low resolution colorful backlight panel combined with a high resolution color filter-less LC panel generated a "green-based multi-color" field-image which showed greater image luminance in the first field (Fig. 5-2). The 180Hz Stencil-FSC algorithm was similar to 240Hz Stencil-FSC method, including applying local color-backlight dimming first, and then ingeniously dividing into three field-images. An input image was recalculated to obtain three primary-color backlight signals, BL_R, BL_G, and BL_B. Moreover, the LC transmittance values of R, G, and B fields, T_R, T_G, and T_B, were compensated using Eq. 4-3 (section 4.2.3), where I_i^{full} and I_i denote image luminance; BL_i^{full} and BL_i denote intensities of the traditional full-on backlight and the HDR blurred backlight signal respectively (Fig. 5-3(b)). The difference from 240Hz Stencil-FSC was the first field LC signals. To fully display green information in the first field, the green LC signal (T_G) of each LC pixel was taken as the first field LC signal. From Eq. 5-1, the new red and blue-field LC signals (T_R' and T_B') were determined for the red and blue field-images (Fig. 5-3(c)).

$$\begin{bmatrix} T_R \\ T_G \\ T_B \end{bmatrix} = \begin{bmatrix} BL_R^{full}/BL_R & 0 & 0 \\ 0 & BL_G^{full}/BL_G & 0 \\ 0 & 0 & BL_B^{full}/BL_B \end{bmatrix} \begin{bmatrix} T_R^{full} \\ T_G^{full} \\ T_B^{full} \end{bmatrix} \qquad (4\text{-}3)$$

$$\begin{bmatrix} T_R^{'} \\ T_B^{'} \end{bmatrix} = \begin{bmatrix} T_R \\ T_B \end{bmatrix} - T_G \qquad (5\text{-}1)$$
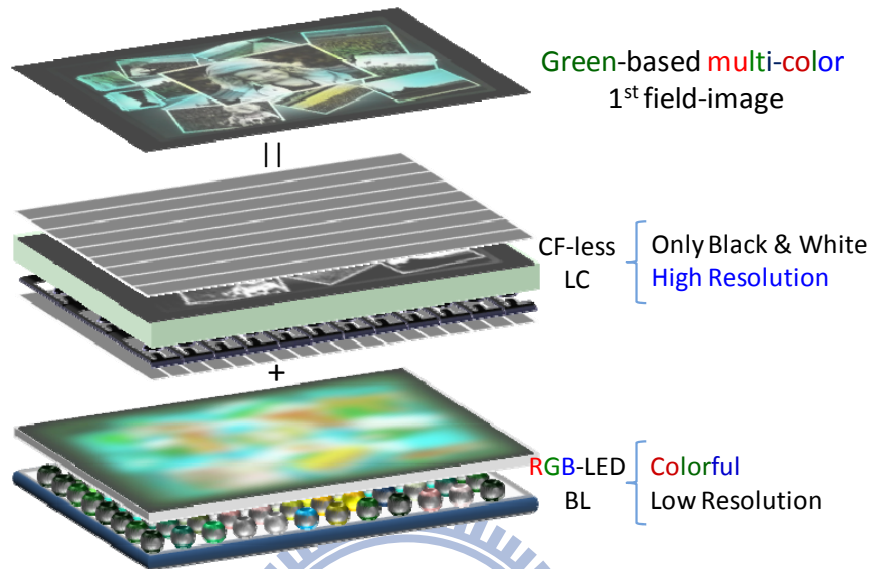
Fig. 5-2   A "green-based multi-color" image is yielded by a low resolution RGB-LED backlight and a high resolution color filter-less LC cell.
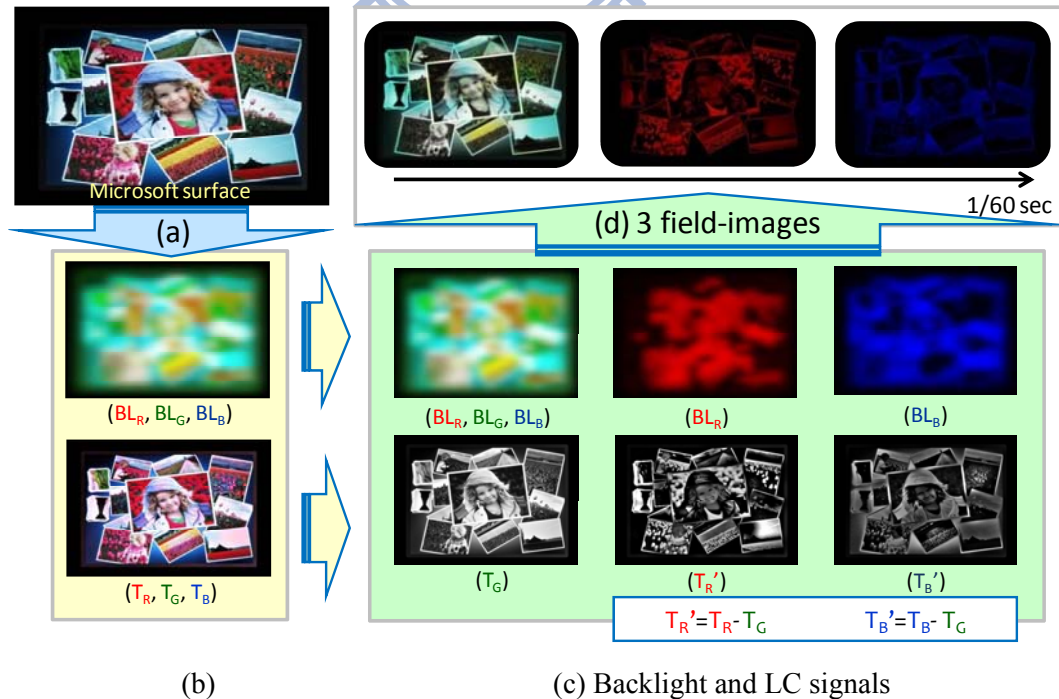
Fig. 5-3   180Hz Stencil-FSC algorithm. (a) Input image, Girl (©Microsoft), (b) local color-backlight dimming technology, (c) backlight and LC signals, and (d) 3 yielded field-images.

To prevent T_R' or T_B' from being a negative value which indicates redundant red or blue light was propagated to the first field and resulted in the reduction of green saturation, as illustrated in Fig. 5-4. Consequently, green backlight determination (BL_G) was different from the red and blue backlight determination (BL_R and BL_B) methods. In this dissertation, the image was evenly divided into non-overlapping rectangles corresponding to the number of backlight divisions. We directly averaged the red and blue pixel values that subtended the rectangular region in front of each given backlight division independently as red and blue backlight signals, BL_R and BL_B, (e.g. the Average method). BL_G was calculated by averaging the green LC pixel signals and then took its square root to enhance the signal (e.g. the Square-Root method) [9][10]. Therefore, if the average red, green, and blue pixel signals in a certain backlight division are similar values, the BL_G will be larger than BL_R and BL_B. Consequently, most compensated red and blue LC signals (T_R and T_B) will be larger than green signal (T_G) which avoids negative T_R' and T_B' and maintains image fidelity.
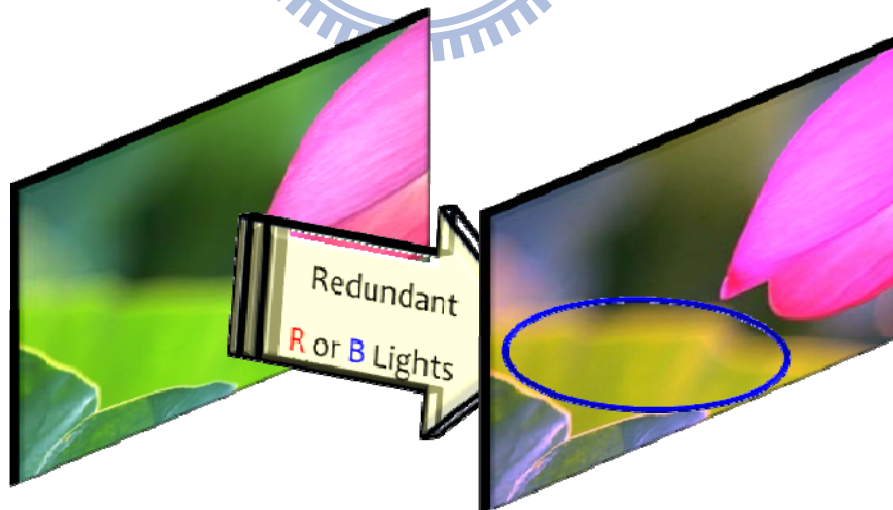
Fig. 5-4   Redundant red or blue light propagates through the first green-based sub-frame resulting in reduction of green color saturation (blue circle part).

After determining each field-image backlight and LC signals, each field LC signal was put on the color filter-less panel as a stencil mask, the RGB-LED backlights were painted onto each mask sequentially to produce each field-image. According to the stencil concept, the three primary-color backlight signals (BL_R, BL_G, and BL_B) and the green LC signal (T_G) were combined to display a high luminance green-based color image in the first field. Likewise, combining the BL_R with T_R' and BL_B with T_B', created residual less-luminance red and blue field-images (Fig. 5-3(d)). Finally, displaying these three field-images at 180Hz generated less CBU and a vivid color image. The direct and simple 180Hz Stencil-FSC signal processing also heightened the image contrast and lowered power consumption because local color-backlight dimming technology was used.

5.1.2 Optimization of 180Hz Stencil-FSC

To suppress CBU more efficiently and maintain image fidelity, the point spread function (PSF) of a backlight division and the number of backlight divisions while using the 180Hz Stencil-FSC method were optimized. Except the test images in Table 4-1, six more high contrast ratio or rich color content test images (Fig. 5-5) were included in the 180Hz Stencil-FSC optimization. In addition, to simulate a relative velocity between the screen object and the human eye, a CBU image was produced by composing the three field-images with 60 total pixel shifts which is equivalent to a velocity of about 180 cm/sec. The PSF was also simulated as a Gaussian distribution in this optimization (Eq. 4-2). By controlling the standard deviation (S.D.) of the Gaussian distribution (σ_x and σ_y), the PSF was modulated (Fig. 5-6 (a)). To help determine the optimal arrangement of backlight divisions, twelve different configurations were formed as shown in Fig. 5-6 (b).

$$g(x,y) = e^{-\left(\frac{x^2}{2\sigma_x^2} + \frac{y^2}{2\sigma_y^2}\right)}$$

(4-2)

Fig. 5-5   Six more test images-- top: Lily, Girl, Blossom; bottom: Basketball, Soccer, and Color Ball.

(a) Simulated backlight intensity distribution

p	4	8	8	12	12	16	24	24	32	48	48	64
q	4	4	8	8	12	12	12	24	24	24	48	48
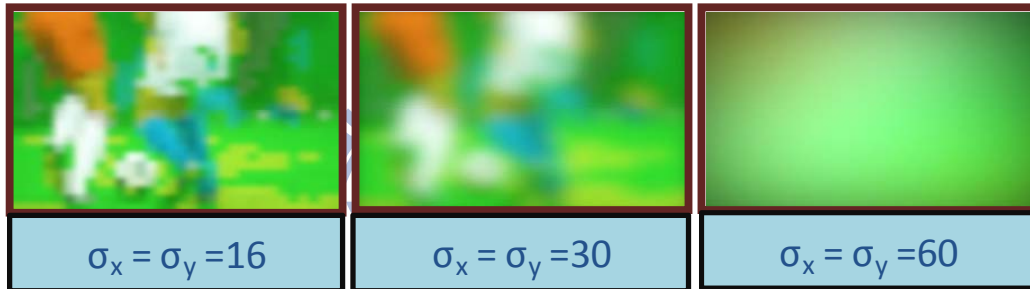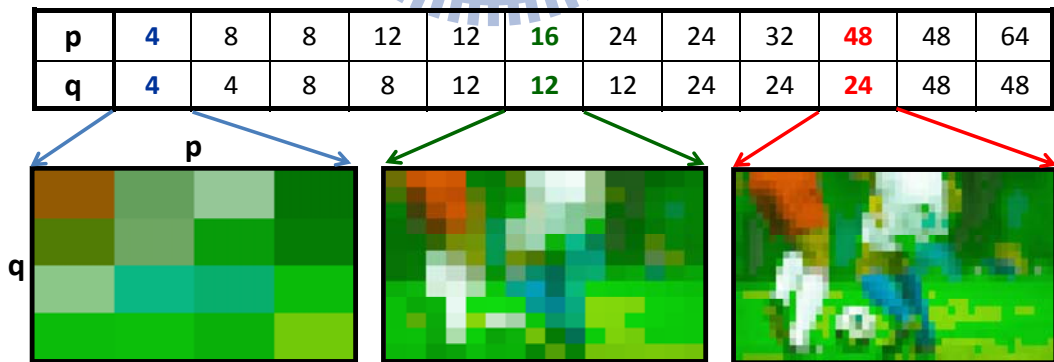
(b) Backlight division combinations

Fig. 5-6   (a) Simulated backlight intensity distribution in various Gaussian standard deviation: σ_x=σ_y=16, 30, and 60 pixels. (b) Simulation backlight division combinations with three corresponding backlight images for the test image_ Soccer. (p is the column number and q is the row number) (*: taken by Jacky Lee, http://jac3158.com/blog)

The color difference of the CIEDE2000 (ΔE_{00}) was also calculated [28]-[49] to evaluate CBU reduction and image fidelity. After summing up ΔE_{00} value of each pixel between a test image and its CBU image ($\Sigma \Delta E_{00}$), a *relative CBU$_{RGB}$* index was defined as the ratio of total color difference between p×q backlight division and conventional RGB-driving, as shown in Eq. 4-7. In addition, the average ΔE_{00} between test images and 180Hz Stencil-FSC simulated images was also calculated to evaluate image fidelity.

$$relative\ CBU_{RGB} \equiv \frac{\sum \Delta E_{00}(Target, Stencil)_{p*q}}{\sum \Delta E_{00}(Target, RGB\_driving)} \times 100\% \quad p,q: division\ number \quad (4-7)$$

When considering to CBU suppression and image fidelity, the proper PSF was optimized for each backlight division first and is shown in Fig. 5-7. A larger number of backlight divisions required smaller σ_x and σ_y which suggested that backlight intensity distribution was localized. Using the optimized PSF, the number of backlight divisions was furthermore analyzed. Figs. 5-8 and 5-9 show the number of backlight divisions versus CBU reduction and image fidelity respectively. From the simulation results, both CBU reduction and image fidelity tended to be independent of the number of backlight divisions after 32×24 (768). In addition, the average ΔE_{00} values after 32×24 were less than 3 which indicated acceptable image fidelity. Considering CBU reduction and practical applications, 32×24 with a Gaussian PSF of σ_x=40 pixels and σ_y=26 pixels might be the optimal parameters for using the 180Hz Stencil-FSC method, as shown in Fig. 5-10.
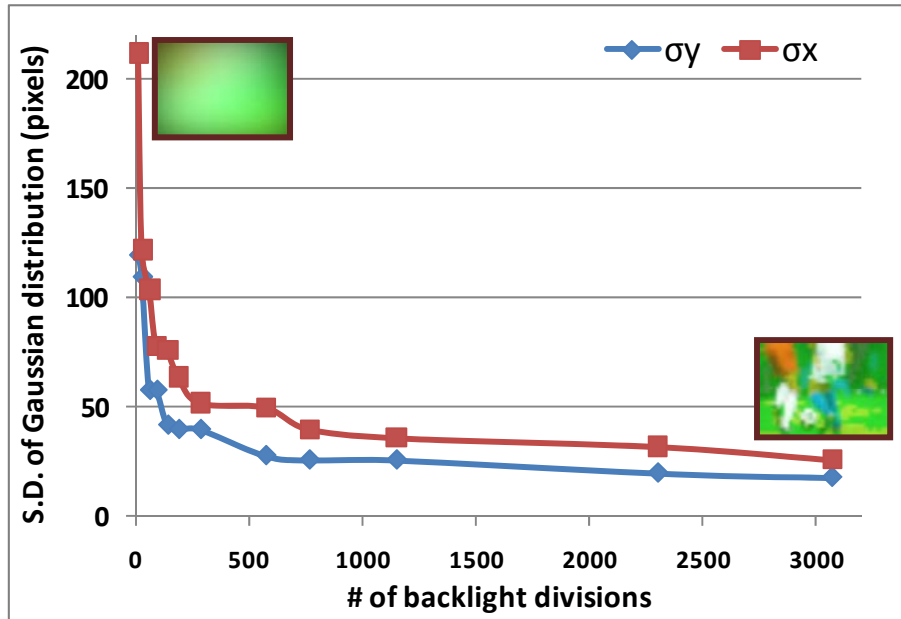
Fig. 5-7   Optimized S.D. (σ_x and σ_y) of a Gaussian PSF for different number of backlight divisions.
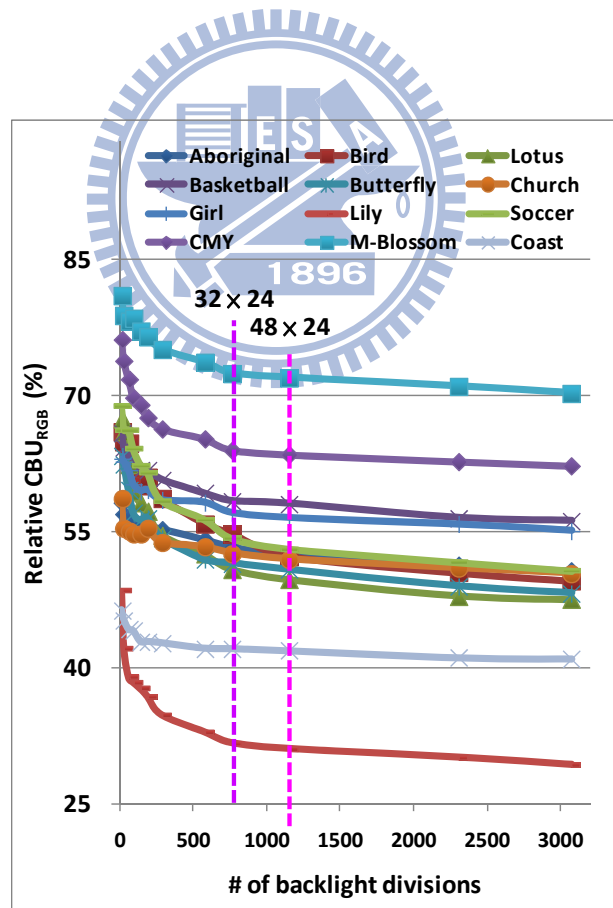
Fig. 5-8   Simulation result of the number of backlight divisions vs relative CBU$_{RGB}$ in the twelve test images.
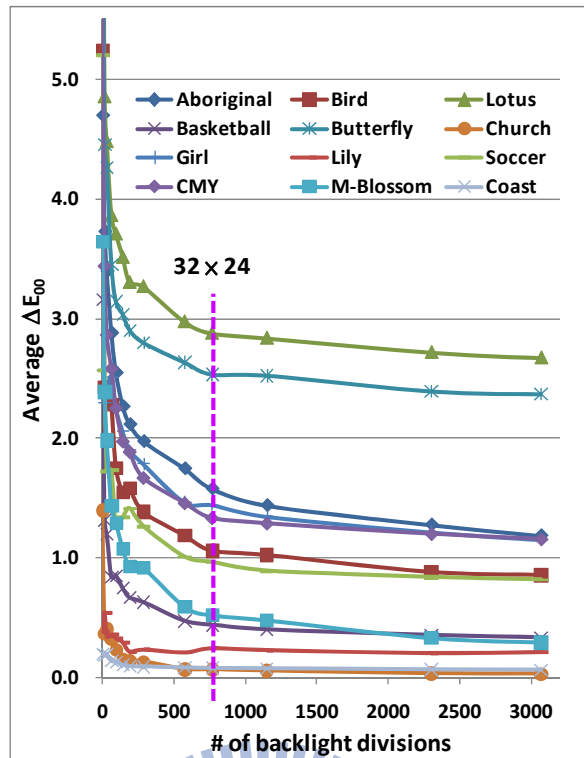
Fig. 5-9   Simulation result of the number of backlight divisions vs. average ΔE_{00} in the twelve test images.
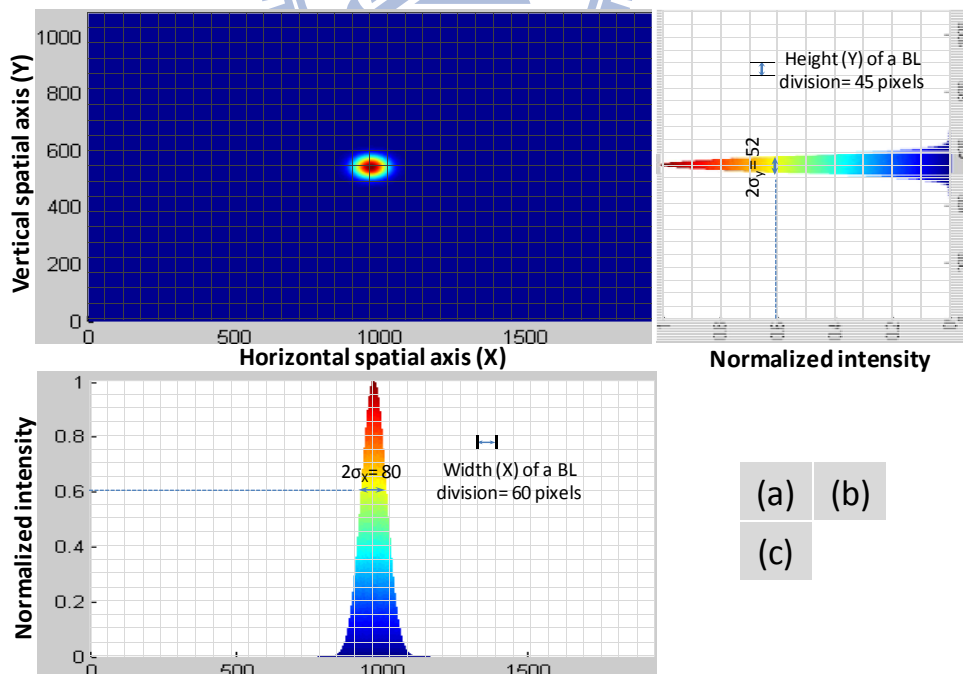
Fig. 5-10   The optimized Gaussian PSF with σ_x=40 pixels and σ_y=26 pixels in the 32×24 backlight division combination. PSF views from (a) vertical, (b) lateral (y-direction), and (c) bottom (x-direction).

| (a) Original images | (b) Simulated images | (c) Error images |
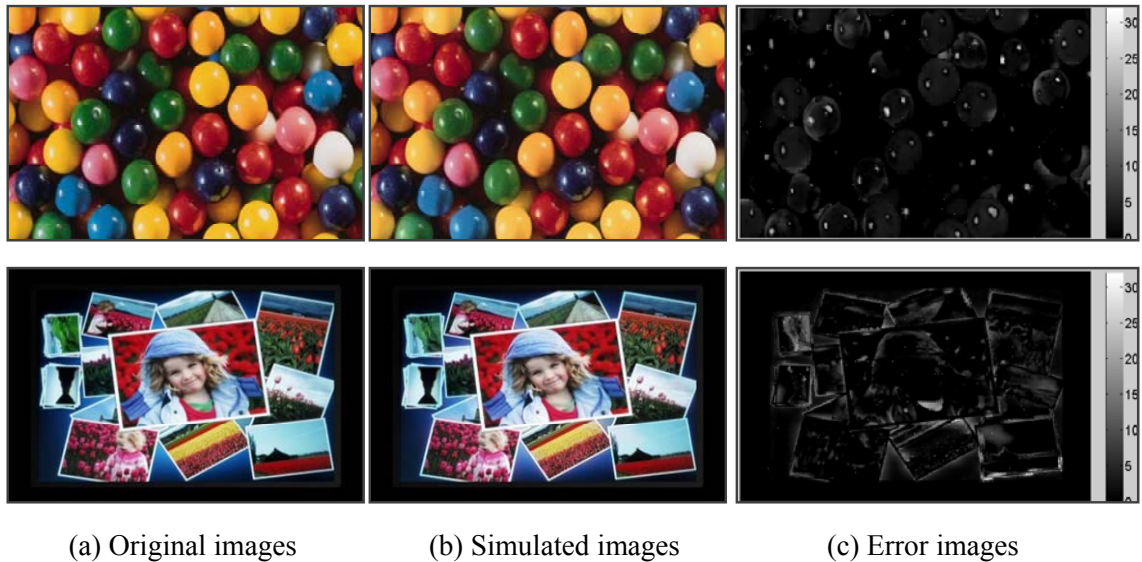
Fig. 5-11   (a) Two test images of Color Ball and Girl. (b) Simulated images after 180Hz Stencil-FSC processing. (c) CIEDE2000 error images between test and processed images with average ΔE_{00} of 1.3 and 1.4 respectively.

Consequently, two test images, *Color Ball* with vivid color information and *Girl* with high image detail were simulated using the optimized conditions. Fig. 5-11 shows their simulated images and CIEDE2000 error images with average ΔE_{00} values of 1.3 and 1.4 respectively at 32×24 backlight divisions. It is difficult to distinguish the differences from the original and simulated images but finding out the differential parts from the CIEDE2000 error images.

5.2 CBU Suppression Comparisons via Simulations

5.2.1 Comparison to other Reduction Methods

CBU suppression using 180Hz Stencil-FSC was compared to methods of double field rate (360Hz-RGB) and black-fields insertion of 360Hz-RGBKKK [63] using simulations. The field-images of each test image were separated in 60 pixels/frame, and the average ΔE_{00} value of the eighty test images (see appendix) using these three suppression methods were calculated and then divided by the ΔE_{00} value using conventional 180Hz RGB-driving

(i.e. index of *relative CBU$_{RGB}$*). The average *relative CBU$_{RGB}$* values using the 360Hz-RGBRGB, 360Hz-RGBKKK, 240Hz Stencil-FSC, and 180Hz Stencil-FSC methods were 76.1%, 60.7%, 52.1%, and 52.7% respectively (Fig. 5-12). The CBU reductions of 360Hz-RGBKKK and two Stencil-FSC methods were close; however, the slow LC response time prevented the 360Hz-RGBKKK from large-sized FSC-LCD applications. The issues are discussed in next section (section 5.2.2). In conclusion, the Stencil-FSC method was more effective than increasing the field rate, when CBU suppression and hardware implementation were considered.
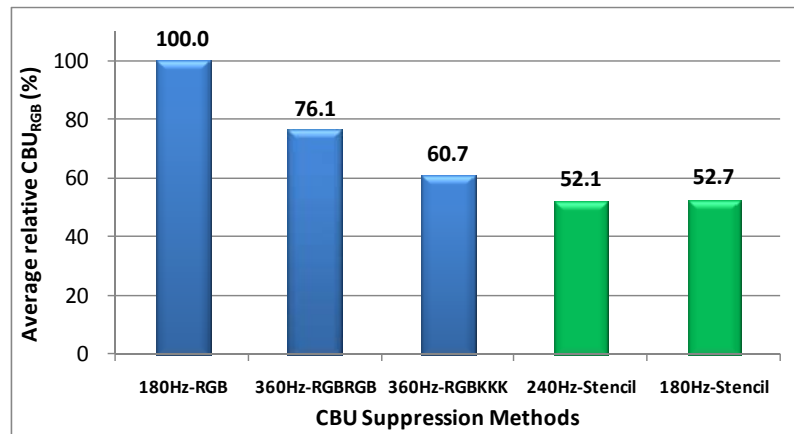
Fig. 5-12   Comparison of the average relative CBU$_{RGB}$ using conventional RGB-driving, double field rate (360Hz-RGBRGB), black-fields insertion (360Hz-RGBKKK) [63], 240Hz Stencil-FSC, and 180Hz Stencil-FSC methods for the eighty test images (see appendix).

5.2.2 360Hz-RGBKKK, 240Hz Stencil-FSC, and 180Hz Stencil-FSC

Since the black-fields insertion method (360Hz-RGBKKK) was concluded as the best practical CBU suppression method [63], we compared this method to two Stencil-FSC methods through simulations. Full-HD (1920×1080 resolution) images were simulated. Eq. 4-8 explains each required time in an FSC-LCD, where *f* is frame rate (60Hz), *N* and *n* are the number of fields and effective scanning backlight divisions respectively [69]. t_{TFT}, t_{LC}, and t_{LED} are the data addressing time, LC response time, and LED-BL flashing time. We assumed the addressing time for each gate-line was 5 μs, LED-BL flashing time was 1.5 ms,

and there were 5 (*n*=5) effective scanning backlight divisions in the Stencil-FSC system. The 180Hz Stencil-FSC method only required 3 fields to show a colorful image, therefore, the LC had 3 ms to completely response which maintained the image brightness and avoid color shift occurring. The 240Hz Stencil-FSC method required 4 fields, it meant one more field was required and resulted in the compression of available time. If image brightness would be maintained, the LC response time should be much shorter than 1.6 ms [70]. Besides, if LC response could not be speeded up, the LED-BL flashing time would be compressed and the LED pulse intensity should be enhanced to maintain image brightness. Once, the LED intensity vs. power was operated at nonlinear region, and then the power consumption would also be raised. That is the reason why the power consumption using 180Hz Stencil-FSC was lower than 240Hz Stencil-FSC (Table 5-1). The 360Hz-RGBKKK also had the same issue. Therefore, its power consumption might be larger than 68 Watts of using conventional 180Hz RGB-driving method.

$$\frac{1}{Nf} = \frac{t_{TFT}}{n} + t_{LC} + t_{LED}$$ (4-8)

Table 5-1   Comparisons between the conventional RGB-driving, 360HZ-RGBKKK [63], 240Hz Stencil-FSC [33]-[35], and 180Hz Stencil-FSC [36][37].

		Conventional RGB-driving	360Hz-RGBKKK	Stencil-FSC	
				240Hz	180Hz
Number of fields		3	6	4	3
*Required LC response time (ms)		3	0.2	1.6	3
Hardware implementation		Easy	Hard	High cost	Easy
**Average Power consumption (W)		68	>68 (estimated)	~35	<35 (estimated)
Optimization	BL divisions	Global	Global	24×24 (576)	32×24 (768)
	PSF (pixels) (Gaussian)	None	None	σ_x= 54 σ_y= 32	σ_x= 40 σ_y= 26
CBU		Serious (100%)	Imperceptible (57.2%)	Imperceptible (55.6%)	Imperceptible (50.4%)
Image fidelity		Good	Good	Good	Acceptable
*: Effective number of scanning backlight divisions: 5 [69]; LED flashing time: 1.5 ms; addressing time: 5 µs; number of gate-lines: 1080					
**: Based on the same brightness using the 15 test images (Table 4-1 and Fig. 5-5)					

5.3 Verification on a 120Hz 46-inch MVA LCD

The 180Hz Stencil-FSC method was verified on a 120Hz 46-inch MVA LCD. The pictures of *Soccer, Lily, and Color Ball* were used as the test images, and CBU images were taken by a digital still camera which was set up 2 meters from the LCD on a moving stage with a horizontal velocity of 200 cm/sec to simulate eye movement, as illustrated in Fig. 4-21. Because the 180Hz Stencil-FSC method showed most image luminance in the first field, the CBU phenomenon was much slighter when compared to the conventional RGB-driving method (top).

(a) Soccer   (b) Lily
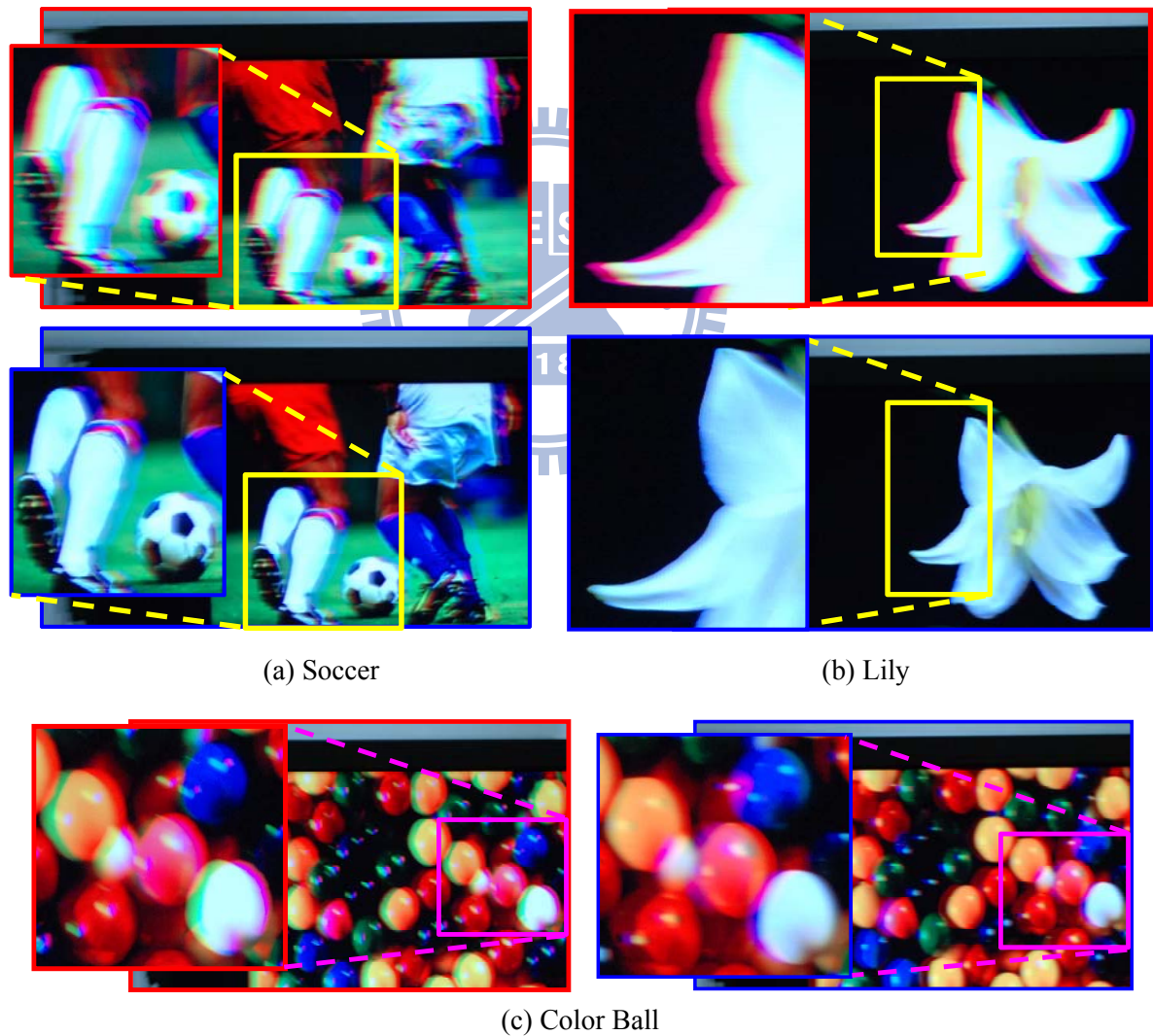
(c) Color Ball

Fig. 5-13   Experimental photos using conventional RGB-driving (red frame) and 180Hz Stencil-FSC methods (blue frame) of (a) Soccer, (b) Lily, and (c) Color Ball.

5.4 Summary

To make Stencil-FSC more feasible, we further reduced the field rate from 240Hz to 180Hz and proposed the 180Hz Stencil-FSC method to suppress the color breakup (CBU) issue. Using local color-backlight dimming technology, a high luminance green-based multi-color image was generated on a color filter-less LCD. Therefore, the luminance of residual red and blue color images was greatly reduced and effectively suppressed CBU. From the optimization results, 32x24 backlight divisions with two directional standard deviations of the Gaussian point spread function (σ_x=40 pixels and σ_y=26 pixels) suppressed CBU by 50% and made CBU almost imperceptible in experimental photos. Using the 180Hz Stencil-FSC method, the average image color differences of CIEDE2000 (ΔE_{00}) were less than 3 indicating acceptable image fidelity. In addition, the power consumption was further reduced to less than 35 Watts which was lower than that of 240Hz Stencil-FSC because of longer backlight flashing time. Finally, the 180Hz Stencil-FSC algorithm processing was also direct and simple, only including backlight determination, liquid crystal compensation, and simple subtraction. As a result, the 180Hz Stencil-FSC LCD has strong potential for future large-sized "Eco-Display" applications.

Chapter 6

CONCLUSION AND FUTURE WORK

A conventional liquid crystal display consists of a backlight module and a TFT-array LC panel which displays an image or video. Some researchers concerned that this combination was neither economical nor necessary, so several studies were focused on developing self-illuminating displays, such as plasma display panels (PDPs) or organic light emitting diode (OLED) displays. While LCD is more cost effective, OLED is considered to be a better technology, because of its high color gamut, high contrast ratio in all viewing angles, low power consumption while showing average image contents, and a thin profile. Even though the debate has been brewing for some time over the superiority of LCD or OLED display technologies, currently LCDs have dominated flat panel display market. Although current OLEDs have price and lifetime issues which limit OLED market, LCD manufacturing is still developing advanced technologies to further enhance image performance and cost-competitiveness. Consequently, this dissertation proposed novel methods to improve both high dynamic range and field sequential color technologies.

6.1 Conclusion

Reducing power consumption while enhancing image quality was successfully demonstrated using Stencil-FSC methods based on a dual-panel structure: a low resolution controllable RGB-LED backlight and a high resolution LC panel. The dual-panel provided more flexibility to present a vivid image or video. The backlight module first displayed a colorful, high contrast image, and then a high optical throughput LC panel maintained image details. The well-combined structure invalided the argument of using two optical structures to display an image. Following, this chapter reviewed the proposed methods of backlight module

and the whole LCD system including the dynamic backlight and the color filter-less LC panel (Fig. 6-1).
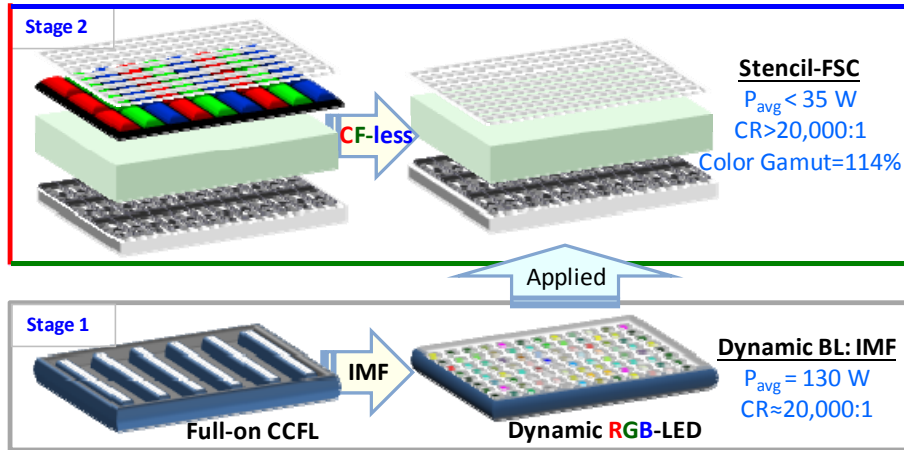
Fig. 6-1   Whole schema of final dissertation results.

6.1.1 Backlight Module: IMF for Dynamic Backlight Control

Differing from prior backlight determination methods, the inverse of a mapping function (IMF) method provided "dynamic" gamma functions for each input image to produce high contrast images. The IMF method was demonstrated on a 37-inch HDR-LCD. The experimental results achieved a high contrast ratio (~20,000:1) image, preserved clearer image details with low distortion (D=3.17%) compared to the prior backlight methods. Furthermore, IMF still maintained high brightness to present a more vivid image for human vision with an average power reduction of 30% compared to an LED full-on backlight LCD (~190W).

6.1.2 LC Panel: Color Filters Removed

For the LC panel, the optical throughput was further enhanced by a factor of 3 while getting rid of color filters in an FSC-LCD, as illustrated in Fig. 6-2. However, a lethal issue, color breakup (CBU) degraded image clarity and caused viewer discomfort. Most prior CBU suppression methods involved either inserting additional mono-color fields or

increasing the field rate. Unfortunately, LC response time prevented the implementation of these methods in large-sized FSC-LCDs.
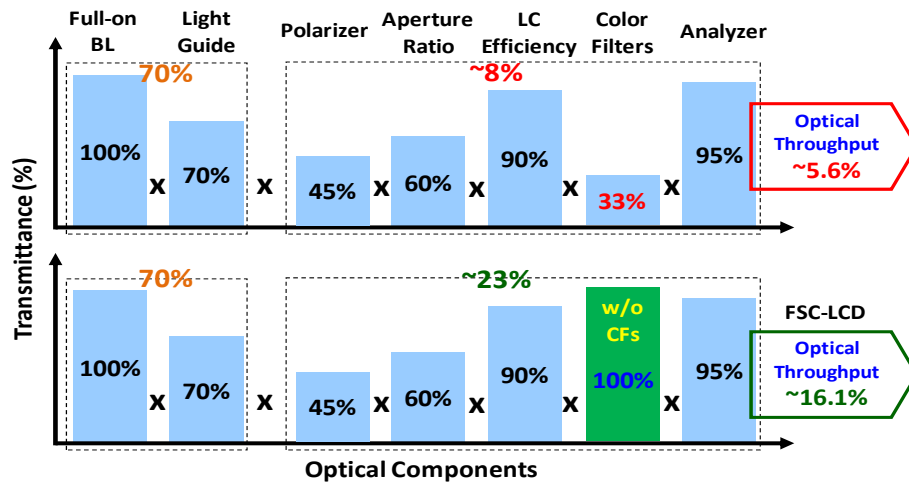
Fig. 6-2   Comparison of optical throughputs between a conventional LCD (top) and a color filter-less LCD (FSC-LCD).

6.1.3 Whole LCD System Based on Stencil-FSC Methods

In order to efficiently suppress CBU, the Stencil-FSC method ingeniously applied local color-backlight dimming technology to an FSC-LCD. The originality of Stencil-FSC was to use a multi-color image concentrating image luminance in a single field. The intensities of the residual primary-color sub-images were therefore greatly reduced. Using this concept, two field rates, 240Hz (4-field) and 180Hz (3-field), Stencil-FSC methods were demonstrated. Through simulations, CBU was suppressed by 50% for eighty test images when compared to conventional RGB-driving and made CBU almost imperceptible in experimental photos.

240Hz Stencil-FSC was realized on a 32-inch OCB-mode FSC-LCD which demonstrated in 35 Watts average power consumption, and a wide color gamut of 114% NTSC. Using the test image, *Lily*, 240Hz Stencil-FSC yielded a high static contrast of 26,000:1, power consumption of less than 28 Watts.

Furthermore, the field rate was reduced to 180Hz to make Stencil-FSC more feasible. A green-based multi-color image replaced the multi-color image of 240Hz Stencil-FSC. Therefore, the luminance of residual red and blue color images was also greatly reduced. The average power consumption was further reduced to less than 35 Watts because only three fields were required. The features of low field rate, simple, and direct algorithm processing made the 180Hz Stencil-FSC method more feasible in a color filter-less LCD.

In summary, Stencil-FSC successfully improved three main drawbacks of conventional LCDs: low optical throughput, imperfect dark state, and low color saturation. The experimental results verified a Stencil-FSC LCD has strong potential for future large-sized "Eco-Display" applications.

Table 6-1   Dissertation comparisons between objectives and results on a 32-inch LCD.

	Objectives	Stencil-FSC		Status
		240Hz	**180Hz**	
Contrast Ratio	> 20,000 : 1	**26,000 : 1**	**26,000 : 1** (estimated)	**V**
Color Gamut (% NTSC)	> 110	**114**	**114**	**V**
Power Consumption (W)	55	**35**	**< 35** (estimated)	**V**
Color Breakup (Relative CBU$_{RGB}$)	Imperceptible	**Imperceptible** (52.1%)	**Imperceptible** (52.7%)	**V**
Field Rate (Hz)	180	**240**	**180**	**V**
Image Fidelity	Good	**Good**	**Acceptable**	**Δ**
Ps: Power of conventional 32-inch LCDs (W) :		*CCFL-BL 110* *LED-BL 190*		

6.2   Remaining Issues

Comparing the results with the objectives of this dissertation, the 180Hz Stencil-FSC method almost reached all the objectives except for a minor issue in image fidelity, as shown in Table 6-1. To reduce the field rate from 240Hz to 180Hz, the green-field content was moved to the first multi-color field because the human eye is the most sensitive to green color.

However, an issue resulted from only choosing green information as the base color for all images. The issue was especially apparent in the image which contained abundant green information, such as illustrated in the purple circle of Fig. 6-3. To quantify the color distortion, a pixel distorted ratio ($PDR(\Delta E_{00}>3)$) is given by Eq. 6-1 which is defined as the ratio of the number of distorted pixels divided by the number of total pixels, where a distorted pixel means that its pixel color difference is larger than the acceptable value ($\Delta E_{00}>3$).

$$PDR(\Delta E_{00} > 3) \equiv \frac{\# \text{ of color distorted pixels}}{\# \text{ of total pixels}} \times 100\% \tag{6-1}$$

For the two test images, *Butterfly* and *Lotus*, their pixel distorted ratio ($PDR(\Delta E_{00}>3)$) were 46% and 40% respectively which was equivalent to half number of total pixels were distorted and reduced green color saturation. As mentioned in section 5.1.1, the first field LC signals were taken from green color; in this case, the red and blue color LC signals were lower than green LC signals. Therefore, even though the red and blue backlight intensities under the purple circles were low, the red and blue lights also propagated through the first field and contributed redundant luminance resulting in reduction of green color saturation.

|(a) Original images|(b) Simulated images|(c) Error images|
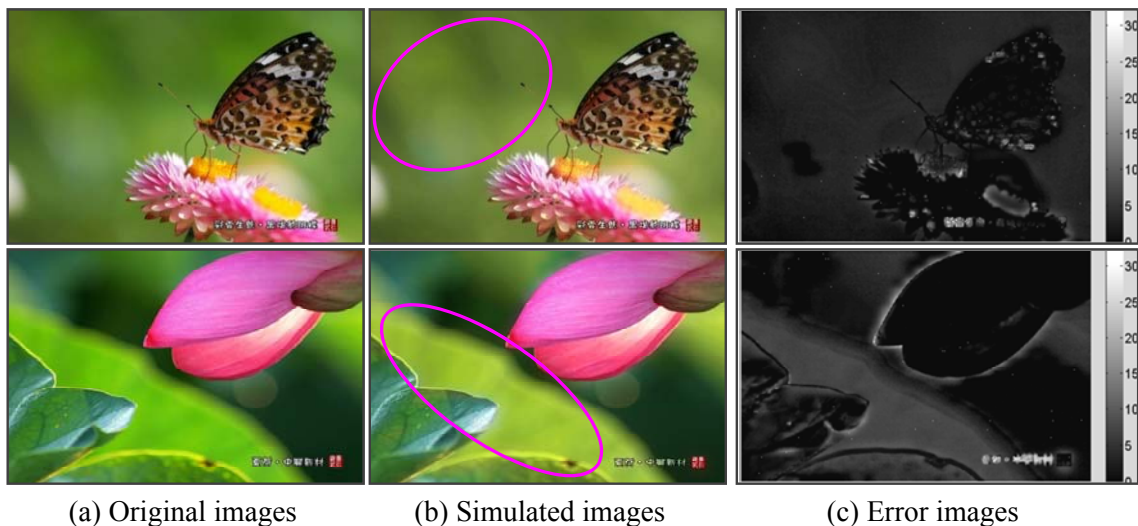
Fig. 6-3 Redundant red or blue light propagates through in the first green-based field-image resulting in reduction of green color saturation, especially in the purple circle. (a) Two test images of Butterfly and Lotus. (b) Simulated images after the 180Hz Stencil-FSC processing. (c) CIEDE2000 error images between test and processed images with PDRs($\Delta E_{00}>3$) of 46% and 40% respectively.

6.3   Future Work-- Green-Color Saturation Improvement

To resolve the minor issue of reduction of green color saturation, the 180Hz Stencil-FSC algorithm should be further improved. The distortion appeared when the LC signal of the first field (green LC signal in original algorithm) is not the minimum signal in each single pixel. Then, the redundant residual colors propagated through the first field. The preliminary suggestion is to dynamically choose the base-color for the first field instead of only using green base-color. The first base-color should be chosen in accordance with the least color of the test image content. In other words, the green-based field should be replaced with the minimum color field (named min-based field). The improved algorithm is shown in Fig. 6-4. The primary-colors of a test image should be averaged first, and then sorted by their magnitudes. Take *Lotus* as an example, the average value of blue color is less than those of red and blue colors. The blue color is inferred the minimum color content with the most minimum pixel value for *Lotus* from the average values sequence. Consequently, the blue color is chosen as the based-color and shown in the first field. The improved algorithm avoids redundant lights and produces higher image fidelity.

The average ΔE_{00} of *Butterfly* and *Lotus* are further reduced from 2.5 to 0.4 and 2.9 to 0.3, while *PDRs(ΔE_{00}>3)* are simultaneously reduced from 46% to 3.6% and 40% to 2.5%, respectively. The simulated images are difficult to distinguish from the original images, as shown in Fig. 6-5. Observing the CIEDE2000 error images (Fig. 6-5(c)), the color differences are almost imperceptible.

The image fidelity issue is nearly solved, but the green information is no longer to hide in the first multi-color field. Consequently, CBU suppression and image fidelity must be further balanced in the future. Finally, hardware parameters, including the number of backlight divisions and a point spread function, must also be optimized for implementation.

(a) Test image   (b) BL and LC panels   (c) Three field-images

If $Avg_B < Avg_R < Avg_G$
Min-color: color[min(Avg_R,Avg_G,Avg_B)]→Blue
Max-color: color[max(Avg_R,Avg_G,Avg_B)]→Green
Mid-color: color[middle(Avg_R,Avg_G,Avg_B)]→Red
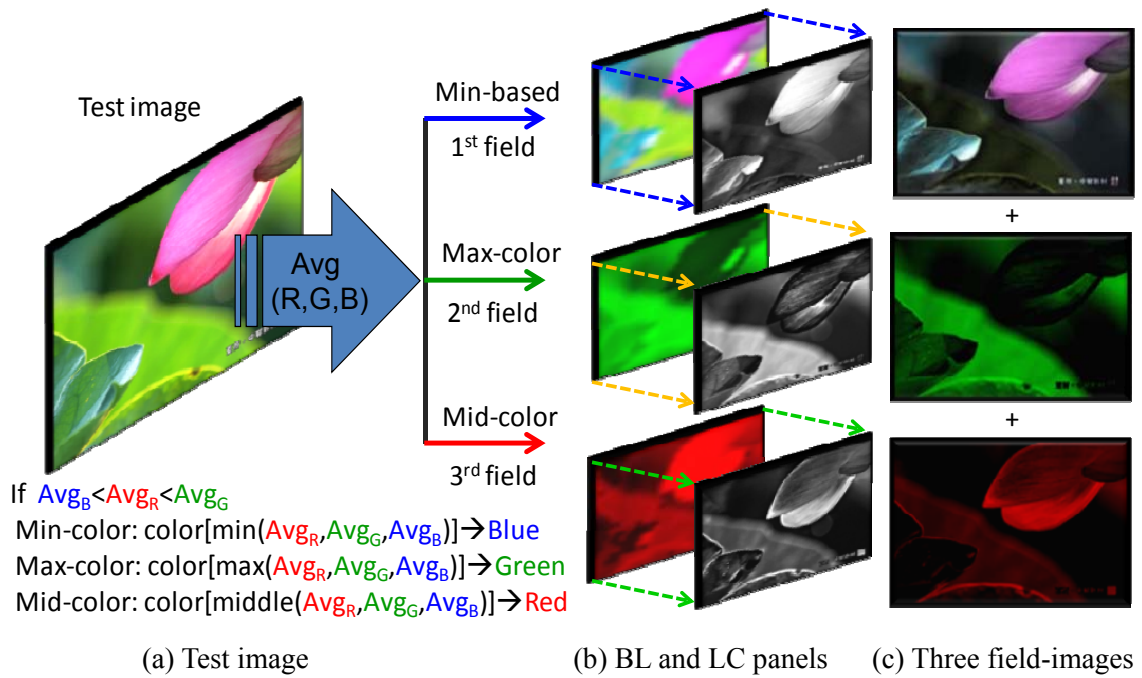
Fig. 6-4   The improved algorithm of the 180Hz Stencil-FSC method. (a) Test image-Lotus, (b) backlight and LC images, and (c) three field-images yielded.

(a) Original images   (b) Simulated images   (c) Error images
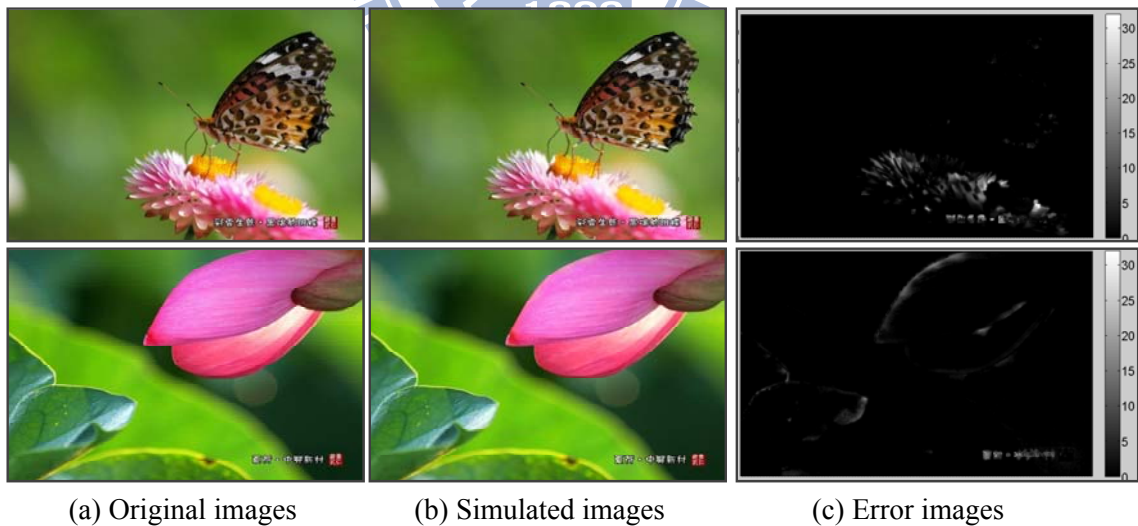
Fig. 6-5   The improved 180Hz algorithm avoids the redundant lights propagating through the first field-image and maintains image fidelity. (a) Two test images of Butterfly and Lotus. (b) Simulated images after the improved 180Hz Stencil-FSC processing. (c) CIEDE2000 error images between test and processed images with PDRs($\Delta E_{00}>3$) of 3.6% and 2.5% respectively.

6.4　Future Perspectives

6.4.1　Is 120Hz Stencil-FSC Possible? — Further Field Rate Reduction

Except for reduction of green saturation, the 180Hz field rate might be further decreased. The OCB-mode LC response time may reach 3 ms making a 180Hz field rate practicable. Nevertheless, the cost of an OCB-mode LCD is still higher than that of current commercial LC modes, such as twisted nematic (TN), multi-domain vertical alignment (MVA), or in-plane switching (IPS) because of high demand-and-supply cost and the particular compensated film was required. Therefore, the cost issue must be noticed for future mass production. If the field rate could be reduced to 120Hz, current commercial LC modes would be used on a color filter-less LCD by the proposed Stencil-FSC to reduce power consumption and panel material cost [71].
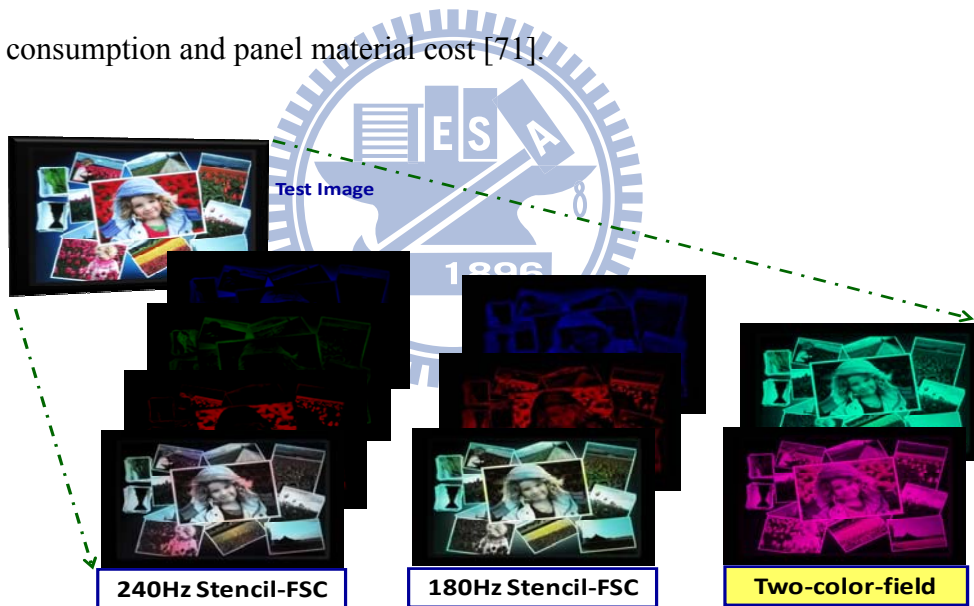
Fig. 6-6　Target image_ Girl (©Microsoft), and each field-image using the 240Hz Stencil-FSC, 180Hz Stencil-FSC, and upgraded 120Hz Stencil-FSC methods [71].

6.4.2　Is an LCD Powered by a Battery Possible?— Further Power Reduction

An amazing concept is an LCD-TV powered by a battery, which was presented in 2009 SID held in San Antonio, TX, USA [72]. Currently, the Stencil-FSC LCD-TV uses a 3-in-1 RGB-LED backlight system to enhance image quality while simultaneous reducing power

consumption to less than 35 Watts. However, the average power efficiency of RGB-LED is only 40 lm/W, which is lower than that of a CCFL. To make a battery-powered more practicable for a Stencil-FSC LCD-TV, the high power efficiency of 150 lm/W white-light LED [6] should be added onto the RGB-set to be a 4-in-1 RGBW backlight system, as illustrated in Fig. 6-7.
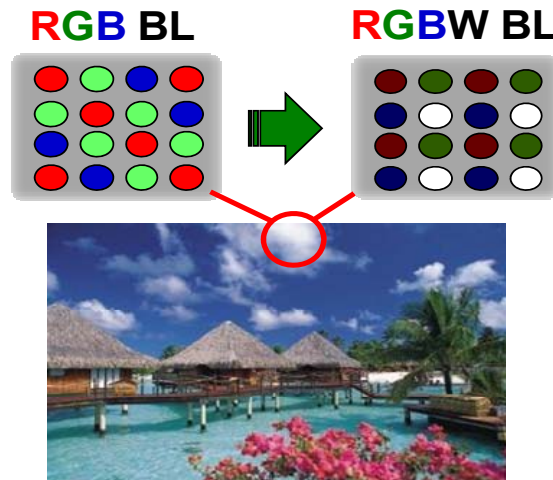
Fig. 6-7   Further power reduction through using RGBW 4-in-1 LED in the backlight system.

As we enjoy the convenience and entertainment from increasingly developed technologies, have we ever considered that the Earth is gradually moving forward catastrophe? "Love Our Earth" is no longer a slogan; in fact, we have a moral obligation to maintain a healthy Earth. As a global citizen, small changes to our daily routine (e.g. biking, carpooling, or taking mass transportation wherever possible) can add up to big differences in helping the Earth continue. As engineers, we wish to design new products and develop advanced technologies while simultaneously considering practicability and eco-friendliness. This dissertation successfully demonstrated the Stencil-FSC method on a high optical throughput color filter-less LCD and showed a good image quality using only 35 Watts average power consumption on a 32-inch LCD. The required power is equivalent to 20% of the same size full-on LED backlight LCD-TV. In the future, we expect that human beings will enjoy multimedia with families or friends and simultaneously help the Earth.

REFERENCES

[1] An Inconvenient Truth Official Site: retrieved on June 18, 2009, from the:
http://www.climatecrisis.net/

[2] H. Kawamoto, "The History of Liquid-Crystal Displays," in *Proceedings of the IEEE*,
vol. **90**(4), pp. 460-500 (2002).

[3] "Realizing a dream of television hanging on the wall 8.6 inch liquid crystal museum,"
Sharp Corp. News Release, Apr. 25, 1991.

[4] LED Backlighting for LCDs Requires Unique Drivers, in Power Electronics Technology:
retrieved on June 26, 2009, from the:
http://powerelectronics.com/power_management/led_drivers/led-backlighting-lcd-power
-efficiency-0512/

[5] 32" LCD TV materials cost structure (Q4' 2008): retrieved on June 24, 2009, from the:
http://www.displaysearch.com/cps/rde/xchg/displaysearch/hs.xsl/TFT_Cost_Report_Rel
ease.asp

[6] NICHIA Corporation: retrieved on June 18, 2009, from the: http://www.nichia.com/

[7] S. Sakai, "A Thin LED Backlight System with High Efficiency for Backlighting 22-in.
TFT-LCDs," in *Proceedings of SID Symposium Digest*, vol. **35**, pp. 1218-1221 (2004).

[8] ClearLCD featuring Aptura™, "Dynamic Scanning Backlight makes ClearLCD™ TV
come alive."
http://www.press.ce.philips.com/apps/c_dir/e3379701.nsf/0/2515E879E57E9131C12570
5B0032FB00/$File/ClearLCD_Aptura%20technical%20backgrounder.pdf

[9] H. Seetzen, Lorne A. Whitehead, and Greg Ward, "A High Dynamic Range Display
Using Low and High Resolution Modulators," in *Proceedings of SID Symposium Digest*,
vol. **34**, pp. 1450-1453 (2003).

[10] H. Seetzen, W. Heidrich, W. Stuerzlinger, G. Ward, L. Whitehead M. Trentacoste, A.
Ghosh, and A. Vorozcovs, "High Dynamic Range Display Systems," *SIGGRAPH 2004,
ACM Transactions on Graphics*, vol. **23**(3), pp. 760-768 (2004).

[11] E. Y. Oh, S. H. Baik, M. H. Sohn, K. D. Kim, H. J. Hong, J. Y. Bang, K. J. Kwon, M. H.
Kim, H. Jang, J. K. Yoon, and I. J. Chung, "IPS-mode dynamic LCD-TV realization with
low black luminance and high contrast by adaptive dynamic image control technology,"
J. Soc. Info. Display, vol. **13**, pp. 215-219 (2005).

[12] M.Trentacoste, W. Heidrich, L. Whitehead, H. Seetzen, and G. Ward, "Photometric
image processing for high dynamic range displays", *J. Visual Communication and Image
Representation*, vol.**18**, pp. 439-451 (2007).

[13] H. Chen, J. Sung, T. Ha, and Y Park, "Locally pixel-compensated backlight dimming on
LED-backlit LCD TV," *J. Soc. Info. Display*, vol. **15**, pp. 981-988 (2007).

[14] Y. K. Cheng, Y. H. Lu, C. H. Tien, and H. P. D. Shieh "Design and Evaluation of Light Spread Function for Area-Adaptive LCD System," *J. Display Technol.*, vol. **5**(1), pp. 34-39 (2009).

[15] E. H. A. Langendijk, R. Muijs, and W. van Beek, "Contrast gain and power savings using local dimming backlights," *J. Soc. Info. Display*, vol. **16**, pp. 1237-1242 (2009).

[16] M. G. Clark and I. A. Shanks, "A field-sequential color CRT using a liquid crystal color switching," in *Proceedings of SID Symposium Digest*, vol. **13**, pp. 172–173 (1982).

[17] R. Vatne, P. A. Johnson, Jr., and P. J. Bos, "A LC/CRT field-sequential color display," in *Proceedings of SID Symposium Digest*, vol. **14**, pp. 28–29 (1983).

[18] H. Hasebe and S. Kobayashi, "A full-color field sequential LCD using modulated backlight," in *Proceedings of SID Symposium Digest*, vol. **16**, pp. 81–83 (1985).

[19] T. Miyashita, P. J. Vetter, Y. Yamaguchi, and T. Uchida, "Wide-Viewing-Angle Display Mode for Active-Matrix LCDs Using a Bend-Alignment Liquid-Crystal Cell," *J. Soc. Info. Display*, vol. **3**(1), pp. 29-34 (1995).

[20] F. Yamada, H. Nakamura, Y. Sakaguchi, Y. Taira, "Sequential-color LCD based on OCB with an LED backlight," *J. Soc. Info. Display*, vol. **10**, pp. 81-85 (2002).

[21] J. H. Lee, X. Zhu, and S. T. Wu, "Novel Color-Sequential Transflective Liquid Crystal Displays," *J. Display Technol.*, vol. **3**(1), pp. 2-8 (2007).

[22] B. Hoefflinger (Ed.), *High-Dynamic-Range (HDR) Vision*, pp. 1-4, Springer (2007).

[23] L. Kerofsky and S. Daly, "Brightness Preservation for LCD Backlight Dimming," *J Soc Info Display*, vol. **14**, pp. 1111-1118 (2006).

[24] Meyer CH, Lasker AG, Robinson DA, "The Upper Limit of Human Smooth Pursuit Velocity," *Vision Research*, vol. **25**(4), pp. 561-563 (1985).

[25] Toni Järvenpää, "Measuring Color Breakup of Stationary Images in Field-Sequential-Color Displays," in *Proceedings of SID Symposium Digest*, vol. **35**, pp. 82-85 (2004).

[26] Yohso and K. Ukai, "How color break-up occurs in the human-visual system: The mechanism of the color break-up phenomenon," *J. Soc. Info. Display*, vol. **14**(12), pp. 1127-1133 (2006).

[27] T. Kurita and T. Kondo, "Evaluation and Improvement of Picture Quality for Moving Images on Field-sequential Color Displays," *International Display Workshop*, pp. 69-72 (2000).

[28] J. B. Eichenlaub, "Development and Preliminary Evaluation of Field Sequential LCD Free of Color Breakup," in *Proceedings of SID Symposium Digest*, vol. **25**, pp. 293-296 (1994).

[29] T. Jarvenpaa, "Measuring Color Breakup of Stationary Image in Field-Sequential-Color Displays," *J. Soc. Info. Display*, vol. **13**, pp. 139-144 (2005).

[30] Miettinen, R. Näsänen, and J. Häkkinen, "Effects of Saccade Length and Target Luminance on the Refresh Frequency Threshold for the Visibility of Color Break-Up," *J. Display Technol.*, vol. **4**(1), pp. 81-85 (2008).

[31] F. C. Lin, C. Y. Liao, L. Y. Liao, Yi-Pai Huang, Han-Ping D. Shieh, Po-Jen Tsai, Te-Mei Wang, and Yao-Jen Hsieh "Inverse of Mapping Function (IMF) Method for Image Quality Enhancement of High Dynamic Range LCD TVs," in *Proceedings of SID Symposium Digest*, vol. **38**, pp. 1343-1346 (2007).

[32] F. C. Lin, L. Y. Liao, C. Y. Liao, Y. P. Huang, H. P. D. Shieh, T. M. Wang, and S. C. Yeh, "Dynamic Backlight Gamma on High Dynamic Range LCD TVs," *J. Display Technol.*, vol. **4**(2), pp. 139-146 (2008).

[33] F. C. Lin, C. M. Wei, Y. P. Huang, and H. P. D. Shieh, "Stencil-FSC Method for CBU Suppression and Low Power Consumption in Field-Sequential LCDs," in *Proceedings of SID Symposium Digest*, vol. **39**, pp. 1108-1111 (2008).

[34] F. C. Lin, Y. P. Huang, C. M. Wei, and H. P. D. Shieh, "Color Breakup Suppression and Low Power Consumption by Stencil-FSC Method in Field-Sequential LCDs," *J. Soc. Info. Display*, vol. **17**(3), pp. 221-228 (2009).

[35] F. C. Lin, Y. P. Huang, C. M. Wei, and H. P. D. Shieh, "Color Breakup Suppression and Low Power Consumption by Stencil-FSC Method in Field-Sequential LCDs," accepted by *J. Display Technol.* (2009/6).

[36] F. C. Lin, Y. P. Huang, C. C. Tsai, and H. P. D. Shieh, "Color Breakup Reduction by 180Hz Stencil-FSC Method in Large-Sized Color Filter-Less LCD-TVs," in *Proceedings of SID Symposium Digest*, vol. **40**, pp. 235-238 (2009).

[37] F. C. Lin, Y. P. Huang, and H. P. D. Shieh, "Color Breakup Reduction by 180Hz Stencil-FSC Method in Large-Sized Color Filter-Less LCDs," accepted by *J. Display Technol.* (2009/6).

[38] P. J. Bos and K. R. Koehler, "The pi-Cell: A Fast Liquid-Crystal Optical-Switching Device," *Molecular Crystals and Liquid Crystals*, vol. **113**, pp. 329-339 (1984).

[39] Y. Yamaguchi, T. Miyashita and T. Uchida, "Wide-Viewing-Angle Display Mode for the Active-Matrix LCD Using Bend-Alignment Liquid-Crystal Display," in *Proceedings of SID Symposium Digest*, vol. **24**, pp. 277-280 (1993).

[40] Simple Anatomy of the Retina, retrieved on July 12, 2009, from the: http://webvision.med.utah.edu/sretina.html

[41] Eugene Hecht, *Optics* (3rd Edition), Addison Wesley Longman, Inc., pp. 203-207 (1998).

[42] G. A. Osterberg, "Topography of the layer of rods and cones in the human retina," *Acta Ophthalmol Suppl*. vol. **13**, pp.1-103 (1935).

[43] CIE 170-1:2006 Cone Fundamentals for Various Field Sizes and Observer Ages, retrieved on July 12, 2009, from the: http://www.cis.rit.edu/mcsl/online/cie.php

[44] Some Characteristics of Early Color Vision: retrieved on July 14, 2009, from the: http://www.ling.upenn.edu/courses/ling525/color_vision.html

[45] CIE 1931 color space, in Wikipedia, retrieved on July 14, 2009, from the: http://en.wikipedia.org/wiki/CIE_1931_color_space

[46] Mark D. Fairchild, *Color Appearance Models*. John Wiley & Sons, Ltd, 2005.

[47] Roy S. Berns, *Principle of Color Technology*, John Wiley & Sons, Inc. pp. 63-121 (2000).

[48] CIE, "Improvement to industrial colour-difference evaluation," *CIE Publication*, No. 142-2001, Central Bureau of the CIE, Vienna (2001).

[49] G.M. Johnson and M.D. Fairchild, "A top down description of S-CIELAB and CIEDE2000," *Color Research and Application*, vol. **28**, pp. 425-435 (2003).

[50] M. R. Luo, G. Cui, and B. Rigg, "The development of the CIE 2000 colour difference formula," *Color Research and Application*, vol. **26**, pp. 340-350 (2001).

[51] R. C. Gonzalez and R. E. Woods, *Digital Image Processing* (2nd Edition), Prentice-Hall, New Jersey, pp. 75-214 (2002).

[52] T. C. Jen, Brian Hsieh, and S. J. Wang, "Image Contrast Enhancement Based on Intensity-Pair Distribution," *Proc IEEE'05 International Conference on Image Processing*, vol. **1**, I-913-16 Genova (2005).

[53] Frosio, G. Ferrigno, and N. A. Borghese, "Enhancing Digital Cephalic Radiography With Mixture Models and Local Gamma Correction," *IEEE Trans Medical Imaging*, vol. **25**(1), pp. 113-121 (2006).

[54] T. C. Hsu, T. M. Lin, and Y. C. Chen, "Fuzzy Contrast Correction (FCC) for Image Contrast Enhancement," in *Proceedings of SID Symposium Digest*, vol. **37**, pp. 303-305 (2006).

[55] C. C. Sun, S. J. Ruan, M. C. Shie, and T. W. Pai, "Dynamic Contrast Enhancement based on Histogram Specification," *IEEE Trans Consumer Electronics*, vol. **51**(4), pp. 1300-1305 (2005).

[56] L. Y. Liao, F. C. Lin, Y. P. Huang, H. P. D. Shieh, and S. C. Yeh, "A Real-Time Liquid Crystal Signal Compensation Method for High Dynamic Range LCD," *International Display Workshop*, vol. **14**, DES5-1L (2007).

[57] L. Y. Liao, Y. P. Huang, and S. C. Yeh, "A Real-Time Image Compensation for High Dynamic Range LCDs," in *Proceedings of SID Symposium Digest*, vol. **39**, pp. 764-767 (2008).

[58] Konica Minolta Sensing: Measurement Inst. CA-210, Retrieved July 1, 2009, from the: http://www.konicaminolta.com/instruments/products/display/color-analyzer/ca210/featur es.html

[59] E. H. A. Langendijk, S. Swinkels, D. Eliav, and M. Ben-Chorin, "Suppression of color breakup in color-sequential multi-primary projection displays," *J. Soc. Info. Display*, vol. **14**, pp.325-329 (2006).

[60] M. Mori, T. Hatada, K. Ishikawa, T. Saishouji, O. Wada, J. Nakamura, and N. Terashima, "Mechanism of color breakup in field-sequential-color projectors," *J. Soc. Info. Display*, vol. **7**, pp. 257-259 (1999).

[61] P. C. Baron, P. Monnier, A. L. Nagy, D. L. Post, L. Christianson, J. Eicher, and R. Ewart, "Can Motion Compensation Eliminate Color Breakup of Moving Objects in Field-

Sequential Color Displays?" in *Proceedings of SID Symposium Digest*, vol. **27**, pp. 843-846 (1996).

[62] N. Koma and T. Uchida, "A new field-sequential-color LCD without moving-object color break-up," *J. Soc. Info. Display*, vol. **11**, pp. 413-417 (2003).

[63] K. Sekiya, T. Miyashita, and T. Uchida, "A Simple and Practical Way to Cope with Color Breakup on Field Sequential Color LCDs," in *Proceedings of SID Symposium Digest*, vol. **37**, pp. 1661-1664 (2006).

[64] C. H. Chen, F. C. Lin, Y. T. Hsu, Y. P. Huang, and H. P. D. Shieh, "A Field Sequential Color LCD Based on Color Fields Arrangement for Color Breakup and Flicker Reduction," *J. Display Technol.*, vol. **5**(1), pp. 34-39 (2009).

[65] Y. P. Huang, K. H. Chen, C. H. Chen, F. C. Lin, and H. P. D. Shieh, "Adaptive LC/BL Feedback Control in Field Sequential Color LCD Technique for Color Breakup Minimization," *J. Display Technol.*, vol. **4**(3), pp. 290-295 (2008).

[66] F. Li, X. Feng, I. Sezan, and S. Daly, "Two approaches to derive LED driving signals for high-dynamic-range LCD backlights," *J. Soc. Info. Display*, vol. **15**, pp. 989-996 (2007).

[67] C. H. Chen and H. P. D. Shieh, "Effects of Backlight Profiles on Perceived Image Quality for High Dynamic Range LCDs," *J. Display Technol.*, vol. **4**(2), pp. 153-159, 2008.

[68] Rafael C. Gonzalez and Richard E. Woods, *Digital Image Processing, 2nd Edition* (Prentice Hall, 2002), p.176.

[69] N. Koma, T. Miyashita, and T. Uchida, "A novel driving method for field sequential color using an OCB TFT-LCD," *J. Soc. Info. Display*, vol. **9**(4), pp. 331-336 (2001).

[70] S. Gauza, X. Zhu, W. Piecek, R. Dabrowski, and S. T. Wu, "Fast Switching Liquid Crystals for Color-Sequential LCDs," *J. Display Technol.*, vol. **3**(3), pp. 250-252 (2007).

[71] Y. K. Cheng, Y. R. Cheng, Y. P. Huang, and H. P. D. Shieh, "Two-Color Field-Sequential Method for Color-Filter-Free MVA-LCDs," in *Proceedings of SID Symposium Digest*, vol. **40**, pp. 239-242 (2009).

[72] H. P. D. Shieh, Y. P. Huang, F. C. Lin, H. M. P. Chen, and Y. K. Cheng, "Eco-Display – an LCD-TV Powered by a Battery?" in *Proceedings of SID Symposium Digest*, vol. **40**, pp. 228-231 (2009).

APPENDIX

80 Test Images
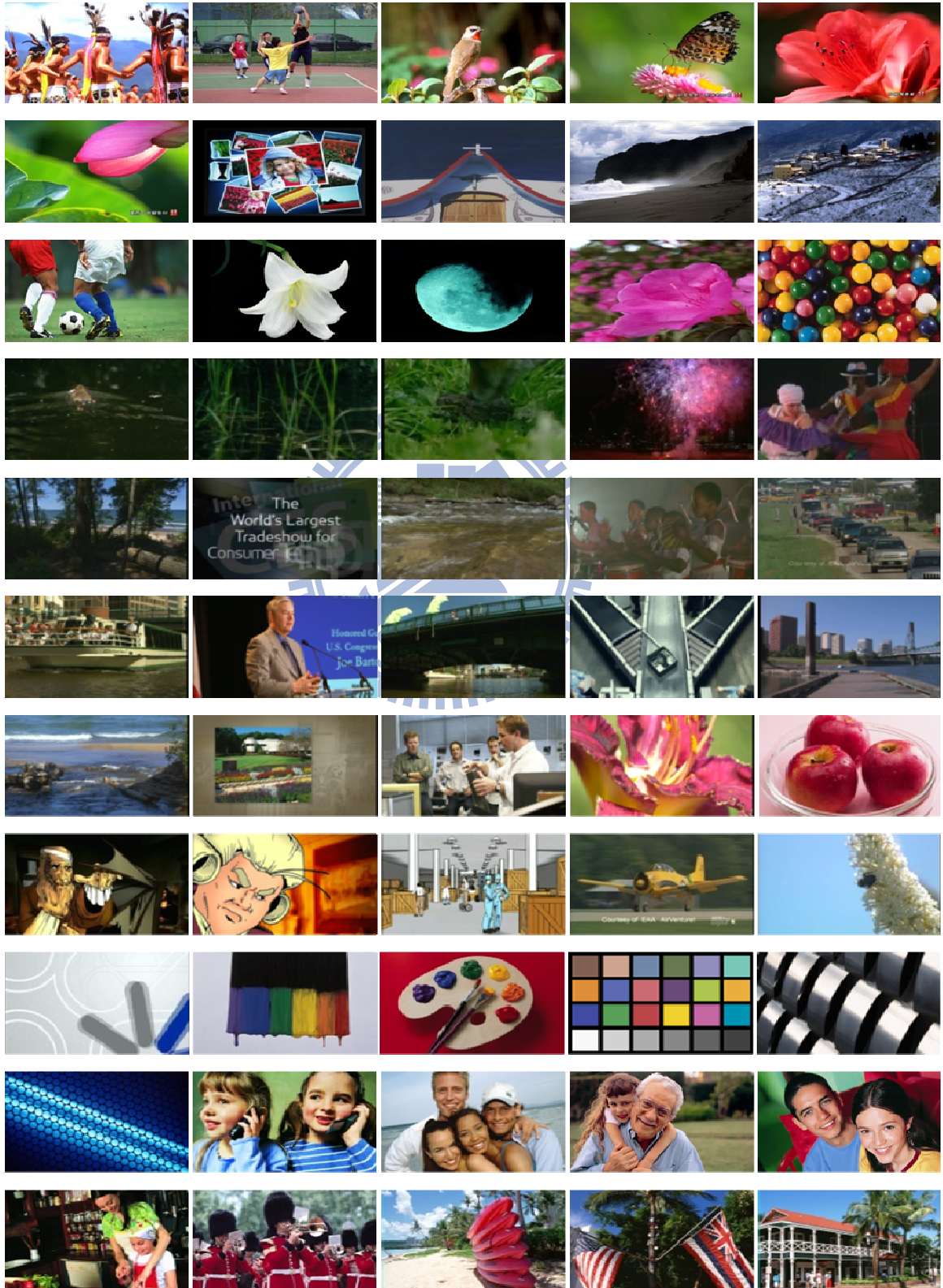
CURRICULUM VITAE

- ## PERSONAL INFORMATION

  - Date of Birth－1978/02/10
  - Place of Birth－Taichung, Taiwan
  - Nationality－Taiwan
  - Gender－Male
  - Marital Status－Married
  - Language－Chinese and English
  - Academic Degree－Ph.D.
  - E-mail: fclin.eo93g@nctu.edu.tw
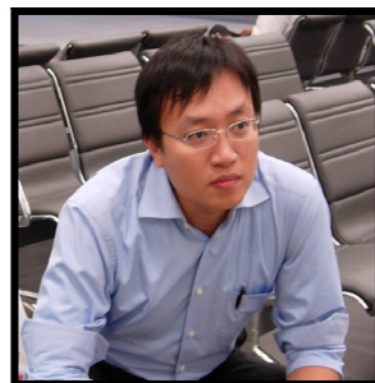
- ## EDUCATION

  - **2005/07- 2009/08   Ph. D. in Institute of Electro-Optical Engineering**

    National Chiao Tung University, Hsinchu, Taiwan

    * Dissertation－"A High Image Quality and Low Power Consumption
         Eco-LCD Using Stencil Field-Sequential-Color Methods"

    * Advisors－Prof. Han-Ping D. Shieh and Prof. Yi-Pai Huang

  - **2000/09- 2002/06   MS in Department of Physics**

    National Cheng Kung University, Tainan, Taiwan

    * Thesis－"Spectroscopy Studies of the Cs_2 $B^1\Pi_u$ State"

    * Advisor－Prof. Chin-Chun Tsai

  - **1996/09- 2000/06   BS in Department of Physics**

    National Cheng Kung University, Tainan, Taiwan

    * Project－"Image Processing with LabVIEW Software"

    * Advisor－Prof. Chin-Chun Tsai

- ## EXPERIENCE

  - **2005/07- 2005/08   Internship in Research & Design Center**

    Chuanghwa Picture Tubes, LTD., Taoyuan, Taiwan

    * Project－"Field-Sequential-Color with OCB-Mode LCDs"

  - **2005/01- 2005/04   ESL Student**, Hunter College, NYC, USA

  - **2003/07- 2005/01   Artillery Officer,** Kaoshiung, Taiwan

  - **2002/09- 2003/06   Physics Intern,** Tainan Girls' Senior High School, Tainan, Taiwan

- **AWARDS**
  - 2007/12: Student Paper Award by Optics & Photonics Taiwan
  - 2007/12: Student Paper Award by Optics & Photonics Taiwan
  - 2008/04: Paper Invited for publication in the Special Section of JSID titled "Best of the SID'08 Symposium."
  - 2008/07: Best Industry-University Cooperative Research Award by Chuanghwa Picture Tubes.
  - 2008/09: First Award of Display Design Competition of Northern Taiwan.
  - 2008/11: The Second Place of 2008 National Display Design Final Competition.
  - 2008/12: Student Paper Award by Optics & Photonics Taiwan
  - 2009/06: Research Paper Award of 2008 National Innovative Education Program on Image Display Technology

Time		Title	Organization	
2007	Dec.	Student Paper Award	Optics & Photonics Taiwan	
	Dec.	Student Paper Award	Optics & Photonics Taiwan	
2008	Apr.	Best of the SID'08 Symposium	Journal of SID	
	July	Best Industry-University Cooperative Research	CPT	
	Sep.	First Award of Display Design Competition	Ministry of Education	
	Nov.	Second Place of 2008 National Display Design Final Competition	Ministry of Education	
	Dec.	Student Paper Award	Optics & Photonics Taiwan	
2009	June	Research Paper Award of 2008 National Innovative Education Program on Image Display Technology	Ministry of Education	
	Sep.	NSC Scholarship (千里馬-博士後研究)	National Science Council	

● <u>PUBLICATIONS</u>

■ **Journal Papers**

(1) **Fang-Cheng Lin**, Lin-Yao Liao, Cheng-Yu Liao, Yi-Pai Huang, Han-Ping D. Shieh, Te-Mei Wang, and Szu-Che Yeh, "Dynamic Backlight Gamma on High Dynamic Range LCD TVs," *J. Display Technol.*, vol. **4**(2), pp. 139-152 (2008). [NSC96-2628-E-009-020-MY3]

(2) Yi-Pai Huang, Ke-Horng Chen, Chun-Ho Chen, **Fang-Cheng Lin**, and Han-Ping D. Shieh, "Adaptive LC/BL Feedback Control in Field Sequential Color LCD Technique for Color Breakup Minimization," *J. Display Technol.*, vol. **4**(3), pp. 290-295 (2008). [NSC96-2221-E- 009-113-MY3]

(3) Chun-Ho Chen, **Fang-Cheng Lin**, Ya-Ting Hsu, Yi-Pai Huang, and Han-Ping D. Shieh, "A Field Sequential Color LCD Based on Color Fields Arrangement for Color Breakup and Flicker Reduction," *J. Display Technol.*, vol. **5**(1), pp. 34-39 (2009).

(4) **Fang-Cheng Lin**, Yi-Pai Huang, Ching-Ming Wei, and Han-Ping D. Shieh, "Color Breakup Suppression and Low Power Consumption by Stencil-FSC Method in Field-Sequential LCDs," *J Soc Info Display*, vol. **17**(3), pp. 221-228 (2009). [NSC96-2221-E-009-113-MY3]

(5) **Fang-Cheng Lin**, Yi-Pai Huang, Ching-Ming Wei, and Han-Ping D. Shieh, "Color Filter-Less LCDs in Achieving High Contrast and Low Power Consumption by Stencil-Field-Sequential-Color Method," accepted by *J. Display Technol.* (2009/6)

(6) **Fang-Cheng Lin**, Yi-Pai Huang, and Han-Ping D. Shieh, "Color Breakup Reduction by 180Hz Stencil-FSC Method in Large-Sized Color Filter-Less LCDs," accepted by *J. Display Technol.* (2009/6)

■ **Conference Papers**

<u>International</u>:

(1) **Fang-Cheng Lin**, Cheng-Yu Liao, Lin-Yao Liao, Yi-Pai Huang, Han-Ping D. Shieh, Po-Jen Tsai, Te-Mei Wang, and Yao-Jen Hsieh "Inverse of Mapping Function (IMF) Method for Image Quality Enhancement of High Dynamic Range LCD TVs," *SID Symposium Digest Tech Papers*, vol. **38**, pp. 1343-1346, (2007/5).

(2) Shu-Ping Yan, Yu-Kuo Cheng, **Fang-Cheng Lin**, Ching-Ming Wei, Yi-Pai Huang, and Han-Ping D. Shieh, "A Visual Model of Color Break-Up for Design Field-Sequential LCDs," *SID Symposium Digest Tech Papers*, vol. **38**, pp. 338-341 (2007/5).

(3) Cheng-Yu Liao, **Fang-Cheng Lin**, Lin-Yao Liao, Yi-Pai Huang, and Han-Ping D. Shieh, "Inverse of Mapping Function Method for Image Quality Enhancement of Dual-Panel Displays," *IDMC 2007*, pp.431-434 (2007/7).

(4) Ya-Ting Hsu, **Fang-Cheng Lin**, Chun-Ho Chen, Yi-Pai Huang, and Han-Ping D. Shieh, "Drive and Control Circuitry of OCB Field-Sequential Color LCD with High Data Rate," *IDMC 2007*, pp.435-438 (2007/7).

(5) Sheng-Chang Chen, Shu-Ping Yan, Yu-Kuo Cheng, **Fang-Cheng Lin**, Ching-Ming Wei, Yi-Pai Huang, and Han-Ping D. Shieh, "A Human Visual Model for Color Break-Up Artifact in Design Field-Sequential Color LCDs," *IDMC 2007*, pp. 872-875 (2007/7).

(6) Yi-Pai Huang, **Fang-Cheng Lin**, Cheng-Yumr Liao, Ya-Ting Hsu, Wei-Kai Huang, Cheng-Han Tsao, Lin-Yao Liao, Chun-Ho Chen, Han-Ping D. Shieh, "Advanced technologies for high quality LC display," *Optical Fiber Communication and Optoelectronics Conference*, Asia, pp. 12-14 (2007/10).

(7) Ya-Ting Hsu, **Fang-Cheng Lin**, Chun-Ho Chen, Yi-Pai Huang, and Han-Ping D. Shieh, "A Field Sequential Color LCD Based on Color Field Arrangement for Color Breakup and Flicker Reduction," *IDW'07*, pp. 59-62 (2007/12).

(8) Lin-Yao Liao, **Fang-Cheng Lin**, Yi-Pai Huang, Han-Ping D. Shieh, and Szu-Che Yeh, "A Real-Time Liquid Crystal Signal Compensation Method for High Dynamic Range LCD," *IDW'07*, pp. 1433-1434 (2007/12).

(9) **Fang-Cheng Lin**, Yi-Pai Huang, Ching-Ming Wei, Han-Ping D. Shieh, Chi-Chung Tsai, and Wen-Chih Tai, "Stencil-FSC Method for Color Break-Up Suppression and Low Power Consumption in Field-Sequential LCDs," *SID Symposium Digest Tech Papers*, vol. **39**, pp. 1108-1111 (2008/5). [NSC96-2221-E-009-113-MY3]

(10) Guo-Zhen Wang, Yi-Pai Huang, **Fang-Cheng Lin**, Han-Ping D. Shieh, and Szu-Che Yeh, "Delta-Color Adjustment (DCA) Method for Color Controlled Backlight of High Dynamic Range LCD-TVs," *SID Symposium Digest Tech Papers*, vol. **39**, pp. 768-771 (2008/5). [NSC96-2221-E-009-113-MY3]

(11) Shih-Hsun Chien, Chun-Ho Chen, **Fang-Cheng Lin**, Yi-Pai Huang, Han-Ping D. Shieh, Shian-Jun Chiou, and Wen-Chih Tai, "Adaptive Backlight in Field Sequential Color Display for Optimizing Color Breakup Suppression," *IDMC 2009*, Wed-S10-04 (2009/4).

(12) Chi-Chu Tsai, **Fang-Cheng Lin**, Yi-Pai Huang, Ching-Ming Wei, Han-Ping David Shieh, Shian-Jun Chiou, and Wen-Chih Tai, "Color Breakup Suppression in Color Filter-Less LCDs by Optimized Stencil-Field-Sequential-Color Method," *IDMC 2009*, Wed-P5-18 (2009/4).

(13) Han-Ping D. Shieh, Yi-Pai Huang, **Fang-Cheng Lin**, Huang-Ming P. Chen, and Yu-Kuo Cheng, "Eco-Display– an LCD-TV Powered by a Battery?" *SID Symposium Digest Tech Papers*, vol. **40**, pp. 228-231 (2009/6). [NSC96-2628-E009-021-MY3]

(14) **Fang-Cheng Lin**, Yi-Pai Huang, Ching-Ming Wei, and Han-Ping D. Shieh, "Color Breakup Reduction by 180Hz Stencil-FSC Method in Large-Sized Color Filter-Less LCD-TVs," *SID Symposium Digest Tech Papers*, vol. **40**, pp. 235-238 (2009/6).

Domestic:

(1) Lin-Yao Liao, **Fang-Cheng Lin**, Yi-Pai Huang, Han-Ping D. Shieh, Szu-Che Yeh, and Julienne Lyu, "A Liquid Crystal Signal Compensation Method with Lower Computational Complexity for Dynamic Range LCD," *OPT2007*, GO-006 (2007/11). **[Student Paper Award]**

(2) Jian-Lung Wu, **Fang-Cheng Lin**, Chun-Ho Chen, Yi-Pai Huang, and Han-Ping D. Shieh, "A 5.6-Inch Field Sequential Color LCD with Less Color Break-Up," *OPT2007*, GO-004 (2007/11). **[Student Paper Award]**

(3) **Fang-Cheng Lin**, Lin-Yao Liao, Cheng-Yumr Liao, Yi-Pai Huang, and Han-Ping D. Shieh, "Backlight Determination of High Dynamic Range LCDs," *OPT2007*, GO-012 (2007/11). [NSC96-2628-E-009-020-MY3]

(4) Ching-Ming Wei, **Fang-Cheng Lin**, Chao-Chiun Liang, and Yi-Pai Huang, "Utilize RGBW$_{min}$ Color Sequence to Suppress CBU Phenomenon on FSC-LCDs," OPT2007, GO-014 (2007/11).

(5) Guo-Zhen Wang, **Fang-Cheng Lin**, Yi-Pai Huang, Han-Ping D. Shieh, Szu-Che Yeh, and Julienne Lyu, "Delta-Color Adjustment Method for HDR-LCD TVs," *OPT2007*, GO-021 (2007/11).

(6) Chien-Liang Wu, Chun-Ho Chen, Fang-Cheng Lin, Yi-Pai Huang, and Han-Ping D. Shieh, "Demonstration of a Mobile-Sized Field Sequential Color LCD for Color Break-up Suppression," *Taiwan Display Conference*, No. E003 (2008/6).

(7) Ching-Ming Wei, **Fang-Cheng Lin**, Chao-Chiun Liang, and Yi-Pai Huang, "Stencil-FSC Method for CBU Suppression and Low Power Consumption in Field-Sequential LCDs," *Taiwan Display Conference*, No. E004 (2008/6).

(8) Guo-Zhen Wang, **Fang-Cheng Lin**, Yi-Pai Huang, Han-Ping D. Shieh, and Szu-Che Yeh, "Delta-Color Adjustment (DCA) Method for Color Backlight of High Dynamic Range LCD-TVs," *Taiwan Display Conference*, No. E005 (2008/6).

(9) **Fang-Cheng Lin**, Yi-Pai Huang, Ching-Ming Wei, and Han-Ping D. Shieh, "Stencil-FSC Method Achieving a Green LCD-TV," *OPT2008*, S13-01 (2008/12). [NSC96-2221-E-009-113-MY3] **[Student Paper Award]**

■ **PENDING PATENTS**

(1) 林芳正,廖振宇,廖凌嶢,黃乙白,謝漢萍,汪德美, "液晶顯示器之背光控制方法."
台灣申請號(TW)：96103083 @2007/01/26   公開號：200832320@2008/08/01
大陸申請號(CN)：200710088722 @2007/03/20 公開號：101021639@ 2007/08/22
美國申請號(US)： 11/896378 @2007/08/31 公開號： US20080180383A1
@2008/07/31   "Backlight control method for high dynamic range LCD"

(2) 許雅婷,<u>林芳正</u>,黃乙白,謝漢萍,陳建宏,洪集茂, "閃爍抑制應用於色序法液晶顯示器."

台灣申請號(TW)：<u>96137168</u> @2007/10/03　　公開號：<u>200917207</u> @2009/04/16

大陸申請號(CN)：<u>200710168284</u> @2007/11/01　公開號：<u>101149904</u> @ 20080326

(3) 廖凌嶢,<u>林芳正</u>,黃乙白,汪德美,葉斯哲,謝漢萍, "高動態範圍液晶顯示器液晶補償演算."

台灣申請號(TW)：<u>96140811</u> @2007/10/30　　公開號：<u>200920122</u> @2009/05/01

大陸申請號(CN)：<u>200710170329</u> @2007/11/12 公開號：<u>101187756</u> @ 2008/05/28

(4) 王國振,<u>林芳正</u>,黃乙白,汪德美,葉斯哲,謝漢萍, "高動態範圍液晶顯示器彩色背光演算."

台灣申請號(TW)：<u>96141050</u> @2007/10/31　　公開號：<u>200919412</u> @2009/05/01

大陸申請號(CN)：<u>200710187301</u> @2007/11/19 公開號：<u>101162565</u> @ 2008/04/16

(5) 黃乙白,孫沛立,<u>林芳正</u>,魏景明,謝漢萍, "色序顯示器之色彩資料處理裝置及其方法."

台灣申請號(TW)：<u>096141445</u> @2007/11/02　　公開號：<u>200921628</u> @2009/05/16

(6) <u>林芳正</u>,黃乙白,魏景明,謝漢萍, "降低液晶顯示器色分離之顯示方法."

台灣申請號(TW)：<u>096141627</u> @2007/11/05　　公開號：<u>200921609</u> @20090516

美國申請號(US)：<u>12/003,995</u> @2008/01/04 公 開 號 ： <u>US 20090115719 A1</u> @2009/05/07　　<u>"Display method for LCD device with reduced color break-up"</u>

(7) <u>林芳正</u>,黃乙白,魏景明,謝漢萍, "壓縮反應時間之畫面控制訊號產生方法."

台灣申請號(TW)：<u>096146958</u>　　@2007/12/10 公開號：<u>200926120</u> @2009/06/16

美國申請號(US)：<u>12/007,323</u> @2008/01/09　　公開號：<u>US 20090146990 A1</u> @2009/6/11 <u>"Method of generating frame control signal for reducing reaction time"</u>

(8) 魏景明,黃乙白,<u>林芳正</u>,謝漢萍, "應用於色序法顯示器之新色場決定法."

台灣申請號(TW)：<u>97131042</u> @2008/08/14